Cell cycle inhibition as a mode of abnormal development: the role of cell cycle checkpoint proteins and cyclin-dependent kinase inhibitors in neurodevelopmental toxicant defense

Elizabeth J. Gribble

A dissertation submitted in partial fulfillment of the requirements for the degree of

Doctor of Philosophy

University of Washington

2005

Program Authorized to Offer Degree:
Public Health and Community Medicine - Environmental and Occupational Health Sciences

University of Washington
Graduate School

This is to certify that I have examined this copy of a doctoral dissertation by

Elizabeth J. Gribble

and have found that it is complete and satisfactory in all respects,
and that any and all revisions required by the final
examining committee have been made.

Chair of the Supervisory Committee:

Elaine Faustman

Reading Committee:

Elaine Faustman

Terrance Kavanagh

Christopher Kemp

Date: 12.19.05

In presenting this dissertation in partial fulfillment of the requirements for the doctoral degree at the University of Washington, I agree that the Library shall make its copies freely available for inspection. I further agree that extensive copying of the dissertation is allowable only for scholarly purposes, consistent with "fair use" as prescribed in the U.S. Copyright Law. Requests for copying or reproduction of this dissertation may be referred to Proquest Information and Learning, 300 North Zeeb Road, Ann Arbor, MI 48106-1346, to whom the authos has granted "the right to reproduce and sell (a) copies of the manuscript in microform and/or (b) printed copies of the manuscript made from microform."

Signature Elizabeth Gibbs

Date 12·14·05

University of Washington

Abstract

Cell cycle inhibition as a mode of abnormal development: the role of cell cycle checkpoint proteins and cyclin-dependent kinase inhibitors in neurodevelopmental toxicant defense

Elizabeth J. Gribble

Chair of the Supervisory Committee:
Professor Elaine Faustman
Department of Environmental and Occupational Health Sciences

Neurodevelopment is an intensively complex process involving the production and organization of over a trillion cells into regions with specialized functions. Patterning of these structures is orchestrated via signaling pathways that provide cues for immature precursor cells to continue proliferating or exit the cell cycle and differentiate into mature, functional neurons and glia. The transition from the proliferative to differentiated state is ultimately accomplished via cell cycle regulatory proteins that act to confer cell cycle exit. This same class of proteins also responds to stress signaling to prevent cellular growth in suboptimal conditions or to repair DNA. Little is known regarding the adverse effects of premature cell cycle exit, effected by these cell cycle regulators, following toxicant exposure during neurodevelopment. Using methylmercury (MeHg) as a model toxicant, this dissertation explores the involvement of cell cycle regulatory proteins in the balance between necrosis, apoptosis, cell cycle inhibition at specific cell cycle phases, and neuronal differentiation following MeHg exposure. Mouse embryonal fibroblasts wildtype and null for Tp53 (p53) are utilized to ascertain the role of p53 signaling pathways in MeHg's effects on cell cycle arrest and cell death. This experimentally

derived data is then compared to a literature based mathematical model of the cell cycle that uses rates to describe p53 controlled cell cycle checkpoints and apoptotic pathways. The mathematical model accurately predicts cell cycle phase distribution and is of utility to inform mechanism specific dose-response predictions of toxicant exposures that cause cell cycle inhibition. In order to examine the involvement of cell cycle regulatory proteins on cell cycle exit during differentiation and toxicant response, we established a novel embryonic mouse midbrain neural precursor cell (NPC) culture and demonstrated a role for both p27 and p53 proteins in effecting differentiation in vitro and in vivo. Midbrain NPC cultures were then used to test the hypothesis that sub-lethal exposure of cycling NPCs to MeHg would result in cell cycle arrest and premature neuronal differentiation in a p53 dependent manner. At a concentration of MeHg resulting in a 50% reduction of cells able to reach a new round of cycling (0.5 μM), we observed increases in cholinergic and GABAergic but not dopaminergic neurons in p53+/+ but not p53-/- NPCs. Taken as a whole, this body of work demonstrates a significant role for p53 in neurodevelopmental toxicant defense, and supports cell cycle inhibition and premature differentiation as possible modes of abnormal development following low dose toxicant exposures.

TABLE OF CONTENTS

	Page
List of Figures	iii
List of Tables	v
Chapter 1: Background and Significance	
1.1 Neurodevelopmental disorders and public health	1
1.2 Dynamics of nervous system development and toxicant susceptibility	1
1.3 Cell cycle inhibition as a mode of abnormal development	2
1.4 Fundamentals of cell cycle regulation	3
1.5 Connectivity of cell cycle and cell fate in neurodevelopment	4
1.6 Knockout mouse models of cell cycle regulatory proteins	5
1.7 Identification of the embryonic midbrain as a region of interest	10
1.8 Methylmercury as a model neurodevelopmental toxicant	11
1.9 Mathematical modeling of biological processes	12
1.10 Summary, hypotheses, and specific aims	14
Chapter 2: The role of p53 in MeHg toxicity and changes in cell cycle kinetics in mouse embryonal fibroblasts	
2.1 Introduction	26
2.2 Methods	29
2.3 Results	31
2.4 Discussion	35
Chapter 3: A mathematical model connecting molecular signaling with cell cycle dynamics in p53+/+ and p53-/- mouse embryonal fibroblasts	
3.1 Introduction	46
3.2 Model development	48
3.3 Model predictions and experimental validation	52
3.4 Discussion and future directions	53
Chapter 4: Dynamic characterization of an embryonic mesencephalon neural precursor cell culture system	
4.1 Introduction	59
4.2 Methods	62
4.3 Results	65
4.4 Discussion	69

Chapter 5: A role for p53 and p27 in normal and perturbed midbrain development
5.1 Introduction 86
5.2 Methods 87
5.3 Results 92
5.4 Discussion 97

Chapter 6: Summary and Conclusions 114

References 128

Appendix 154

LIST OF FIGURES

Figure Number	Page
1.1 Timeline of murine nervous system development	16
1.2 Regulation of cyclin/CDK complexes	17
1.3 NPC cell exit is controlled by cell cycle regulatory proteins	18
1.4 Connectivity of cell cycle and cell fate in neuronal determination	19
1.5 Impacts of Mehg on proliferation	25
2.1 Wildtype p53 MEFs are preferentially susceptible to MeHg cytotoxicity	40
2.2 Growth inhibition by MeHg	41
2.3 Cell cycle inhibition by MeHg	42
2.4 G2/M cell cycle inhibition by MeHg	43
2.5 Apoptosis in p53+/+ and p53-/- MeHg treated MEFs	44
2.6 Apoptosis and necrosis in p53+/+ and p53-/- MeHg treated MEFs	45
3.1 Model schematic	55
3.2 Model simulation of cell cycle phase distribution	57
3.3 Comparison of predicted and observed cell cycle phase distribution	58
4.1 Morphology of mesencephalon cultures	75
4.2 Examination of proliferation: cell counts in mouse and rat	76
4.3 Characterization of cell cycle kinetics: BrdU uptake	77
4.4 Western blot analysis of proliferation markers	78
4.5 Western blot analysis of differentiation markers	79
4.6 Assessment of dopaminergic neuronal phenotype	80
4.7 Assessment of GABAergic neuronal phenotype	81
4.8 Assessment of cholinergic neuronal phenotype	82
4.9 Cell cycle regulatory protein expression in vitro	83
4.10 Cell cycle regulatory protein expression in vivo	84
4.11 Summary and comparison of protein expression in vitro and in vivo	85
5.1 Immunohistochemical staining of p27 and p53 in the mouse midbrain	104
5.2 Cell counts of midbrain NPCs from p53+/+ and p53-/- mice	105
5.3 Assessment of proliferation of p53+/+ and p53-/- NPCs	106
5.4 Comparison of differentiation characteristics of p53+/+ and p53-/- NPCs	107
5.5 Cell viability following MeHg exposure in p53+/+ and p53-/- NPCs	108
5.6 Cell cycle inhibition in p53+/+ and p53-/- NPCs	109
5.7 Cytoplasmic and nuclear localization of p53, p27, and p21 following MeHg exposure	110
5.8 Upregulation of p53 protein following MeHg exposure	111
5.9 Effect of MeHg on differentiation of p53+/+ NPCs	112
5.10 Comparison of differentiation in p53+/+ and p53-/- NPCs following MeHg treatment	113
6.1 A role for p53 in midbrain NPC early differentiation following sublethal MeHg exposure	123
6.2 Implications of toxicant induced early differentiation	124

6.3 Use of the parallelogram approach to compare effects of MeHg across species and experimental system 125
6.4 Ability of experimental systems to assess and predict neurodevelopmental toxicity 127

LIST OF TABLES

Table number	Page
1.1 Knockout models of cell cycle regulatory proteins	20
1.2 Developmental abnormalities in p53 null mice	23
1.3 Developmental abnormalities in p27 null mice	24
3.1 Parameters for model	56
4.1 Markers of neuronal differentiation	74
6.1 Functional overlap of structural homologues of p53	126

ACKNOWLEDGEMENTS

I would like to express my gratitude to my advisor, Elaine Faustman, and dissertation committee for their enthusiasm, support, and suggestions for this work. I have been blessed with the unwavering support of my family and friends, especially my devoted mother. Finally, thank you, Matthew, for your daily companionship, patience, ridiculous sense of humor, and wisdom.

CHAPTER 1. BACKGROUND AND SIGNIFICANCE

1.1. Neurodevelopmental disorders and public health

Identifying preventable causes of neurodevelopmental disorders is an important goal with significant potential to improve public health. Diagnoses of these disorders in live births reported worldwide are in the range of 0.3%-0.7% for autism spectrum disorders, 1% for mental retardation and in the range of 5%-10% for learning disabilities including ADHD. Overall, it is currently estimated that between 3% to 8% of babies born each year in United States will be diagnosed with a neurodevelopmental disorder (Weiss and Landrigan, 2000). These disorders come with enormous financial, social, and emotional costs. While an estimated 15%-25% of disorders can be explained by genetic causes such as the chromosomal abnormalities causing Down's syndrome and another 10% by identified environmental factors such as alcohol, smoking, infections, metals, and prescription drugs, the cause of the large majority of neurodevelopmental disorders is unknown (Little, 2000; Brent, 2001). Lack of basic knowledge as to the causes and mechanisms of these disorders prevents the formulation of strategies to prevent or reduce incidence.

1.2. Dynamics of nervous system development and toxicant susceptibility

Generation of the mammalian central nervous system is a formidable process involving the production, organization, and differentiation of over a trillion cells. Four major phases can be identified and are illustrated in Figure 1.1. In late gastrulation, neural induction biases the ectoderm towards a neural fate. Next, neuralation establishes the neural groove on the dorsal ectodermal surface and copious stem cell proliferation generates the neural progenitor cells. Symmetric division of neural progenitor cells then begins to change and at least one daughter cell permanently exits the cell cycle and further narrows its specific neuronal cell fate. Cell cycle exit is generally thought of as the commencement of differentiation and the loss of progenitor or precursor cell status. Immature neurons then migrate to form distinct structures such

as retina or cerebellum, acquire further neuronal phenotypes and forge communication pathways through synaptogenesis. Lastly, most of the brain, with the exception of the glial cells and a few other localized regions such as a stem cell like population in the cerebral cortex, enters a quiescent state (usually post-natal). The temporal and spatial organization of nervous system development proceeds in a step-like fashion with each subsequent step dependent on proper completion of the previous step. This unilateralism renders it particularly susceptible to even minor insults and exemplifies the principle of timing of exposure in developmental toxicology (Rice and Barone, 2000; Rodier, 1995). Developmental timing of proliferation, differentiation, migration, and apoptosis differ by brain region conferring potential for time and structure specific effects of neurodevelopmental toxicants.

1.3. Cell cycle inhibition as a mode of abnormal development

Alteration of proliferation is implicated in several neurodevelopmental disorders including spina bifida, exencephaly, anencephaly, and craniofacial defects such as cleft palate (Sulik and Sadler, 1993; Rodier et al., 1979, 1994, 1995). Furthermore, many environmental exposures that adversely affect neurodevelopment have been demonstrated to inhibit proliferation including metals (methylmercury and arsenic), valproic acid, rubella, heat stress, fungicides, ethanol, and ionizing radiation (Finnell et al., 2000; Wlodarczyk et al., 1996a, 1996b; Walsh and Morris, 1989; Burbacher et al., 1990; Miller, 1986; Ponce et al., 1994; Gribble et al., 2005). Because inhibition of proliferation can be a general, internally originating, protective mechanism, giving the cell time to repair or wait for external conditions to improve, it is likely to be especially important for low-dose environmental exposures that do not cause outright cell death. For example, Wlodarczyk et al. induced exencephaly following arsenate exposure in mice and demonstrated associated upregulation of cell cycle inhibitory genes (1996). They concluded cell cycle delay prevented neural tube closure in the absence of apoptosis. Similarly, low dose ethanol exposure in humans and in experimental animals has consistently demonstrated time and dose dependent effects on brain

morphology and function (Coles et al., 1991). Proposed mechanisms include inhibition of proliferation and migration and several groups have documented ethanol's effects on cellular proliferation. Li et al. (2001) exposed rat cerebellar granule progenitor cells to sub-cytolethal concentrations of ethanol and observed increases in the total cell cycle length and decrease in the number of cycling cells that corresponded to changes in cell cycle regulatory proteins. These examples demonstrate the balance between proliferation and cell cycle exit and differentiation is sensitive to toxicant perturbation and that cell cycle arrest, an intended defense mechanism, can result in severe neurodevelopmental outcomes.

1.4 Fundamentals of cell cycle regulation

The cell cycle is a tightly regulated process that is described most simply as the time during which the cell divides into two new cells (mitosis) and the time spent preparing to divide again (interphase). Interphase can be partitioned into Gap phase I (G1), DNA synthesis phase (S), and Gap phase II (G2) (Figure 1.2). Sequential progression through these phases is fundamentally driven by fluctuating levels of cyclins which partner with specific cyclin-dependent kinases (CDKs) to phosphorylate proteins necessary for phase transition. As Figure 1.2 indicates, movement from G1 phase into S phase is regulated by the activities of D-type cyclins and Cdk4/6 and E-type cyclins and Cdk2, while G2 to M transition requires activation of the A-type cyclins and Cdk2 and the cyclin B/Cdk1 complex. Further regulation is achieved through the selective synthesis and degradation, activation and deactivation of cyclin-dependent kinase inihibitors (CKIs), tumor suppressors, protooncogenes, and components of other signaling pathways (Chan, 2000; Agarwal et al., 1998; Stewart, 2001). These regulators compose a kind of molecular surveillance program to ensure integrity of the genome and optimal conditions at each phase transition before the cell cycle can proceed. While the fundamentals of cell cycle regulation as described above in proliferating cells in adult organisms are believed to be fairly well understood, the

details of how cell cycle regulation proceeds during development and interfaces with differentiation of cells are less clear.

1.5 Connectivity of cell cycle and cell fate in neurodevelopment

Following proliferation of neuronal cell precursor pools during neurogenesis, cells exit the cell cycle and terminally differentiate into their specific neuronal phenotypes. In contrast to many other organ systems, this cell cycle exit is almost always permanent. Such precise timing of cell cycle exit and differentiation organizes functional and morphological specialization of cells (Cunningham et al., 2002). What are the molecular controls of this process? Figure 1.3 demonstrates the transition of a proliferating, neuronal precursor cell into a quiescent, differentiated cell. This process most obviously involves exiting the cell cycle, changes in morphology, and eventual acquisition of functional neuronal properties such as synaptic transmission and action potentials. In theory, cell cycle exit could result from the cell's response to extrinsic cues such as a reduction of growth factors such as platelet-derived growth factor (PDGF), or accumulation of an external inhibitor, or from intrinsic adjustments to cell cycle regulation (Edlund and Jessell, 1999; Conlon and Raff, 1999). Experimental evidence suggests a complicated interaction between extrinsic and intrinsic factors. For instance, targeted null mutations for PDGF indicate that this factor is essential for proper patterning and proliferation of many types of precursor cell populations including the development of oligodendrocytes (reviewed in Betsholtz et al., 2001; Hoch and Sorriano, 2003). However, in wildtype cultured oligodendrocyte precursors (cells that necessarily depend on PDGF for maintenance in culture), cell cycle exit and differentiation still occur in the presence of saturating conditions of PDGF (Raff et al., 1988). This is also observed for sonic hedgehog (Shh): it acts as a notable and necessary factor for patterning and proliferation by organizing the ventral neural tube into specific precursor cell populations including cortical NPCs, midbrain NPCs and cerebellar NPCs (Wijgerde et al., 2002). Shh is a potent mitogen for cultured cerebellar precursor cells yet they still differentiate in its presence (Miyazawa et al., 2000).

Furthermore, across several days of isolation in cultured cerebellar precursor cells and oligodendrocytes, the number of cellular divisions before cell cycle exit observed in vitro closely parallels in vivo timing and has been associated with accumulation of cell cycle inhibitory proteins, specifically p27 (Miyazawa et al., 2000; Tokumoto et al., 2002; Durand et al., 1997).

These examples point to several important aspects of the work contained in this dissertation. Firstly, that upstream signaling pathways during neurodevelopment likely converge to direct and utilize the basic cell cycle control pathways consisting of cyclins, cyclin dependent kinases, and cell cycle inhibitory molecules identified and fairly well characterized in adult organisms. Figure 1.4 illustrates some examples of how extrinsic signaling has been demonstrated to connect to cell cycle regulatory proteins in specific neuronal cell populations. For example, while cell cycle exit of the two cell types mentioned above has been associated with accumulation of p27, other cell types appear to critically utilize alternate cell cycle inhibitors including p53 in nerve growth factor (NGF) treated neuroblastoma cells, p21 in glial cells, and p57 in amacrine neurons (Figure 1.4). This demonstrates both the redundant nature of cell cycle control pathways and that the specific inhibitory signal to effect cell cycle exit is cell type specific. Second, in vitro proliferative behavior of primary neuronal precursor cell culture systems may reflect intrinsic differentiation "timers" and closely resemble in vivo behavior, thus providing an approximate model for mechanistic investigations. Finally, it is suggested that toxicant or stressor-induced cell cycle inhibition may molecularly mimic the signals directing normal physiological cell cycle exit and lead to premature differentiation.

1.6 Knockout mouse models of cell cycle regulatory proteins

The most common strategy employed in elucidating the function of a protein or signaling pathway in development relies on the inference of functionality via the observed phenotype following the deliberate disruption of functional protein expression. In Table 1.1, we present a summary and description of knockout mice

phenotypes for cell cycle regulatory proteins. Cell cycle regulatory proteins can be distinguished by their critical (Cyclin A2, Cyclin B1, and Cdk5) or non-critical role during development as indicated by whether their absence induces embryonic lethality. This table is not intended as an exhaustive summary of the literature describing the role of cell cycle regulators in development, but relays reported phenotypic anomalies in order to demonstrate the apparent developmental use of cell cycle regulatory proteins in a tissue or time specific manner. While some functional redundancies exist among the cell cycle regulators, examinations of null phenotypes has revealed development-specific roles for these proteins. For example, while Cyclin A1 and Cyclin A2 can pair with Cdk2 to promote G1/S transition, Cyclin A1 null mice are developmentally normal except for male infertility (Liu et al., 1998), whereas Cyclin A2 mice cease development shortly after implantation. Obviously, descriptions of these mice are also limited by how closely and specifically the knockouts were examined. For example, the p27 null mouse was not discovered to be hearing impaired (due to inappropriate proliferation of hair cells in the Organ of Corti) until a few years after it was originally reported but most likely this would have gone unnoticed had the mouse not proven to be a very interesting model and been utilized by several groups (Lowenheim et al., 1999; Fero et al., 1996). Three null mouse models contained in Table 1.1, Cyclin D1, Cdk5, and p53, exhibit abnormal brain development, indicating that these proteins may be especially important during neurodevelopment. Cyclin D1 null mice exhibit general growth retardation, reduced viability, and symptoms of neurological impairment. Cyclin D1 RNA is expressed at high levels in the developing retina in wildtype embryos and accordingly, impaired proliferation of retinal cells in the null mice is observed (Sicinski et al., 1995). Cdk5 was classified as a cyclin dependent kinase on the basis of sequence homology but has not been demonstrated to pair with any cyclins or regulate cell cycle activity (Wang et al., 2005). Instead, it forms a heterodimer with p35 and p39, activators only expressed in the nervous system, and appears to principally influence neuronal survival and apoptosis (Zheng et al., 1998). Mice null for Cdk5 die between embryonic day 16.5 and 12 hours post-birth and exhibit severe

defects throughout the CNS including cerebral and cerebellar cortices, hippocampus, and brain stem (Ohshima et al., 1996). Cells in these brain regions exhibit chromatolysis and increased immunoreactivity for neurofilaments leading the authors to suggest that Cdk5 may developmentally regulate cytoskeletal changes during neuronal differentiation (Ohshima et al., 1996). In contrast to Cdk5 and Cyclin D1, the p53 protein is responsive to stress signaling and also appears to play a role in neurodevelopment. The work described in this dissertation utilizes in vitro cultures from p53 null mice to explore the role of this protein in neurodevelopmental toxicant exposure and differentiation of midbrain neurons. As previously described, the p53 protein is a critical effector of cell cycle arrest and apoptosis following stress and has been implicated as a differentiation factor in several cell types. p53 null mice are reportedly developmentally normal except for a low incidence of strain and sex-dependent neural tube abnormalities (described in more detail below). We hypothesized a role for p53 in midbrain neuronal differentiation and developmental neurotoxicant exposure and utilized a null culture system to further examine the potential substituted expression of other cell cycle regulators such as p21 and p27 in its absence. The p53 and p27 knockout mouse models are described below as a summary of the established functional role of these proteins during development.

p53 knockout mouse

The p53 null mouse provides an exceptional model for investigation of toxicant-induced perturbation of the cell cycle during development. First developed via gene targeting in embryonic stem cells by Donehower et al. (1992), several more groups have since generated p53 knockout lines (Jacks et al., 1994; Purdie et al., 1994; Tsukada et al., 1993; Gondo et al., 1994). Early reports indicated that, surprisingly, the mice were developmentally normal, but developed spontaneous tumors at an exceedingly rapid rate: two separate studies reported nearly 90% of the animals had died with tumors by 6 months of age (Donehower et al., 1992, Jacks et al., 1994). However, subsequent analysis by Sah et al. (1995) and Armstong et al. (1995) revealed

8–23% prevalence of strain- and female-associated neural tube defects, primarily exencephaly, implicating an important role for p53 in neurodevelopment. Analysis at gestational day 13.5 by Sah et al. (1995) revealed 8.8% of p53 -/- embryos from a mixed genetic background (129/Sv x C57BL/6) and 16% of p53-/- embryos from an inbred background (129/Sv) exhibited overgrowth of forebrain and midbrain tissue preventing normal cranium formation. All the exencephalic embryos were female, a bias concordant with other exencephalic-prone mouse strains and neural tube defect prevalence in humans. In contrast to Sah et al., Armstrong et al. (1995) examined 15 p53-/- embryos with exencephaly between gestational day 11.5 and birth and 4 p53-/- anencephalic new-born embryos and reported a spectrum of additional craniofacial and neural abnormalities. Fusion of the upper incisors was observed in 5 of the 19 embryos, retinal dysplasia in 5 of 19, and adhesion of the lens to the cornea in 13 of 19. Ocular abnormalities were also observed in many of the unaffected p53-/- littermates. The exencephalic phenotype again solely appeared in females with the exception of a single male embryo. Table 1.2 presents a phenotypic summary of several different p53 null mouse lines.

Exencephaly results from failure of neural tube closure followed by an overgrowth of tissue from the neural plate. Two hypotheses exist for the increased incidence of this defect in p53 -/- mice. First, p53 may play an important role during neural tube closure, a process highly dependent on changes in cell cycle rates, cell division, and cell apoptosis. Alternatively, higher mutation rates in the haploid gametes of p53 null parents may lead to an increased rate of exencephaly. If the latter were true, however, we would expect to see a spectrum of developmental abnormalities and these are not observed with the single exception of Armstrong's observations of ocular and craniofacial defects (1995). While the penetrance of the exencephalic phenotype varies with strain, it is exaggerated with dietary folate reduction and irradiation of male mice prior to mating indicating the multifactorial nature of neural tube closure (Choi and Donehower, 1999; Armstrong, 1995). The p53 null mouse phenotype also supports our hypothesis of a non-essential role for p53 in normal development but a possibly more

critical role following environmental stress. To note, the mouse strain used in our studies is the same backcross as Donehower et al. and exhibits low frequency of neural tube defects.

p27 knockout mouse

P27-/- mice appear to be fully viable (Table 1.3). The most obvious feature of disruption of the p27 gene is a gene dose-dependent growth enhancement (Nakayama et al., 1996; Fero et al., 1996; Kiyokawa et al., 1996). P27-/- mice are larger than their wildtype counterparts without obesity or gross morphological abnormalities. This weight difference is not evident at birth but quickly becomes significant at 2-3 weeks of age and is due to an approximate 20-40% enlargement of all organs (Fero et al., 1996). Specifically, obvious enlargements of the thymus, pituitary, and adrenal glands, spleen and gonadal organs were observed though endocrine changes were not evident. Fero et al. speculate the observed gigantism is not due to endocrine effects, rather, the lack of p27 appears to allow cell proliferation in the absence of external mitogenic stimuli (1996). Consistent with evidence for p27's role in granulosa cell luteal differentiation as discussed previously, female p27-/- mice are sterile (Kiyokawa, 1996). In human cancer, reduced p27 expression is observed quite frequently in multiple tumor types including colon, lung, glioma, gastric and ovarian and is associated with aggressive growth and poor prognosis, but complete loss of expression is extremely rare (Philipp-Staheli, 2004). In contrast, and despite hyperplasia, only non-invasive adenomas were observed specifically in the intermediate lobe of the pituitary gland in the p27-/- mice (Nakayama et al., 1996). A more recent report determined hearing impairment in p27-/- mice is likely due to inappropriate proliferation of the supporting cells and hair cells in the organ of Corti in the ear (Chen and Segil, 1999). Precursors of supporting cells in wildtype mice permanently exit the cell cycle and differentiate between ED12 and ED14 concurrent with continued expression of p27 protein. Chen and Segil suggest their work demonstrates that p27 links developmental control of cellular proliferation, differentiation, and morphological development of the inner ear.

1.7 Identification of the embryonic midbrain as a region of interest

While regulation of neuronal differentiation in some cell types (oligodendrocytes, retinal cells, cerebellar precursor cells) and brain regions (cerebellum) has been well studied, information about cell cycle exit in the transition from proliferation to differentiation for most brain regions is lacking. With the recognition that little is known about the regulation of cell cycle exit and differentiation in midbrain neuronal precursor cells, this dissertation includes characterization of an in vitro primary embryonic mouse midbrain cell culture system and further validates this model with in vivo comparisons. Understanding the regulation of cell cycle exit in midbrain cells should have several important applications. First, identifying levels and timing of expression of key proteins involved in midbrain development and comparing our results to other regions of the brain will assist our ability to generalize to patterning of distinct brain regions. Our in vitro cultures mimic in vivo development with several neuronal phenotypes emerging from our isolated precursor cells. Of special interest are the dopaminergic neurons which reside within the adult derivatives of the embryonic midbrain: the substantia nigra pars compacta, the retrorubral field, and the ventral tegmentum (Vitalis et al., 2005). Loss of these neurons is a hallmark of severe neurodegenerative disorders such as Parkinson's disease and understanding the control mechanisms of their cell cycle exit may offer clues on how to target regenerative therapies. Furthermore, culturing these cells in vitro may offer possibilities for transplanting dopaminergic neurons into affected brains.

1.8 Methylmercury as a model neurodevelopmental toxicant

As described in Section 1.3, inhibition of proliferation has been implicated in several neurodevelopmental disorders and observed following low dose exposure to many neurodevelopmental toxicants including methylmercury. Furthermore, Mendoza et al., had previously determined that cell cycle inhibition in response to MeHg was dependent on the p21 protein, indicating responsivity of cell cycle signaling pathways to this toxicant that led to cell cycle arrest (2002). While an underlying premise of this

dissertation is that cell cycle inhibition is a downstream response or convergence for many different stress signaling pathways, we chose to utilize MeHg as a model neurodevelopmental toxicant because of its previously documented impacts on proliferation during neurodevelopment. MeHg is a significant environmental contaminant: nearly 80% of states in the United States currently post fish advisories, principally aimed at preventing MeHg exposure to pregnant women through consumption of contaminated fish. The nervous system of the developing fetus is widely acknowledged as the most sensitive target to MeHg; however subtle changes in structure or function are challenging to diagnose and definitely link to exposure. Figure 1.5 lists observed impacts of MeHg exposure across increasing levels of biological complexity: changes in gene expression and cell signaling, effects on dynamic cellular processes, and alterations in brain morphology, function, and behavior. Reduced brain size and weight, hypoplasia of the cerebellar granule layer, and disorganization of the cortex have been observed following higher dose MeHg exposure in humans, primates, and rodents (Burbacher, 1990; Choi and Simpkins, 1986; Geelen et al., 1990; Choi et al., 1991; Eto et al., 1992; Eto, 1997; Eto et al., 1997; Eto et al., 2002). Observed reduction in cell number without apparent necrosis or changes in protein synthesis implicates a role for MeHg in regulatory disruption of cell dynamic processes, specifically proliferation, differentiation, and migration which are intimately linked (Faustman et al., 2002). Mitotic inhibition has been consistently observed following MeHg treatment in vivo and in in vitro animal studies (Miura et al., 1978; Rodier et al., 1984; Howard and Mottet, 1986; Vogel et al., 1986; Sager, 1988; and Ponce et al., 1994). However, epidemiological evidence from human studies remains controversial as to whether low dose, maternal dietary exposure to MeHg during pregnancy leads to significant impacts on learning and behavior. The oral reference dose for MeHg intake is 0.1 μg/kg-day (NRC, 2000) based on analysis of a cohort of pregnancies in the Faroe Islands (Grandjean et al., 1997). Offspring from mothers with mercury cord blood concentrations of 46 – 70 ppb were observed to exhibit language, memory, attention, and some spatial and motor abnormalities at 7 years of age following controlling for

potential confounders such as PCB exposure. Maternal daily MeHg intake was back calculated from mercury blood and hair concentrations (0.86 – 1.6 μg/kg-day) and an uncertainty factor of ten was applied to achieve the reference dose. However, a second prospective longitudinal study of a fish-eating population in the Seychelles Islands did not find any correlation between maternal hair mercury levels and neurodevelopmental deficits in offspring assessed at 5.5 years of age (Davidson et al., 1995, 1998). Nonetheless, a third, smaller epidemiologic study in New Zealand corroborated the Faroe Island observations of dose dependent effects of maternal mercury exposure on child neuropsychosocial deficits (Crump et al., 1998). Thus uncertainty still exists regarding the risks and toxic effects associated with very low dose MeHg exposure. Human estimates of exposure are further complicated by the necessary use of surrogate measures of true target dose to the developing fetal brain. The work in this dissertation utilizes in vitro cell systems to explore potential impacts of sublethal MeHg exposure. Specifically, we examine the role of p53 in MeHg induced cell cycle inhibition and premature neuronal differentiation. Context for extrapolating our experimental concentrations and observations to assess risk for human neurodevelopment is discussed throughout the text and in the final chapter.

1.9 Mathematical modeling of biological processes

A supplemental approach to our experimental questions contained herein involves the development of a mathematical model of the cell cycle. Modeling the molecular pathways governing the dynamic processes specific to development can provide a critical link between toxicant mechanism of action data, often gathered through in vitro systems, and cellular outcome. For example, a model of neocortical development first established by Leroux et al. (1996) and later expanded upon, simulates rates of asymmetric cell proliferation, cell death, and cell migration. This model has allowed for cross species comparisons of normal and perturbed neocortical development, specification of mechanism of cell death, and has allowed for hypothesis testing of mechanism of toxicant action. Effects of neurodevelopmental toxicants such

as ethanol and radiation have been quantitatively examined and dose-response predictions made (Gohlke et al., 2002; 2004). Of additional interest is the potential for assimilating molecular data into a mathematical model of cell cycle regulation. Pioneered from cell cycle phase distribution and kinetics data garnered from flow cytometric analysis (Aarnaes et al., 1990), work by Tyson and Novak has advanced the field considerably through the adoption of differential equations describing cell cycle checkpoint control. Working most often with simple, easily manipulated models such as yeast and frog eggs, their work provided a strong framework for the very recent emergence of a comprehensive model for a mammalian system (Novak et al., 1998; Borisuk and Tyson, 1998; Cross et al., 2002; Novak et al., 2001; Zwolak et al., 2005; Kramer and Fussenegger, 2005).

As reviewed previously, cell cycle regulation during development differs from cell cycle regulation in a mature organism. Cell cycle regulators are expressed in distinct, spatially and temporally restricted patterns since different effects must be achieved during development than what occurs in the adult organism (Ohnuma et al., 2001). Furthermore, cell proliferation in development is intimately linked to both programmed cell death and differentiation (Bally-Cuif and Hammerschmidt, 2003). In our work we have adapted a simple model of the cell cycle from Besse et al. (2003) in order to predict the cycling properties of embryonic cells and to discriminate the specific role of p53 in each of the places it acts in the cell cycle and its role in apoptotic cell death under normal conditions and following toxicant exposure. It is anticipated that this model can be expanded to incorporate mechanistic data across levels of biological complexity from RNA transcription, translation, post-translational modifications, and protein degradation of key cell cycle regulators. It could also be expanded to a neuronal specific framework to encompass differentiation rates and total midbrain neuroanatomy. Such complementary strategies to experimental investigations should improve the robustness of human health risk assessments in addition to generating new experimental hypotheses.

1.10 Summary, hypotheses, and specific aims

The work in this document addresses our overall premise that cell cycle inhibitory proteins such as p27 and p53 play an important role in both normal neurodevelopment and neurodevelopmental toxicant induced cell cycle delay. In Chapter 2, we utilize p53 wildtype and knockout primary mouse embryonal fibroblasts (MEFs) to examine the effects of methylmercury treatment on changes in cell viability, cell cycle kinetics, and apoptosis. Chapter 3 develops a mathematical model of the cell cycle and estimates rates of cell cycle phase transition, cell cycle entry, necrosis and apoptosis over several cell generations for wildtype and p53 knockout MEFs. Chapter 4 describes the establishment of a novel mouse midbrain neural precursor culture system adapted from the rat and characterizes the dynamic proliferating and differentiating behavior of these cells. Utilizing the new culture system, Chapters 4 and 5 investigate the role of specific cell cycle regulators in normal midbrain cell cycle exit and compare their expression with comparable developmental timepoints in vivo. Then, following methylmercury exposure, cultured midbrain cells wildtype and null for p53 are examined for cell cycle regulator protein expression and phenotypic specific differentiation. The final chapter provides overall conclusions from the dissertation. The hypotheses and corresponding specific aims are outlined as follows.

Hypothesis: MeHg causes cell cycle inhibition and cell death via p53 signaling pathways.

Specific Aim I. Determine the role of p53 in MeHg toxicity including changes in cell viability, cell cycle dynamics, and apoptosis using wildtype and null mouse embryonal fibroblasts (MEFs).

Hypothesis: Quantitative modeling of the underlying molecular mechanisms governing cellular proliferation can accurately predict cell cycle phase distribution of multiple generations of MEFs.

Specific Aim II. Develop a mathematical model to connect molecular signaling with cell cycle dynamics and validate with experimental observations from Specific Aim I.

Hypothesis: Cultured mouse midbrain neural precursor cells will behave similarly to rat midbrain cultures with regard to proliferation and differentiation. Proliferation and differentiation of cells can be monitored by several endpoints that are sensitive and responsive across time in culture.

Specific Aim III. Establish and characterize rates of proliferation and differentiation in an embryonic mouse midbrain micromass system.

Hypothesis: The p21, p27 and p53 proteins play an important role in the transition from proliferation from proliferation to differentiation in the embryonic mouse midbrain.

Specific Aim IV. Characterize temporal expression of p21, p27, and p53 protein during cell cycle exit and differentiation in mouse midbrain in vivo and in vitro.

Hypothesis: Toxicant exposure during the transition from proliferation to differentiation can result in cell cycle inhibition via p27 and p53 signaling that corresponds to inappropriate differentiation.

Specific Aim V. Determine the role of p21, p27, and p53 in response to neurodevelopmental toxicant exposure in micromass. Measure changes in protein expression and markers for proliferation and differentiation by genotype in wildtype and p53 null cells.

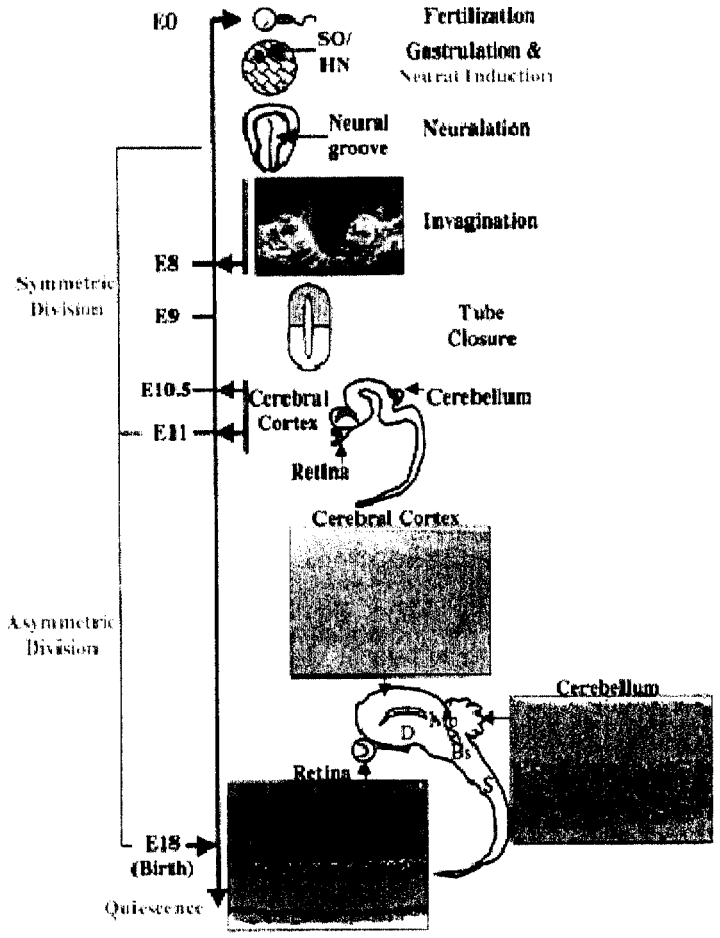

Figure 1.1 Timeline of murine nervous system development. Following fertilization, designated E0, the process of gastrulation establishes anterior and posterior poles within the developing embryo. Specification of the Speamann's organizer (*SO*) or Hensen's node (*HN*), a region through which gastrulating cells move through to form the future head and neck, marks the beginning of neural induction. The neural groove on the dorsal ectodermal surface eventually invaginates (E8) and fuses (E9) to form the neural tube. Major cellular proliferation in ventricular zones (VZs) between E10.5 and E11 forms the beginnings of future brain structures such as the retina, cerebral cortices, and the cerebellum. Unique to the developing CNS, proliferating cells progressively switch from symmetric to asymmetric division with at least one daughter cell permanently exiting the cell cycle such that most of the CNS is quiescent by birth. *Bs*, brainstem; *D*, diencephalon; *Mb*, midbrain; *Sc*, spinal cord. This figure is taken from Cunningham and Roussel, 2001.

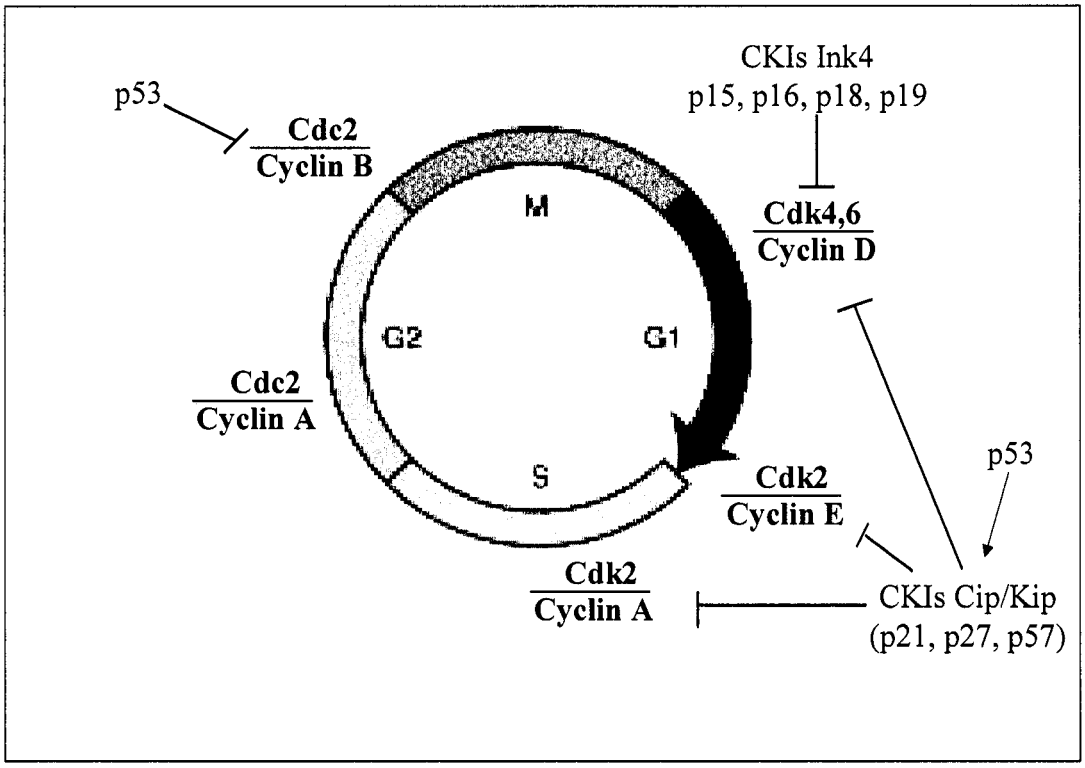

Figure 1.2 Regulation of cyclin/CDK complexes. Cell cycle progression relies on the sequential pairing and activation of cyclins and cyclin-dependent kinases which successively act together to promote unidirectional progression through the stages of the cell cycle. In response to cellular stress or damage, cyclin-CDK complexes are precisely regulated and inhibited by cyclin kinase inhibitors (CKIs) that block their activity. There are two CKI families, the Ink4 family only inhibits cyclinD/CDK complexes to effect G1 arrest while the Cip/Kip family principally inhibits cyclin E to prevent G1/S transition. The Cip/Kip CKIs have been observed to bind other cyclin/cdk complexes but the functional significance of this binding is controversial. P53 is a major cell cycle regulator with many downstream targets including the Cip/Kip family and can effect arrest at the G1/S or G2/M transition. Modified from Ohnuma et al., 2001.

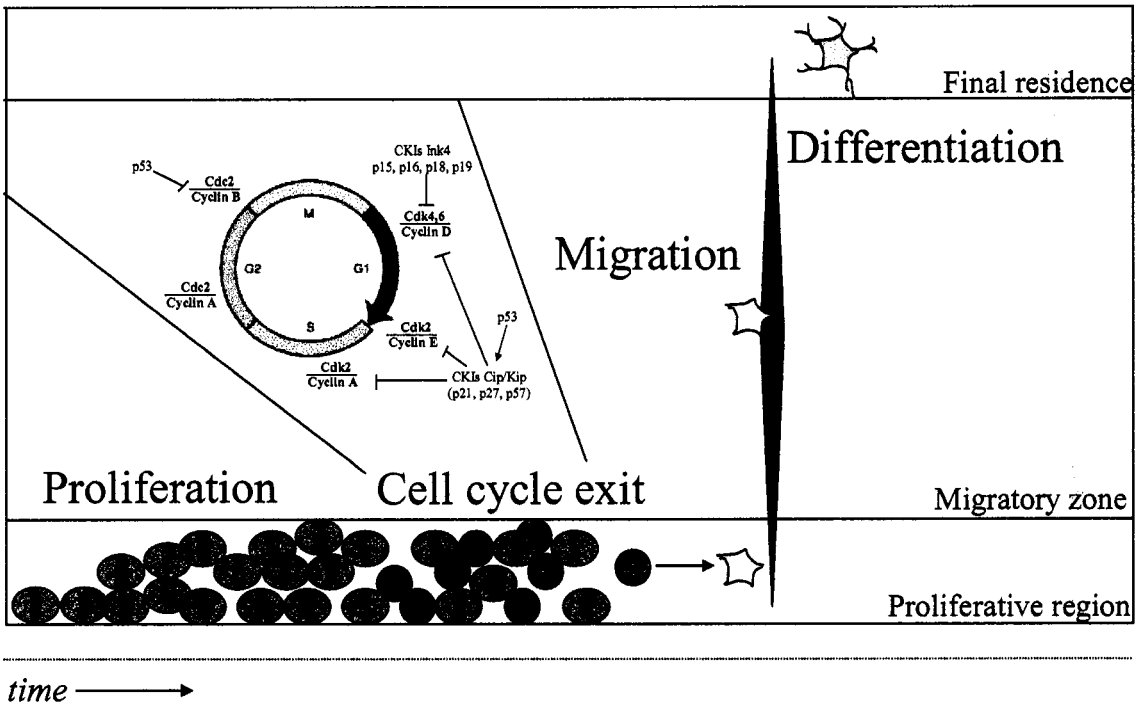

Figure 1.3 Neural precursor cell cycle exit is controlled by cell cycle regulatory proteins. During neurodevelopment, proliferating, pluripotent neural precursor cells are concentrated in proliferative or ventricular regions throughout the developing CNS. Cell cycle exit is the first step in the transition to the differentiated state and this is molecularly achieved through cell cycle signaling. Following cell cycle exit, immature neurons begin to express phenotypic specific markers and migrate to the developing region of their final residence. Here, they undergo further differentiation and form synapses with other neurons.

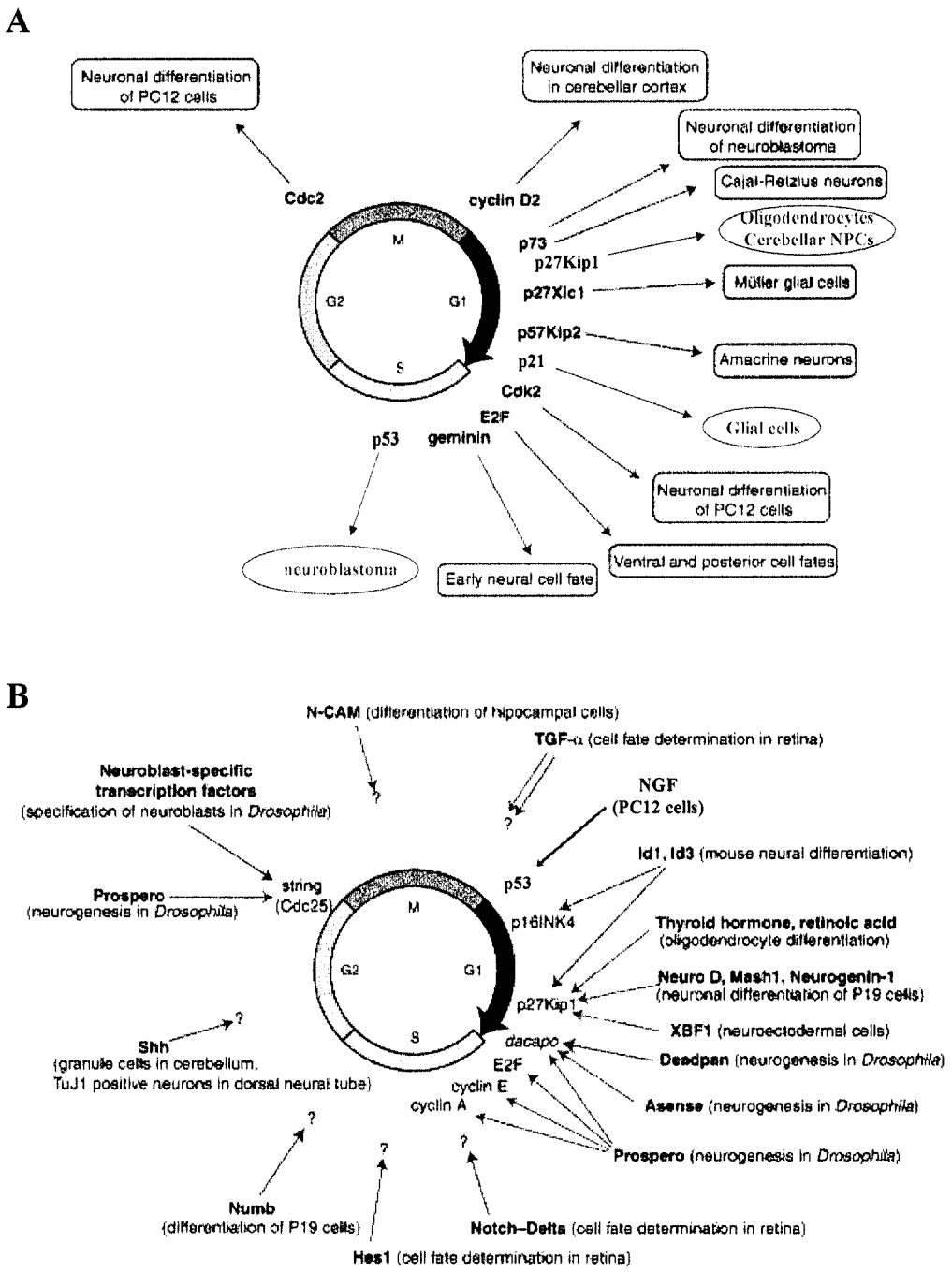

Figure 1.4 Connectivity of cell cycle and cell fate in neuronal differentiation. Specific cell cycle regulatory proteins have been experimentally demonstrated to be critical for determining cell fate and the acquisition of specific neuronal phenotypes (A). Alternatively, upstream neuronal determination factors can act through cell cycle regulatory proteins to promote cell cycle exit and differentiation (B). Adapted from Ohnuma et al., 2001.

Table 1.1 Knockout models of cell cycle regulatory proteins

Gene	Role in cell cycle	Viability of Null Mutant	Phenotype	References
Cyclins				
CyclinA1	Partners with cdk2 during G1/S transition, active in S phase, appears to be expressed predominantly in germ cells but not somatic tissues	Adulthood	Developmentally normal. Males infertile due to arrest of spermatogenesis during late meiotic prophase.	Liu et al., 1998
CyclinA2	Partners with cdk2 during G1/S transition and is active in S phase	Embryonic lethal between day 5.5 and day 8.5	Cease development shortly after implantation	Murphy et al., 1997
CyclinB1	Present in all cells at high levels at prophase and metaphase when binds to cdc2 to form mitosis promoting factor (MPF), necessarily destroyed at anaphase for cytokinesis to proceed	Embryonic lethal (stage not determined)		Brandeis et al., 1998
CyclinB2	Expression levels peak slightly after cyclinB1, possibly also part of MPF, destroyed for mitotic exit	Adulthood. Underrepresented (17%)	Developmentally normal and fertile	Brandeis et al., 1998
CyclinD1	Responsive to growth stimulatory signals in G1 and partners with cdk4 and cdk6, phosphorylates the Rb protein, sequesters p21 and p27.	Juvenile death (0-5 months)	Growth retardation, neurological defects, reduction of cell number of neural retina, fertile but impairment of pregnancy-associated mammary tissue proliferation	Sicinsky et al., 1995 Deletion of p27 restores normal development Geng et al., 2001
CyclinD2	Responsive to growth stimulatory signals in G1 and partners with cdk4 and cdk6, phosphorylates the Rb protein, sequesters p21 and p27.	Adulthood	Infertility in females. Two-fold reduced sperm count in males.	Sicinski et al., 1996
CyclinE1	Expression peaks sharply at the G1/S transition, associates with cdk2 and cdk3, believed to complete Rb phosphorlation following cyclinD/cdk and drive progression into S phase via other targets.	Adulthood	Developmentally normal but reduced fertility in males.	Geng et al., 2003
CyclinE2	Overlapping function with cyclinE1	Adulthood	Developmentally normal but reduced fertility in males.	Geng et al., 2003
Cyclin dependent kinases				
Cdk2	Binds cyclinE to phosphorylate Rb protein, also associates with cyclinA in G1/S transition	Adulthood. Underrepresented (19%)	Developmentally normal but infertile. Inability of germ cells to enter meiosis. Pre-pubertal and severe atrophy of gonads.	Berthet et al., 2003
Cdk4	Associates with cyclinD1 to facilitate G1/S transition	Adulthood	Growth retardation, infertile, and develop insulin-deficient diabetes within the first two months of life from reduction of beta-islet pancreatic cells	Rane et al., 1999

Table 1.1 (continued)

Cdk5	Not related to cell cycle progression, preferential activity in facilitation of migration of post-mitotic neurons	Death between day 16.5 and 12h post birth	Defects in cerebral and cerebellar cortices and hippocampus	Ohshima et al., 1996; Gilmore et al., 1998
Cyclin kinase inhibitors				
P19	Cdk inhibitor (member of the Ink4 family). Activates p53 by binding and inactivating Mdm2.	Adulthood	Developmentally normal and fertile. No increased sensitivity to ionizing radiation and no cell cycle, proliferative, or differentiative abnormalities in MEFs or immune cells.	Zindy et al., 2000
P21	Cdk inhibitor (member of the Cip/Kip family). Responsible for the G1/S checkpoint. Can be activated by p53 or operate independently.	Adulthood	Developmentally normal. G1/S checkpoint of reduced efficiency depending on toxicant. G2/M checkpoint intact.	Deng et al., 1995 Brugarolas et al., 1995 Schubart et al., 1996
P27	Cdk inhibitor (member of the Ink4 family). Primarily inhibits transition to S-phase through complexing with cyclin E-cdk2 but also binds cyclin D-cdk4 and cyclin A-cdk2.	Adulthood	Developmentally normal but significantly heavier by 3 weeks of age with with disproportionate enlargement of spleen, thymus, and pituitary. In inbred backgrounds, pituitary tumorigenesis leads to early mortality. Female sterility.	Kiyokawa et al., 1996; Nakayama et al., 1996 Fero et al., 1996
Other cell cycle regulatory proteins				
Cdc25c	Activates cyclinb1-cdc2 complex to promote G2/M transition. Cdc25A, -B, and -C expressed in overlapping but time and tissue specific patterns	Adulthood	Developmentally normal and fertile	Chen et al., 2001
P53	Involved in G1/S and G2/M checkpoints. Directs transcription of a network of genes that can induce cell cycle arrest or apoptosis.	Adulthood. Underrepresented (17-20%). Reduced lifespan (varies depending on backcross) due to tumorigenesis	Developmentally normal and fertile though some impaired spermatogenesis. 8-16% incidence of neural tube abnormalities selectively affecting females. Accelerated time to tumor development (4 – 9 months) with lymphomas most prevelant.	Donehower et al., 1992 Harvey et al., 1993 Sah et al., 1995
Mdm2	Ubiquitin ligase that is normally bound to p53 and directs its degradation by the proteosome.	Embryonic lethal between day 4.5 and 7.5, coincides with increase in cell cycle rates between day 5.5 and 6.0	Rescued by loss of p53	Jones et al., 1995 Leveillard et al., 1998
Chk1	Responsive to double strand DNA breaks, activated by ATM and in turn activates Cdc25 which inhibits the activity of cyclinB1/cdc2 to prevent mitotic entry	Embryonic lethal between day 3.5 and 7.5	Day 3.5 blastocytes contained aberrant nuclei (highly condensed nuclear aggregates and irregularly-sized micronuclei) within the rapidly dividing inner portion of embryos. Defective in G2/M checkpoint following toxicant treatment in vitro.	Takai et al., 2000
E2F-1	Transcription factor for genes involved in cell cycle progression from G1/S.	Adulthood	Developmentally normal and fertile except for abnormal cells in the exocrine tissues that	Yamasaki et al., 1996 Field et al., 1996

Table 1.1 (continued)

	Inactivated when bound to Rb.		became more pronounced with age. Males experience testicular atrophy between 9 and 12 months. Broad spectrum of early tumorigenesis beginning at 9 months.	
Rb	Binds E2F proteins to repress gene expression associated with cell cycle progression. Essentially inactivated for G1/S transition.	Embryonic lethal between day 13.5 and 15.5	Widespread neuronal cell death at day 12.5 and deficiency of erythropoiesis in day 13.5 embryos.	Jacks et al., 1992 Mansour et al., 1998

Table 1.2 Developmental abnormalities in p53 null mice.

Reference	Ratio of null offspring	Background mouse strain	Null developmental phenotype
Donehower et al., 1992	23%	C57BL/6-129/SV	Reduced fertility, otherwise developmentally normal, later report of 5% exencephaly in null females
Armstrong et al., 1995	84% reduction of null females at weaning 50% reduction in female homozygotes by weaning	inbred 129/Ola outcrossed to SWR and C57BL/6	in outcross: 23% of null females exhibited exencephaly usually confined to fore- and midbrain region, upper incisor fusion, ocular abnormalities, and one hindlimb polydactyly in same embryos with neural tube abnormalities
Rotter et al., 1993		129/SV	reduced fertility: increased level of multinucleated giant cells in testicular seminiferous tubules
Jacks et al., 1994	17%	C57BL/6	appeared developmentally normal and were fertile.
Sah et al., 1995 from Jacks lab	17% 129/sv 20% 129/sv x C57BL/6	129/SV & 129/SV-C57BL/6	129/SV had higher rates of exencephaly (16%) than mixed background (8%). Exencephaly only observed in females.

Table 1.3 Developmental abnormalities in p27 null mice.

Reference	Ratio of null offspring	Background mouse strain	Null developmental phenotype
Fero et al., 1996	24%	129/Sv x C57/B6J	Female sterility, gigantism, disproportionate enlargement of the thymus, spleen, and pituitary. No hormonal abnormalities. Pituitary adenomas and early mortality due to pituitary tumors in 129/Sv inbred mice but not 129/Sv x C57/B6J hybrids
Kiyokawa et al., 1996	25%	C57BL/6	Female sterility, gigantism, increase in proliferating thymocytes, pituitary intermediate lobe adenomas. No hormonal abnormalities.
Nakayama et al., 1996	25%	129/Ola x C57BL/6	Female sterility, gigantism, disproportionate enlargement of thymus, spleen, testis, ovary, pituitary, adrenal gland, and prostate. No hormonal abnormalities. Increases in proliferating thymocytes but not due to decreased sensitivity to apoptosis. Benign pituitary intermediate lobe adenomas. Disorganization of the cellular layer pattern in the neural retina.
Chen et al., 1999 Lowenheim et al., 1999	25%	129/Sv (from Fero group)	Proliferation in hair cells and supporting cell layers in the organ of Corti and impaired hearing

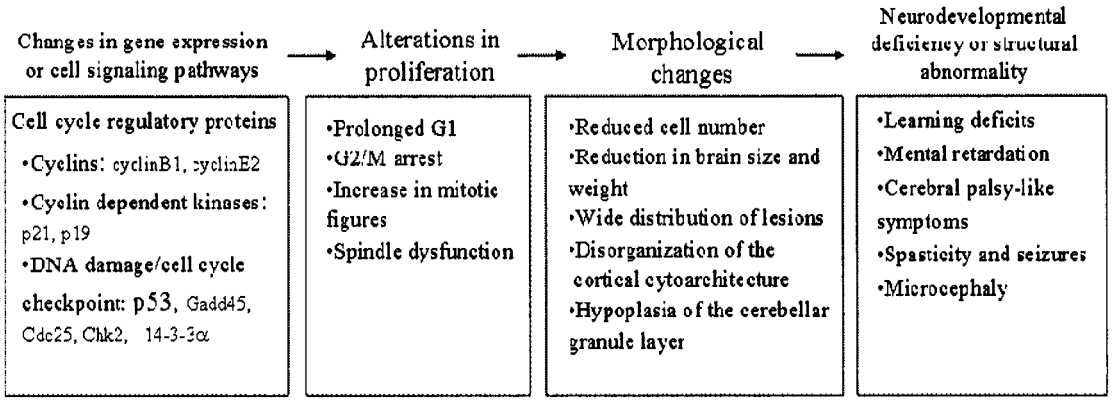

Figure 1.5 Impacts of MeHg on proliferation across levels of biological complexity. MeHg is a known human neurodevelopmental toxicant with documented human exposure resulting in changes in brain function and structure. On a cellular level, MeHg exposure has experimentally been demonstrated to result in a variety of molecular and cellular changes including increases in intracellular calcium levels and binding of MeHg to cellular macromolecules. In proliferating cells, a common response to such stressors is to undergo cell cycle arrest: this has been documented in response to MeHg, even at sublethal concentrations. Cell cycle inhibition has been linked to underlying changes in gene expression of cell cycle regulatory proteins. Please see text for complete references.

CHAPTER 2. THE ROLE OF P53 IN MEHG TOXICITY AND CHANGES IN CELL CYCLE KINETICS IN MOUSE EMBRYONAL FIBROBLASTS

2.1 Introduction

Catastrophic methylmercury (MeHg) poisonings in the past fifty years in Minimata Bay, Japan and Iraq have served to remind us that MeHg is a potent, ubiquitous toxicant demanding vigilant exposure reduction strategies. Neurodevelopmental effects in the absence of maternal toxicity are well established, yet the dose response for subtle clinical deficits is difficult to identify and definitively link to exposure. Knowledge of mechanisms of action for low-dose MeHg exposure can greatly serve to identify safe exposure levels for pregnant mothers and aid our general understanding of both metals and neurodevelopmental toxicants.

Prenatal MeHg pathology in humans, primates, and rodents presents with reduced brain size and weight, hypoplasia of the cerebellar granule layer, and disorganization of the cortex (Choi and Simpkins, 1986; Geelen et al., 1990; Choi, 1991; Eto et al., 1992; Eto 1997; Eto et al., 1997; Eto et al., 2002). Observed reduction in cell number without apparent necrosis or changes in protein synthesis implicates a role for MeHg in regulatory disruption of cell dynamic processes, specifically proliferation (Faustman et al., 2002). Mitotic inhibition has been consistently observed following MeHg treatment in vivo and in in vitro animal studies (Miura et al., 1978; Rodier et al., 1984; Sager, 1984; Howard and Mottet, 1986; Vogel et al., 1986; Sager, 1988; Ponce et al., 1994). However, disruption of neuronal migration has also been observed in response to MeHg exposure and recently, Kakita et al. (2003) observed abnormal neuronal migration through the cortical layers on P28 following MeHg exposure on E16 and E21, a period of overlapping neurogenesis and migration. Proliferation and migration are intimately linked during development and it is possibly the duration and timing of MeHg exposure that produces the observed complex neurodevelopmental effects (Takahashi et al., 1996). This emphasizes the need to

specifically examine the impacts of MeHg on each of these processes in order to better understand the molecular mechanisms governing changes in cell cycle.

Exquisite control of the cell cycle is mandatory especially during development where slight disruptions in the processes of proliferation, differentiation, and migration can produce extreme consequences. Molecular checkpoints, activated in response to toxic insult or sub-optimal growth conditions, assure control by arresting the cell in order to repair damage or enter apoptosis. The importance of these signaling pathways for cell cycle control is underscored by their evolutionary conservation (NRC, 2000). At the G_2/M checkpoint, surveillance and potential cellular arrest is largely accomplished through p53-dependent mechanisms (Stewart and Pietenpol, 2001). Cells progress from G_2 to mitosis by formation and activation of the M-phase promoting factor (MPF) consisting of cyclin B1 complexed with p34cdc2 (cdk1). MPF is activated upon entry into mitosis by dephosphorylation of p34cdc2 on Thr-14 and Tyr-15 by cdc25 (Morgan, 1997). The activated complex then acts to phosphorylate many cytoskeletal proteins and must be deactivated for mitotic exit. The p53 protein inhibits mitotic entry through transcriptional repression of *cyclin b1* and *cdc2*, induction of 14-3-3σ to sequester cdc25 in the cytoplasm, and induction of cyclin-dependent kinase inhibitors (CKIs), including $p21^{Cip1}$ that physically inactivate the cyclin B1/cdc2 complex (Taylor and Stark, 2001). Genes transcriptionally activated by p53, including $p21^{Cip1}$ and the *Gadd* (growth arrest and DNA damage) family, also regulate cell cycle transition at the G_1-S border in response to DNA damage. In the absence of p53, cells can still undergo arrest (and apoptosis) via p53-independent signaling pathways such as ATM (ataxia-telangiectasia mutated) and ATR (ATM and Rad-3 related) and phosphorylation of Chk1/Chk2 (Pearce and Humphrey, 2001), p19ARF (Rowland et al., 2002; Tsuji et al., 2002) and ERK (extracellular regulated kinase) (Tang et al., 2002), and inhibition of PARP (poly(ADP-ribose) polymerase) (Saldeen et al., 2003). In most cases, these proteins can also cooperate with p53 to effect similar results although the developmental ontogeny of each specific signaling pathway has not yet been established. For example, Vinson and Hales (2003) recently showed minimal

upregulation of the PI3K (phosphatidylinositol 3-kinase) family including ATM, ATR, and DNA-PK (DNA-dependent protein kinase) following genotoxic stress during mid-organogenesis in the rat conceptus.

The p53 null mouse provides a useful model for investigation of toxicant-induced perturbation of the cell cycle. First developed via gene targeting in embryonic stem cells by Donehower et al. (1992), several more groups have since generated p53 knockout lines (Tsukada et al., 1993; Gondo et al., 1994; Jacks et al., 1994; Purdie et al., 1994). Early reports indicated that, surprisingly, the mice were developmentally normal, but formed spontaneous tumors at a rapid rate: two separate studies reported nearly 90% of the animals had died with tumors by 6 months of age (Donehower et al., 1992; Jacks et al., 1994). However, subsequent analysis by Sah et al. (1995) and Armstrong et al. (1995) revealed an 8–23% prevalence of strain- and female-associated neural tube defects, primarily exencephaly, implicating an important and distinct role for p53 in neurodevelopment. The growth characteristics of p53-deficient mouse embryonal fibroblasts (MEFs) from a mixed C57/BL6 and 129/Sv background, as used in this study, have been reported by Harvey et al. (1993) who indicated that p53-/- fibroblasts, as compared to p53+/+ and p53+/- fibroblasts, divided more rapidly in culture, had a lower percentage of cells in G_0/G_1 phase, did not enter a senescent phase even after 50 passages, and exhibited chromosomal instability with increasing time in culture. The faster cycling times observed in the p53-/- MEFs support the idea of a constitutive and inducible role for p53 in cell cycle control. The p53 protein is post-translationally regulated in a complex manner in order to respond to environmental stress but may also normally participate in a not yet identified interaction to slow the G_0/G_1 transition (Harvey et al., 1993). The MEFs are easily collected, are usually robust in culture and allow for the investigation of specific pathways in proliferation and cell cycle dynamics in embryonic cells but in tissue culture conditions that are not promoting differentiation.

We have previously demonstrated that MeHg treatment (0, 2, 4, and 6 μM) causes G_2/M arrest in asynchronous transgenic mouse embryonal fibroblasts (MEFs)

irrespective of p21 genotype but that progression to a new round of division is partly dependent on p21 (Mendoza et al., 2002). Here, we investigate the involvement of p53, an upstream regulator of p21 and major coordinator of G_2/M arrest, in MeHg induced G_2/M arrest of cells.

2.2 Methods

Cell culture. Mice heterozygous for the wild type and null p53 allele of a C57BL/6 x 129/Sv background were obtained from Dr. Richard Morrison of the Department of Neurological Surgery, University of Washington. Embryonal fibroblasts were prepared according to Robertson et al. (1987) with some modifications. Fourteen days after a successful mating, pregnant mice were euthanized according to IUCAC protocol, and gravid uteri were removed. Isolated embryos were washed separately several times in Earl's Balanced Salt Solution (Gibco BRL, Grand Island, NY). Tissue dissociation of torso and limbs was performed overnight at 4 °C using 0.25% (w/v) trypsin (DIFCO, Detroit, MI). Single-cell fibroblast suspensions were then plated in 100-mm tissue culture dishes (Corning, Acton, MA) and maintained in Dulbecco's modified Eagle's medium (DMEM, Gibco BRL) containing 10% (v/v) fetal bovine serum (FBS, Gibco BRL), 200 units/mL penicillin (Sigma, St. Louis, MO), and 0.1 mg/mL streptomycin (Sigma) at 37 °C with 5% CO_2/95% humidified air. Cells were genotyped at early passage and subsequently genotyped prior to each experiment. At passage 4-7, p53+/+ and p53-/- cells were plated in 60-mm tissue culture dishes (Corning) with DMEM-F12 (Gibco BRL) containing 10% (v/v) Nu-serum (BD Biosciences, Bedford, MA), 200 units/mL penicillin (Sigma), and 0.1 mg/mL streptomycin (Sigma). Initial numbers of cells plated were adjusted in order to ensure uniform sub-confluence (80-90%) prior to treatment (500,000 p53-/-; 1,000,000 p53+/+). Culture stocks were frozen at -80°C in DMEM containing 20% (v/v) FBS and 10% (v/v) dimethyl sulfoxide (DMSO, Sigma).

MeHg treatment. A 10^3-fold dilution of a 1 M methylmercury(II) hydroxide stock solution (Alfa Aesar, Ward Hill, MA) in sterile water was performed to obtain a working solution for MeHg treatments (0.25, 1.0, 2.5, 4.0 μM). Sterile water was used

as a negative control while 50 nM colchicine (Sigma) was used as a positive control. Subconfluent cells were grown overnight in 60-mm dishes and then transferred to serum-free media (DMEM-F12, .05% Nu-Serum) for 24h to synchronize the cells. For flow cytometric analysis, 5-bromo-2'-deoxyuridine (BrdU, Sigma) was added to cultures with treatment at a final concentration of 90 μM. MeHg treated cells were placed in a plexiglass chamber (in order to minimize MeHg exposure) with water to maintain humidity, gassed for 5 minutes with 5% CO_2/95% air, and placed in a 37 °C incubator.

Flow cytometry. After incubation, cells were harvested in 0.05% trypsin, resuspended in Hoechst 33258 (Molecular Probes, Eugene, OR) buffer with 10% NP40 (Sigma) and 10% DMSO, and stored at –20 °C until analysis. Prior to analysis, samples were thawed on ice and 10 μg/mL propidium iodide with 0.1% RNase was added. Cells were taken up into a 25-5/8 gauge syringe, passed through a 40 μm wire mesh filter and run on a Coulter Epics Elite flow cytometer. MPLUS 5.0 software (Phoenix Flow Systems, San Diego, CA) was used to analyze data.

Cytotoxicity. Cell viability assays were carried out using Promega's CytoTox 96®Non-Radioactive Cytotoxicity Assay (Madison, WI). The assay measures lactate dehydrogenase activity through the conversion of a tetrazolium salt (INT) into a red formazan product. Briefly, cells were plated and treated as described for MeHg treatments. At time of assay, 500 μL of media were removed from dishes and placed at 4 °C. Plates were washed once in CMF-PBS and 5 mL of new culture media plus 750 μL of Lysis Solution (9% (v/v) Triton® X-100 in water). Cells were incubated at 37 °C for 45 minutes then 500 μL media collected. 50 μL of each supernatant and 50 μL of Substrate Mix were added in triplicate to a 96-well enzymatic plate, covered in foil, and left at room temperature for 20 minutes. The assay was stopped by adding 50 μL Stop Solution (1 M acetic acid). The plate was read at 490 nm on a Molecular Devices plate reader. Background media absorbance was subtracted from all samples and cytotoxicity was expressed as absorbance due to treatment divided by maximal

absorbance (absorbance of supernatant from lysed cells + absorbance in media supernatant).

Apoptosis. Programmed cell death was measured with the Annexin V-FITC Apotosis Detection kit from Oncogene Research Products (San Diego, CA) according to manufacturer's instructions. Briefly, treated cells were harvested by trypsinization, centrifuged at 800 x g for 5 minutes, and washed twice in 500 μL cold PBS. Cells were washed once and then gently resuspended in 500 μL cold Binding Buffer. Next, 2.5 μL Annexin V-FITC were added and incubated for 15 minutes at room temperature in the dark. Cells were centrifuged at 800 x g for 5 minutes, resuspended in 500 μL cold Binding Buffer, and 10 μL Propidium Iodide (PI) were added. Cells were immediately analyzed on a Coulter Epics Elite flow cytometer with excitation at 488 nm and emission 518 nm (FITC) and 620 nm (PI). MPLUS 5.0 software (Phoenix Flow Systems) was used to analyze data.

Statistical Analysis. Intercooled Stata 7.0 for Windows (StataCorp, College Station, TX) was used to perform all statistical tests. Analysis of variance (ANOVA) and linear regression were used to determine differences in genotype response to toxicant treatment and temporal differences within genotype. Bonferroni's multiple comparisons procedure was used to compare MeHg doses to control. A p value ≤ 0.05 was considered statistically significant.

2.3 Results

Cytotoxicity and inhibition of proliferation by MeHg

The LDH assay quantitatively measures lactate dehydrogenase, a cytosolic enzyme released upon loss of membrane integrity. In this assay, LDH-mediated conversion of lactate to pyruvate is coupled with a colorometric conversion of a tetrazolium salt by diaphorase. Figure 2.1 indicates the differential sensitivity of the p53 +/+ cells to MeHg: while a significant reduction in cell viability at 1.0 μM, 2.5 μM, and 4.0 μM was observed in the p53+/+ at 48h, only a non-significant, shallow dose response was evident with the p53-/- cells. The response to MeHg was statistically

different between the genotypes as determined by ANOVA. In the p53+/+ cells, treatment with 2.5 μM MeHg and 4.0 μM MeHg caused a significant reduction in cell viability at 24h. None of the MeHg treatments caused a significant decline in viability at either 24h or 48h in the p53-/- cells. Treatment with 0.25 μM MeHg was indistinguishable from control for all endpoints measured and is not discussed further.

Figure 2.2 shows growth inhibition by MeHg as measured by total LDH from media plus lysed cells expressed as a percentage of the control at 24h and 48h. In order to approximate a true measure of cell viability, Figure 2.1 expresses percentage of cell death within each treatment. In contrast, Figure 2.2 indicates total cell number, both live and dead, and thus provides a measure of cycling inhibition induced by MeHg treatment. Inhibition is again more dramatic in p53+/+ cells as compared to p53-/-: p53+/+ cultures treated with 2.5 μM MeHg had 76.5% ± 4.4% (24h) and 51.5% ± 3.5% (48h) of control cells versus 86.5% ± 7.2% (24h) and 75.3% ± 6.5% (48h) of control cells in the p53-/-. Because cell number is inclusive of both live and dead cells, reduction in number, as revealed by the LDH assay, is presumably due to a combination of cell cycle delay and the decline of the total proliferating population due to cell death.

Inhibition of cell cycle progression

Cell cycle kinetics and distribution were examined via culture with 5-bromo-2'-deoxyuridine (BrdU), a thymidine analog, and Hoechst 33258 and propidium iodide which both stochiometrically bind DNA. Cells incorporate BrdU into their DNA as they progress through S phase. Hoechst fluorescence is quenched in the presence of incorporated BrdU: progression through multiple cell cycles can thus be tracked by decreased Hoechst fluorescence and by cell cycle stage using propidium iodide fluorescence (Rabinovitch et al., 1998). Cells were gated to exclude clumps and dead cell debris for analysis.

Figure 2.3 expresses MeHg's effect on the cycling population of cells by quantifying the percentage of cells reaching at least a new G_0/G_1 during treatment at

48h. At 24h, no untreated or treated p53+/+ cells have cycled to the next round. In contrast, cell cycle inhibition is evident in the faster-cycling p53-/- cells: 68.2% ± 3.2% of untreated cells have reached a new G_0/G_1 but only 57.8% ± 3.9% (1.0 μM) and 26.5% ± 1.4% (2.5 μM) of treated cells have been able to progress (data not shown). As shown in Figure 2.3, after 48h of culture, 78.6% ± 13.1% of untreated p53+/+ cells and 83.5% ± 8.3% of untreated p53-/- cells reached at least a new G_0/G_1. In comparison, after 48h of MeHg treatment, p53+/+ cycling was severely impacted: at 1.0 μM, 69.8% ± 17.3% of cells reached a new round while at 2.5 μM no p53+/+ cells were able to progress. Treatment with 1.0 μM MeHg affected p53-/- cells similarly to p53+/+ (14% reduction in the progressing population); however, 2.5 μM had a less dramatic effect in the p53-/- cells where 42.6% ± 7.2% of these cells were able to continue cycling.

MeHg causes G_2/M inhibition

MeHg causes a non-permanent G_2/M delay in p53+/+ cells at 1.0 μM (Figure 2.4A, 2.4B). At 24h, the original G_2/M population is elevated by 15.1% over the untreated population; however, by 48h, the untreated and treated (1.0 μM) cell cycle population distributions are nearly indistinguishable. Treatment-induced G_2/M inhibition is accompanied by an inability of G_0/G_1 cells to progress to a new G_2/M. At 24h, 28.9% ± 14.1% of the untreated p53+/+ cells have reached a new G_2/M (G_2/M'), but none of the MeHg treated cells (1.0 μM and 2.5 μM) has cycled to G_2/M'. Higher dose MeHg (2.5 μM) also causes an increase above untreated cells (17.3% ± 9.0%) in the p53+/+ G_2/M population at 24h, and this population increases with time. By 48h, the original G_2/M population in the p53+/+ cells treated with 2.5 μM MeHg is 77.0% ± 7.5% as compared to 7.3% ± 8.4% in the untreated p53+/+ cells.

Compared to the p53+/+ cells, the p53-/- cells cycle more rapidly and cell cycle population distributions cannot be compared directly. P53+/+ cells double in approximately 36h while the doubling time in p53-/- cells is approximately 16h (unpublished observations). For instance, at 24h, the untreated p53-/- cells have 3.1%

± 1.0% of cells in G_2/M, 30.4% ± 12.0% of cells in G_2/M', and a majority of cells in G_0/G_1'. G_2/M populations in the p53-/- untreated cells are smaller as compared to the p53+/+ at 24h and 48h. Strikingly, MeHg treatment also caused a G_2/M specific delay in the p53-/- cells; however, it occurred in the new G_2/M population (Figure 2.4C, 2.4D). At 24h in the p53-/- cells, 2.5 μM MeHg did not effect a change in the G_0/G_1 (data not shown) or G_2/M populations, but the G_2/M' population was increased 26.3% ± 11.1% over the untreated cells with moderate significance (p=0.07). At 48h, the G2/M' population of p53-/- cells treated with 2.5 μM MeHg is significantly elevated 23.5% ± 1.1% over the untreated cells.

Mechanism of cell death

To determine if the increased cell viability of the p53-/- cells following MeHg treatment was due to a decreased capability to induce apoptosis, we treated cells and stained with propidium iodide and annexin V-FITC. In this flow cytometric assay for apoptosis, FITC-conjugated annexin V binds to phosphatidyl serine, a phospholipid only present in the outer membrane of cells undergoing apoptosis. Propidium iodide is excluded from cells with intact membranes. Figure 2.5 presents a representative cytogram showing four distinct cell populations: FITC-/PI- cells are healthy (H), FITC+/PI- cells are early apoptotic (EA), FITC-/PI+ cells are necrotic (N), and FITC+/PI+ cells are late apototic or necrotic (N/LA). As show in Figure 5, for the same concentration and time point, p53+/+ cells undergo more apoptosis than do the p53-/- cells. Treatment with 1.0 μM MeHg causes approximately a 3-fold larger percentage of p53+/+ cells to undergo apoptosis than the p53-/- at 24h and 48h.

Figure 2.6 shows MeHg induced changes in viability by mechanism of cell death: early apoptotic cells (FITC+/PI-) are indicated in black while necrotic cells (FITC-/PI+) and FITC+/PI+) are shown in gray. Assessment of viability by this assay was comparable to the LDH assay and demonstrates that, with the exception of one treatment condition (p53+/+, 2.5 μM, 48h), apoptosis is not a major contributor to MeHg induced cell death in these cells. Early apoptotic cells increased in a

concentration dependent fashion in both genotypes but a larger percentage of apoptotic cells were observed in the p53+/+ cells at all treatment conditions and time points.

2.4 Discussion

First reported as a tumor suppressor, the p53 protein plays a fundamental role in protection from physiological stress and DNA damage through its ability to arrest the cell cycle and induce apoptosis (Cadwell and Zambetti, 2001). Because cell cycle checkpoint pathways are central to controlled proliferation, migration and differentiation, p53 is also likely essential to many developmental processes. In the experiments reported here, the role of p53 in MeHg induced cell cycle arrest and cytotoxicity was explored utilizing wildtype and nullizygous p53 mouse embryonal fibroblasts. In this system, the presence of p53 led to decreased viability, increased apoptosis, and higher rates of cell cycle inhibition and G_2/M arrest following MeHg exposure.

MeHg has been shown to elicit cell death in neuronal cell lines via both necrotic and apoptotic pathways. For instance, Castoldi et al. (2000) demonstrated acute necrosis in primary rat cerebellar granule cells within 1h exposure to 5–10 μM MeHg following impairment of mitochondrial activity and plasma membrane lysis. In contrast, 1 μM MeHg induced depolymerization of microtubules as early as 1.5h followed by nuclear condensation (6–9h); however, the researchers were unable to prevent this apopotosis with taxol, a microtubule-stabilizing agent, or caspase inhibitors (Castoldi et al., 2000). This indicates that microtubule disruption may not be the apoptotic trigger and the mechanism may be caspase independent. In a primary midbrain micromass system, Ponce et al. (1994) demonstrated similar patterns of G_2/M arrest between MeHg and colchicine, a mitotic inhibitor that binds to microtubules, but showed that MeHg was more cytotoxic at equivalent levels of G_2/M arrest. This suggests that while arrest may be connected to cell death, it is not the primary cause. Indeed, in our experiments, temporary and recoverable arrest was observed in p53+/+ cells following treatment with 1.0 μM MeHg that led to G_2/M inhibition at 24h. The

inhibition was ablated by 48h and accompanied by cells progressing to the next round of cycling in proportions similar to controls.

It has been proposed that the availability of sufficient energy to mount the apoptotic response may be the critical determinant of mechanism of cell death (Eguchi et al., 1999). The cytotoxicity assay we used measures the release of lactate dehydrogenase (LDH) into the cell culture media upon loss of cytosolic membrane integrity. While loss of membrane integrity is a late step in both necrosis and the longer process of apoptosis, both mechanisms of cell death should be captured via this assay with the exception of early, apoptotic cells. Our results indicated a much higher rate of cell death in the p53+/+ cells than in the p53-/- after MeHg treatment. For example, 24h treatment with 2.5 μM MeHg caused a 17% reduction in cell viability in p53+/+ that increased to 49% at 48h as compared to untreated cells. At the same concentration in the p53-/-, no cytotoxicity was observed after 24h and viability was only reduced by 12% of the control at 48h. Discrimination of apoptosis and necrosis was accomplished via the annexin V-FITC assay. In concordance with visual inspection of cell morphology, apoptosis does not appear to play a large role in MeHg induced cell death except at conditions with an approximate 50% reduction in viability in the p53+/+ cells (2.5 μM, 48h). While p53-/- cells underwent less apoptosis following MeHg treatment than p53+/+ cells, they experienced less necrosis also. The increased viability of p53-/- cells after MeHg treatment cannot be entirely accounted for by a decreased capacity to undergo apoptosis. MeHg is known to affect mitochondrial membrane potential and reduce ATP production at doses as low as 0.2 μM (Limke and Atchison, 2002). This simultaneous toxic effect may hinder cells from mounting the apoptotic program independent of p53 status.

Following cell cycle checkpoint activation at any stage of the cell, the immediate effect of the resulting signaling is cell cycle arrest (for reviews see Shackelford et al., 1999; Pearce and Humphrey, 2001; Pietenpol and Stewart, 2002). Following MeHg treatment, we observed accumulation of cells with 4N DNA content in both p53 genotypes and a concurrent decline in cells reaching a new G_0/G_1. These

observations agree with previous work in MeHg treated primary rat fetal CNS cells (Ponce et al., 1994) and p21 transgenic MEFs (Mendoza et al., 2002). While Mendoza et al. (2002) observed G_2/M accumulation independent of p21 genotype, we demonstrate a statistically different magnitude of G_2/M accumulation at 48h in p53+/+ cells as compared to p53-/- (Figure 2.4). After 48h of treatment with 2.5 μM MeHg, 77.0% ± 7.5% of p53+/+ cells were in G_2/M phase as compared to 7.7% ± 8.4% of control cells. In contrast, at the same concentration and time point, G_2/M' inhibition was observed in the p53-/- cells but to a lesser degree: 41.8% ± 1.1% of treated cells compared to 18.3% ± 1.4% of untreated. Interestingly, p53-/- cells in G_2/M at the beginning of treatment were not immediately inhibited from cycling and accumulation was observed at the G_2/M' phase (Figure 2.4C, 2.4D). This is likely due to both the accelerated cycling kinetics in these cells as compared to the p53+/+ cells and the potentially related reduced sensitivity to MeHg.

Inhibition of cell cycling is generally considered a protective strategy upon toxic insult. In the context of low dose MeHg exposure, we demonstrate that measurements of cell death must also consider cell cycle inhibition to understand the toxicant's effect on cell number. To quantify true cell death caused by MeHg, we expressed our cytotoxicity data as dead cells divided by total live and dead cells in the same treatment dish. At 24h in both p53+/+ and p53-/- cells, cell viability following 1.0 μM MeHg treatment is the same as untreated controls. However, differences are observed in both genotypes in total cell number (live and dead). Figure 2.2A indicates at 24h, 1.0 μM MeHg caused a 9.8% ± 7.4% reduction of cell number in the p53+/+ cells. Similarly, in the p53-/-, 1.0 μM MeHg treatment led to a 12.3% ± 9.9% decrease in cell number with no associated change in viability; growth inhibition increased to 77.8% ± 4.8% of control at 4.0 μM with no change in viability. These measures are important to note as they provide a bridge between estimating cell death and percentages of cell population reaching a new G_0/G_1. Cell populations in different stages of the cell cycle obtained through cytometry are calculated as percentage of living cells by selectively gating for size, intracellular granularity, and DNA staining

characteristic of live cells. Integration of our results clearly indicates MeHg causes inhibition of cell cycling in the absence of changes in viability.

The p21 protein is an important effector of p53 mediated cell cycle arrest at both the G_1/S and G_2/M transitions (reviewed in Pietenpol and Stewart, 2002). Significant G_2/M accumulation of cells was observed following 24h treatment with 2 μM and 4 μM MeHg irrespective of p21 genotype in transgenic MEFs (Mendoza et al., 2002). Cytotoxicity was also p21 independent. In contrast, we observed G_2/M arrest in p53+/+ cells at 2.5 μM MeHg that was significantly greater than in the p53-/- cells. While p53-/- cells did exhibit significant G_2/M delay with treatment, over 40% of the cell population went on to reach a new round of cycling. In contrast, p53+/+ cells underwent a G_2/M specific inhibition of all cell cycling. This implies p53 plays an important role in MeHg induced cell cycle inhibition, but that redundant pathways are able to cause some cell cycle delay independent of p53 and p21 does not appear to be a major mediator of this G_2/M arrest.

A recent paper by Lewandowski et al. (2003) compared in vivo and in vitro effects of MeHg on cell cycling and proliferation. To permit these comparisons, a common dose metric (μg Hg/g cellular material) was developed that allowed for comparison of tissue concentrations in order to relate these to MeHg toxicity observed in in vitro and in vivo studies. In P19 mouse cells and primary rat midbrain cells, they measured media and intracellular mercury concentrations and found an approximately 3-fold accumulation in cells of the media MeHg concentration (i.e. 1 μM = 3 μg/g). For in vitro data, they saw similar LOAELs (1 μg/g – 3 μg/g) for cell cycle changes in mouse carcinoma, glioma, and leukemia cells, rat midbrain cells, and human fibroblasts. Using the dose metric for comparisons to in vivo mouse studies indicated brain cell cycling effects at similar levels. In contrast, rat in vivo tissues required approximately 2-fold higher doses than in vitro studies and in vivo mouse studies before cell cycling impacts were observed. For perspective, a human LOAEL is estimated at 0.5 μg/g - 1.0 μg/g based on data collected from neonates involved in the Minimata poisoning (Choi et al., 1978), a non-symptomatic Japanese population

(Nishimura et al., 1974) and from Lapham et al.'s study in the Seychelles Islands (1995). A summary of the literature indicates that humans may be more sensitive to MeHg's neurodevelopmental effects than mice, which in turn, are less sensitive than rats. Consistent with the literature, we observed minimal changes in cell viability but significant cell cycle effects at an in vitro concentration of 1 μM (3 μg/g). This concentration is higher than the estimated LOAEL for humans but is consistent with previous studies by Rodier et al. (1984) and Sager et al. (1984) indicating that concentrations of 2 μg/g in vivo and 3 μg/g in vitro can produce neuronal specific cell cycle changes in the mouse.

Consistent with previous work, our results indicate low-dose MeHg causes cell cycle inhibition in the absence of cytotoxicty. Furthermore, this study suggests a hypothesized mechanism involving p53 signaling that may have important implications for the neurodevelopmental toxicity of MeHg. Our results support the relevance of key checkpoint pathways in developmental toxicity and emphasize the importance of bridging molecular mechanisms and cellular outcome following low-dose environmental exposures.

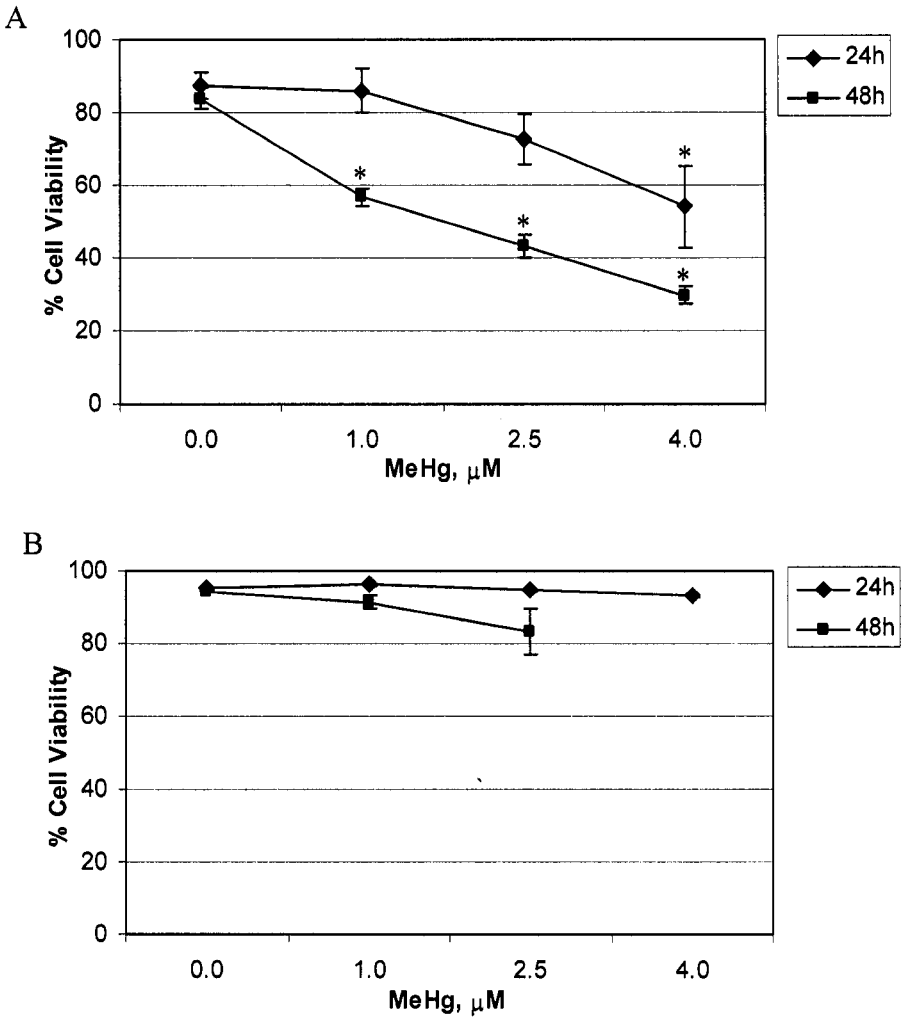

Figure 2.1. Wild type p53 mouse embryonal fibroblasts are preferentially susceptible to cytotoxicity by MeHg. Cytotoxicity in p53+/+ (A) and p53-/- (B) cells is expressed as percentage of viable cells as measured by lactate dehydrogenase release. Concentration and time dependent response was observed in the p53+/+ cells. At 24h, MeHg (4.0 μM) caused a significant reduction of cell viability as compared to the control and at 48h, all concentrations are significantly different. In contrast, a shallow dose response is observed in the p53-/- cells but the trend is not statistically significant. As measured by regression, p53+/+ cells respond significantly differently to treatment than do p53-/- cells. Each point represents the mean ($n \geq 3$) ± SE and concentrations producing a statistically significant change ($p \leq 0.05$) from the untreated control are denoted with an asterisk (*).

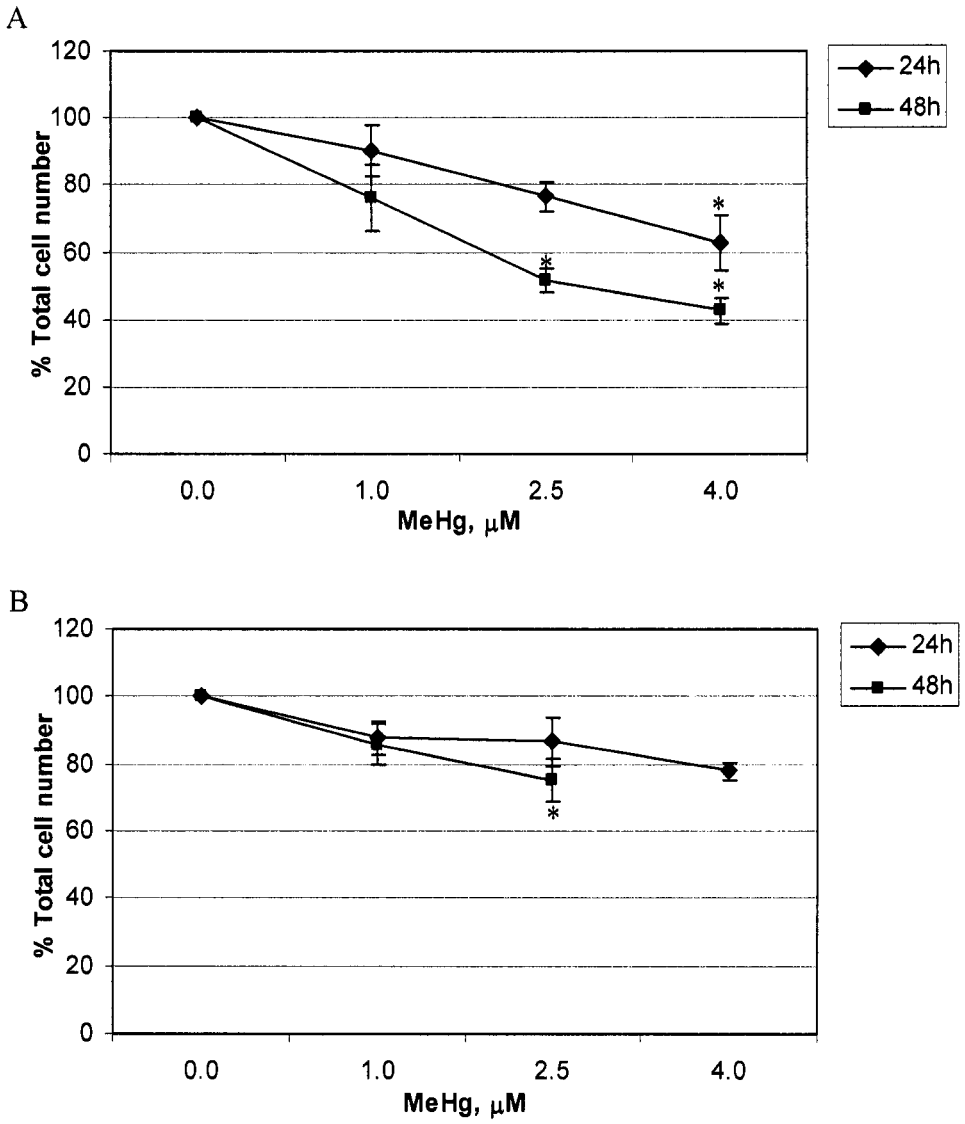

Figure 2.2 Growth inhibition by MeHg. Growth inhibition by MeHg treatment was estimated using LDH data. Because total LDH is proportional to total cell number, Figure 2.2 is a representation of the total cell population at each time point and concentration, both live and dead. In the p53+/+ cells (A), 4.0 μM MeHg caused a significant reduction of cell proliferation as compared to lower concentration treatment at 24h. This trend was even more evident at 48h. In the p53-/- cells (B), 24h treatment with 4.0 μM caused a marginally significant reduction ($p \leq 0.06$) and at 48h, 2.5 μM also became significant. Each point represents the mean ($n \geq 3$) ± SE and concentrations producing a statistically significant change ($p \leq 0.05$) from the untreated control are denoted with an asterisk (*).

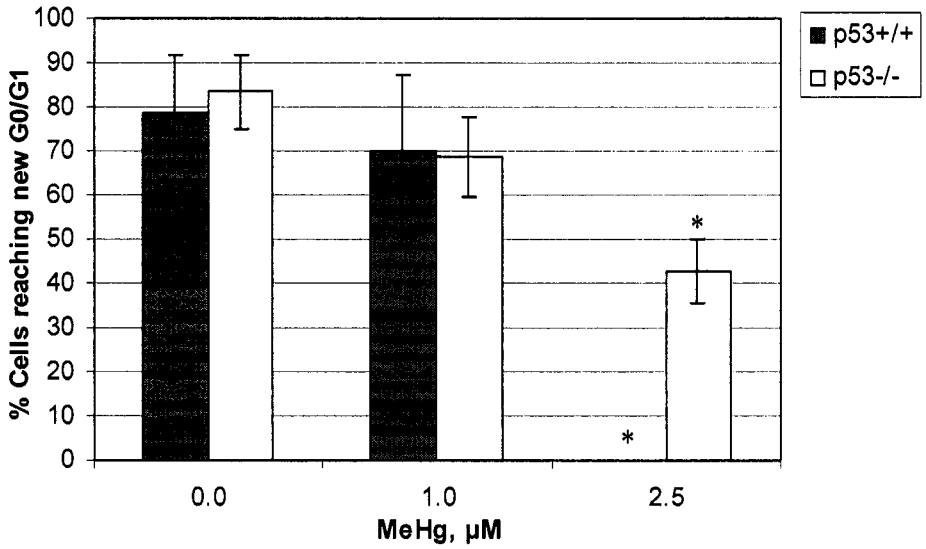

Figure 2.3. Cell cycle inhibition by MeHg. Cells treated with MeHg show a statistically significant concentration-dependent decrease in their ability to reach a new G_0/G_1 by 48h irrespective of genotype. Treatment with 2.5 µM MeHg halted all cycling in the p53+/+ cells while in the p53-/- cells, it significantly decreased the number of cells reaching a new G_0/G_1 during treatment. As measured by regression, the genotypes respond significantly differently to treatment. Each point represents the mean ($n \geq 3$) ± SE and concentrations producing a statistically significant change ($p \leq 0.05$) from the untreated control are denoted with an asterisk (*).

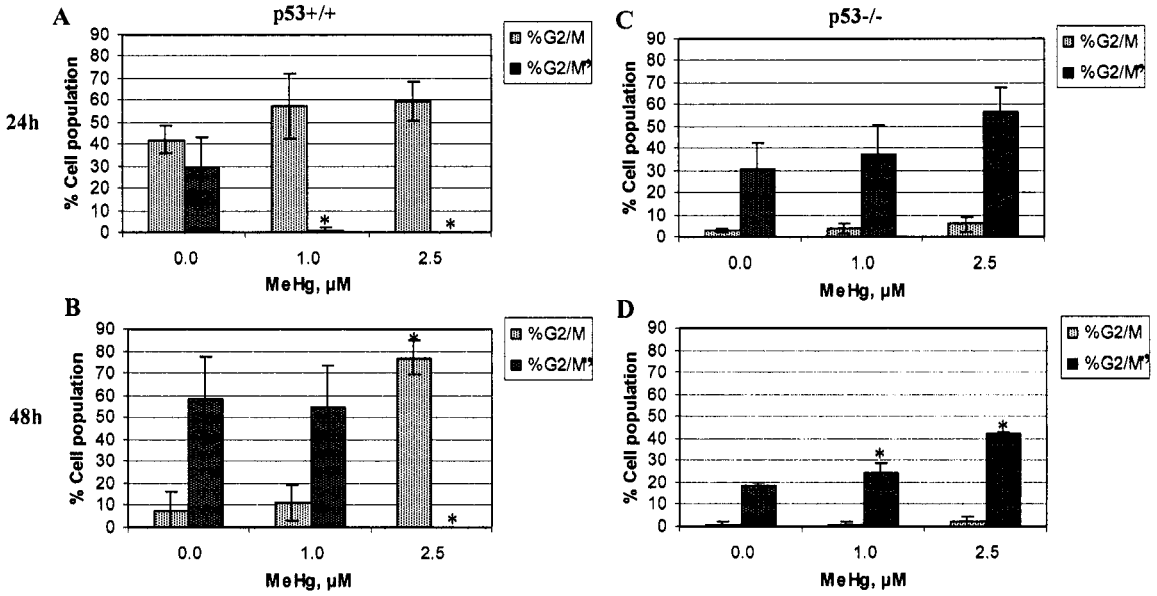

Figure 2.4. G_2/M cell cycle inhibition by MeHg at 24h and 48h. (A) p53+/+ cells, 24h; (B) p53+/+ cells, 48h; (C) p53-/- cells, 24h; (D) p53-/- cells, 48h. In both genotypes, MeHg causes a concentration dependent increase in the number of cells in G_2/M. In the p53+/+ cells at 24h (A), both 1.0 μM and 2.5 μM MeHg caused G_2/M inhibition and resulted in no cells progressing to the second round of G_2/M. By 48h (B), cycling recovery has occurred in the 1.0 μM group. The p53-/- cells indicate a similar pattern but inhibition occurs in the new G_2/M (G2/M'): concentration dependent G_2/M' inhibition is observed at 24h and persists at 48h (C, D). Unlike the p53+/+ cells, 2.5 μM treated p53-/- cells are able to resume cycling by 48h; however, significant accumulation is still observed in the G_2/M' population. Each point represents the mean ($n \geq 3$) ± SE and concentrations producing a statistically significant change ($p \leq 0.05$) from the untreated control are denoted with an asterisk (*).

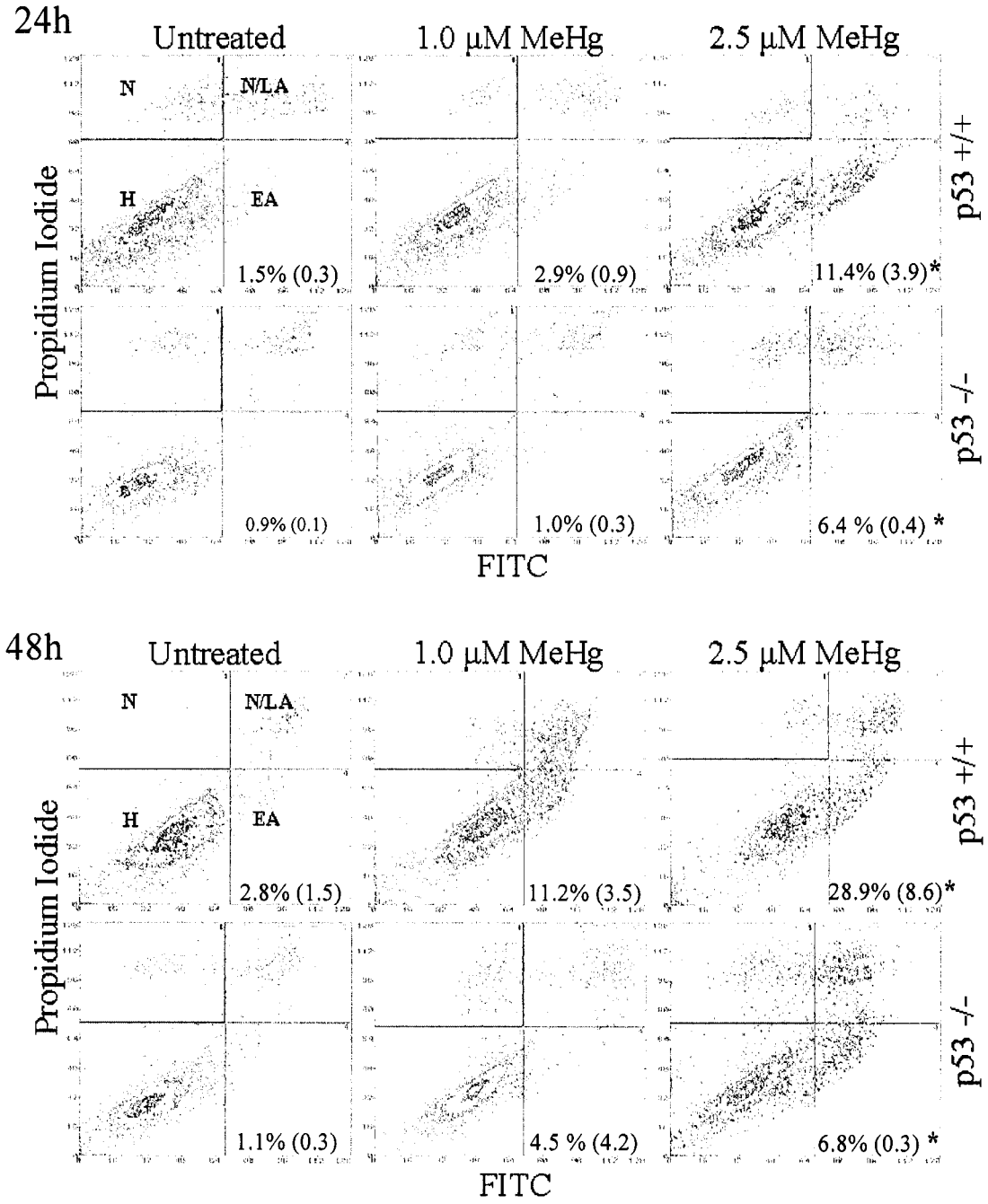

Figure 2.5. Apoptosis in p53+/+ and p53-/- MEFs treated with MeHg for 24h and 48h. Following treatment, cells were harvested and stained with propidium iodide and annexin V-FITC to distinguish between healthy cells (H; lower left quadrant), necrotic cells (N; upper left quadrant), early apoptotic cells (EA; lower right quadrant), and necrotic or late apoptotic cells (N/LA; upper right quadrant). MeHg treatment causes a statistically significant increase in the early apoptotic population in both the p53+/+ and p53-/- cells. Standard deviation is indicated in parenthesis. Cytograms are representative of several experiments ($n \geq 3$) and statistically significant changes in the early apoptotic population ($p \leq 0.05$) from the untreated control are denoted with an asterisk (*).

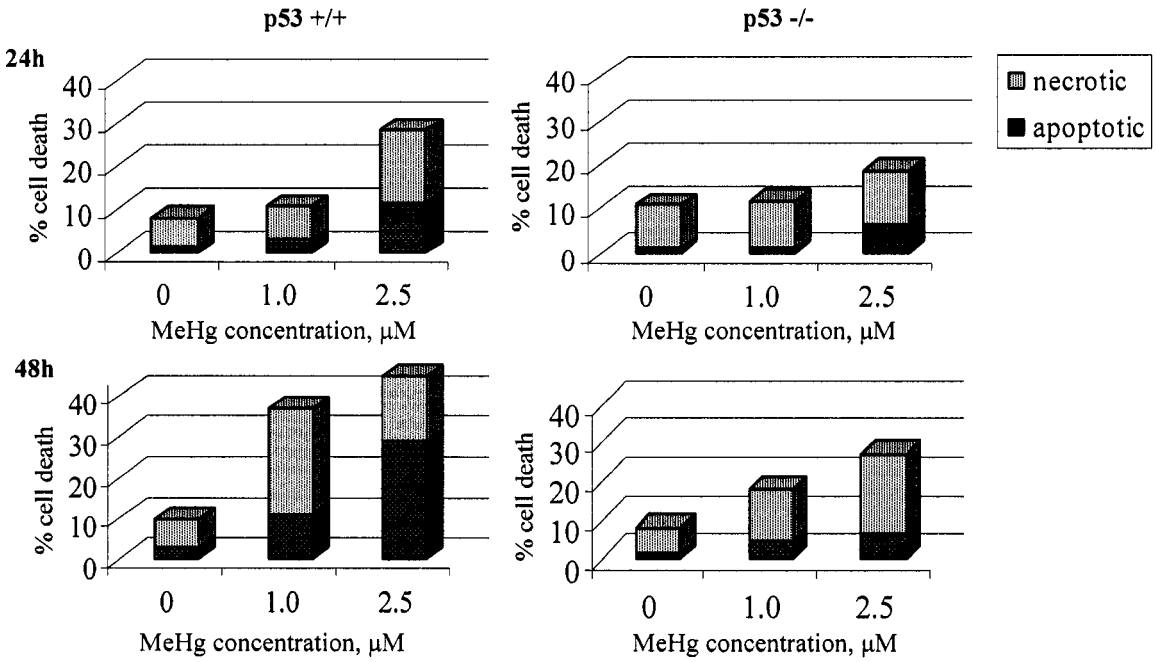

Figure 2.6. Following MeHg treatment, p53-/- cells undergo less apoptosis than the p53+/+ cells. Cells were stained with propidium iodide and annexin V-FITC and analyzed by flow cytometry. Cells that stained positive for propidium iodide, regardless of FITC staining, were counted as necrotic. Apoptosis does not appear to play a major role in the cytotoxicity of MeHg at lower concentrations in either p53+/+ or p53-/- cells. Histograms represent the average of several experiments ($n \geq 3$).

CHAPTER 3. A MATHEMATICAL MODEL CONNECTING MOLECULAR SIGNALING WITH CELL CYCLE DYNAMICS IN P53+/+ AND P53-/- MOUSE EMBRYONAL FIBROBLASTS

3.1 Introduction

The cell cycle is a tightly regulated process that is described most simply as the time during which the cell divides (mitosis) and the time spent preparing to divide again (interphase). Interphase can be divided up into Gap phase I (G1), DNA synthesis phase (S), and Gap phase II (G2). Sequential progression through these phases is fundamentally driven by fluctuating levels of cyclins which partner with specific cyclin-dependent kinases (CDKs) to phosphorylate proteins necessary for phase transition. Movement from G1 phase into S phase is regulated by the activities of D-type cyclins and Cdk4/6 and E-type cyclins and Cdk2, while G2 to M transition requires activation of the A-type cyclins and Cdk2 and cyclin B/Cdk1 complex. Further regulation is achieved through the selective synthesis and degradation, activation and deactivation of cyclin-dependent kinase inihibitors (CKIs), tumor suppressors, protooncogenes, and components of other signaling pathways (for review see Stewart, 2001). These regulators provide a molecular surveillance program to ensure integrity of the genome and optimal conditions at each phase transition before the cell cycle can proceed.

The p53 protein is arguably the most influential of the cell cycle regulatory proteins and participates in signaling to slow the cell cycle in the G1/S transition, the G2/M transition, and following improper spindle alignment. Furthermore, p53 can trigger the apoptotic program. The abundance of p53 is regulated at the level of gene transcription, mRNA translation, phosphorylation, ubiquitination by Mdm2, and acetylation but its principle mode of regulation appears to be post-translational in order to ensure timely cellular responsiveness to stress signaling (Alarcon-Vargas, 2002; Yang et al., 2004; Brooks and Gu, 2003; Giaccia and Kastan, 1998; Sionov and Haupt, 1999). Immediate activation of pre-produced protein can be followed by upregulation of gene transcription to further increase activated protein levels. Transcriptional targets

of activated p53 include genes involved in cell cycle arrest, DNA repair, and apoptosis. For example, the p53 protein inhibits mitotic entry through transcriptional repression of *cyclin b1* and *cdk1*, induction of 14-3-3σ to sequester cdc25 in the cytoplasm, and induction of cyclin-dependent kinase inhibitors (CKIs), including $p21^{Cip1}$ that physically inactivate the cyclin B1/Cdk1 complex (Taylor, 2001). Genes transcriptionally activated by p53, including $p21^{Cip1}$ and the growth arrest and DNA damage (Gadd) family, also regulate cell cycle transition at the G_1/S or restriction checkpoint in response to suboptimal growth conditions or DNA damage. Pro-apoptotic gene targets include Bcl-2 family members *Noxa* and *PUMA*. An area of intense investigation, it has been postulated that the level of activated p53 protein controls balance between cell cycle inhibition and initiation of the apoptotic program. A complimentary suggestion is that the presence of co-activators is required for full induction of the apoptotic program (Yu and Zhang, 2005).

While p53 is an influential protein, other redundant signaling pathways are able to maintain cell cycle responsiveness and cell death. In the absence of p53, cells can still undergo arrest and apoptosis via p53-independent pathways involving proteins such as p21, ATM (ataxia-telangiectasia mutated) and ATR (ATM and Rad-3 related) and phosphorylation of Chk1/Chk2 (Pearce, 2001), p19ARF (Rowland, 2002; Tsuji, 2002) and ERK (extracellular regulated kinase) (Tang, 2002), and inhibition of PARP (poly(ADP-ribose) polymerase) (Saldeen, 2003). Although p53 deficient mice are developmentally normal with a strain and sex dependent low penetrance of neural tube defects, their lifespan is greatly reduced due to increased tumor incidence (Donehower et al., 1992). Experimentally, p53 null mice or cultures of p53 null cells are extensively used to explore cancer susceptibility, initiation, and progression (Kemp, 2005; Phillip-Stahelli et al., 2004), toxicant mechanism of action, DNA repair pathways, cell cycle control, and apoptosis. Usually, however, each of the pathways in which p53 participates is studied in isolation because of the previously described biological complexity. This chapter describes our attempt to mathematically quantify, partition, and integrate p53 signaling in order to understand and predict the relative importance of

its role in cell cycle phase transition from G1 to S, G2 to M, and cell death under normal conditions through the use of MEFs wildtype and null for p53.

Conceptualization of the cell cycle into discrete phases separated by transition checkpoints allows for mathematical descriptions of the temporal progression through the cell cycle. Furthermore, the known molecular signaling pathways governing phase transitions can be modeled as rates. Building on a model from Basse et al. (2003), we describe the movement of cells from one phase to the next, track subsequent generations of cells, and specifically focus on the role of p53 through the use of p53 wildtype (+/+) and p53 null (-/-) cells. The purpose of this work was to adapt an existing model in order to 1) predict the cycling properties of embryonic cells and 2) to discriminate the specific role of p53 in each of the places it acts in the cell cycle and its role in apoptotic cell death under normal conditions. Our model is distinct from the Besse et al. work as we distinguish generations of cells through several divisions, specify death rates by mechanism, omit their DNA content and dispersion terms, and model an embryonic cell system. Furthermore, we explore the specific role of p53, a key protein involved in cell cycle regulation and stress response. The chapter is organized as follows. First, we present the ordinary differential equations that describe the cell cycle and distinguish our specific adaptations to the Basse et al. (2003) model. Next, we summarize the experimental data and parameters upon which our model for p53+/+ and p53-/- cells under normal conditions is based. We then experimentally validate the model's predictions of cell cycle phase distribution and cell death for both genotypes. The final section summarizes our results and conclusions.

3.2 Model development

Differential equations

Progression through the cell cycle is influenced by environmental conditions and stressors: these have been demonstrated to produce cell cycle phase specific inhibition carried out by signaling from cell cycle regulatory proteins. We first sought to develop a simple mathematical model that reflects phase specific cell cycle control

checkpoints and predicts cell cycle phase distribution and death of cells by generation. The dependent variables are thus ${}^{i}G1\ (x,\ t)$, ${}^{i}S\ (x\ ,t)$, ${}^{i}G2\ (x,\ t)$, and ${}^{i}M\ (x,\ t)$ where i indicates generation number and x reflects the number of cells at any given time, t. Figure 3.1 presents our model schematic and demonstrates how exit from M phase leads to the generation of two new cells in G1 phase of the subsequent generation. Working from Besse et al. (2003), we utilized the following ordinary differential equations:

Generation 0

$$\frac{d^{o}G_{1}}{dt} = -({}^{o}k_{1}+{}^{o}\mu_{G_{1}})^{o}G_{1}(t) \tag{1}$$

$$\begin{aligned}\frac{d^{o}S}{dt} &= -{}^{o}\mu_{s}\,{}^{o}S(t)+{}^{o}k_{1}\,{}^{o}G_{1}(t) - I(t;{}^{o}T_{s}) \\ &= -{}^{o}\mu_{s}\,{}^{o}S(t)+{}^{o}k_{1}\,{}^{o}G_{1}(t)-{}^{o}k_{1}\,{}^{o}G_{1}(t-{}^{o}T_{s})e^{-{}^{o}\mu_{s}\,{}^{o}T_{s}}\end{aligned} \tag{2}$$

where ${}^{o}G_{1}(t-{}^{o}T_{s}) = 0$ if $t-{}^{o}T_{s} \le 0$

$$\begin{aligned}\frac{d^{o}G_{2}(t)}{dt} &= I(t;{}^{o}T_{s}) -({}^{o}K_{2}+{}^{o}\mu_{G_{2}})^{o}G_{2}(t) \\ &= {}^{o}k_{1}\,{}^{o}G_{1}(t-T_{s})e^{-{}^{o}\mu_{s}\,{}^{o}T_{s}} -({}^{o}k_{2}+{}^{o}\mu_{G_{2}})^{o}G_{2}(t)\end{aligned} \tag{3}$$

$$\frac{d^{o}M(t)}{dt} = {}^{o}k_{2}\,{}^{o}G_{2}(t)-{}^{o}b\,{}^{o}M(t)-{}^{o}\mu_{\mu}\,{}^{o}M(t) \tag{4}$$

Generation 1

$$\frac{d^{1}G_{1}(t)}{dt} = 2\,{}^{o}b\,{}^{o}M(t) -({}^{1}k_{1}+{}^{1}\mu_{G_{1}})^{1}G_{1}(t) \tag{5}$$

Equation 1 describes the decrease in number of cells in G1 phase of the original population of exponentially growing cells, ^{o}G1. Cells leave ^{o}G1 at a rate equivalent to the probability of transition to S phase, ${}^{o}k_{1}$, plus the rate at which they die, ${}^{o}\mu_{G1}$. Each μ term in equations 1-5 is composed of the rate of necrotic cell death, μ_{n}, plus the rate of

apoptotic cell death, μ_a. Equation 2 describes the loss of cells from S phase due to death, ${}^{o}\mu_{s}{}^{o}S(t)$, plus the appearance of the original population of S phase cells, ^{o}S. In contrast to the Gap phases, S phase in the cell cycle involves the physical process of DNA replication which requires a certain amount of time to be completed. As no cell transits S phase without DNA replication, we introduced an S phase lag time term in order simulate this process. Cells in G2 phase are described by equation (3) with a term expressing cells entering from S phase minus cells leaving at a rate $^{o}k_2$ plus cell death, $^{o}\mu_{G2}$. The first term in equation (4) accounts for the appearance of cells from G2 phase via transition probability, $^{o}k_2$ times the number of cells in ^{o}G2 at a given time, t, while the second term describes cells exiting the ^{o}M compartment, either via the cellular division rate ^{o}b, or death, $^{o}\mu$. Equation (5) demonstrates how each cell leaving ^{o}M phase generates two daughter cells in the next generation of G1 phase, ^{1}G1.

Model parameters

Table 3.1 indicates the model parameters as calculated from previously published literature values characterizing cell cycle kinetics of p53+/+ and p53-/- mouse embryonal fibroblasts from the same transgenic strain and cross as our experiments (C57BL/6 x 129/Sv, then outcrossed to C57BL/6 for 6 generations) (Harvey et al., 1993; Mendoza et al., 1999 (thesis)). Mouse embryonal fibroblasts (MEFs), isolated gd14 and treated at early passages (p4-7) after they have stabilized in culture, are a convenient system for evaluating cell cycle kinetics via flow cytometry. These cells are easily collected, are usually robust in culture and allow for the investigation of specific pathways in proliferation and cell cycle dynamics in embryonic cells but in tissue culture conditions that are not promoting differentiation.

In an asynchronous population of cells, the percentage of cells in each phase of the cell cycle is proportionate to the time spent in that phase of the cell cycle. Percentage cells in each phase of the cell cycle can be experimentally determined by staining for DNA content and analyzing by flow cytometry. Because DNA synthesis is completed in S phase, cells in G2 phase and M phase have the same 4N DNA content

and are not easily distinguished. The following equations by Steel describe time spent in G1, S, and G2/M phase as can be calculated from flow cytometric cell cycle phase distribution data and doubling time of a cell population.

$$T_c \approx T_d \tag{6}$$

$$T_s = T_c \frac{\log\left(\frac{\%S + \%G_2M}{100} + 1\right)}{\log 2} - T_{G_2M} \tag{7}$$

$$T_{G_2M} = T_c \frac{\log\left(\frac{\%G_2M}{100} + 1\right)}{\log 2} \tag{8}$$

$$T_{G_1} = T_c - T_{G_2M} - T_s \tag{9}$$

Time spent in one cell cycle, T_c, is assumed to be approximately equal to the doubling time for a cell population, T_d (Equation 6). From knowing the percentage of cells in each phase of a cell population and the doubling time, we can sequentially calculate time in G2M phase (Equation 8), time in S phase (Equation 7), and finally, time in G1 phase (Equation 9).

Rates for cell cycle phase transition probability were calculated from Takahashi's methods demonstrating the relationship between time spent in each cell cycle phase and phase transition probability, k_1 and k_2, and cell division rate, b (1968). Equation 11 was not utilized for this exercise but is provided for completeness: rate g is the average rate at which DNA content in a cell increases. For our parameter setting, we used a constant rate of cell death for all phases of the cell cycle. As no information regarding background rates of cell death was available in the literature, we used our own data from experiments using FITC-labeled AnnexinV antibody and propidium

iodide staining for flow cytometric analysis. This method allows quantification of apoptotic and necrotic cells at various timepoints; calculated rates are listed in Table 3.1. P53+/+ MEFs experience a higher background rate of both necrosis and apoptosis under normal conditions. Cell death in the p53-/- was considered exclusively necrotic.

$$T_{G1} = \frac{1}{k_1 + \mu_{G1}} \tag{10}$$

$$T_S = \frac{1}{g + \mu_s} \tag{11}$$

$$T_{G2} = \frac{1}{k_2 + \mu_{G2}} \tag{12}$$

$$T_M = \frac{1}{b + \mu_M} \tag{13}$$

3.3 Model predictions and experimental validation

Generation 0 at the beginning of the simulation represents a synchronized cell population following 24h of serum starvation. Figure 3.2 shows model predicted cell cycle phase distributions for p53+/+ and p53-/- cells at 24 and 48h. P53+/+ cells differ from p53-/- cells in several respects and are accurately predicted by the model. Literature values suggest doubling time is approximately 18h in the p53-/- as compared to 36h in the p53+/+ and is evidenced in the model output by earlier appearance of the first and second generation of cells in the p53-/-, ^1X and ^2X, as compared to the p53+/+ cells. G2 and M phase populations have been combined for this output in anticipation of comparing the model prediction with experimental data generated via flow cytometry where populations are defined via DNA staining and G2 and M phases are indistinguishable.

Figure 3.3 gives mathematically predicted distributions of cells in each cell cycle phase and generation compared to our experimental data at 24h and 48h. Observed data were collected following continuous exposure of cells to BrdU, a

thymidine analog useful for tracking cells through progressive divisions, counterstained with propidium iodide, and analyzed via flow cytometry. For both genotypes, the model predicts well the loss of the original population of cells ^{0}X. In p53+/+ cells, the model consistently over and under-predicts G0/G1 phase and G2/M phase, respectively for ^{1}X. For example, while we observed 6.7% of the ^{1}X cell population in G0/G1 and 15.8% in G2/M at 24h, the model predicted 31% and 0.1% for each phase respectively. In the p53-/- cells, the model predicts slightly faster transit through the cell cycle phases and subsequent generations than we observed such that at our 48h timepoint, the expected cell cycle phase distribution for the ^{2}X generation was 14.3% (G0/G1), 27.4% (S), and 46.3% (G2/M). In contrast, we observed 55.1% in G0/G1 phase, 15.4% in S phase, and no cells reaching G2/M. Despite these differences, the model appears to function well and predict a realistic distribution of cell cycle phase for both the p53+/+ and p53-/- MEFs.

3.4 Discussion and future directions for model

Differences in predicted versus observed populations are likely due to several issues: data for rate calculation was taken from the literature; using our cell cycle distributions would likely yield slightly different and more accurate rates. Additionally, the model assumes no constraints on growth; however, the p53-/- cells approach very confluent conditions into their third cycle. Although these cells can grow at high densities, we have observed a reduction in proliferation under conditions achieved between 48 and 72h of culture. This is a likely explanation for the large differences in ^{2}X generation at 48h in the p53-/- cells. Additionally, the model anticipates a homogenous population of G0/G1 phase cells at the beginning of the simulation. Experimentally, following 24h of culture in serum free conditions, we observed imperfect synchronization: approximately 10-20% of p53+/+ cells and 25-35% of the p53-/- cells were in G2/M following serum starvation (unpublished observations). These deviations could significantly affect comparisons of cell cycle phase distribution and would be experimentally observed as a reduction in cell cycle progression as

compared to the scenario modeled. Our next steps to optimize goodness of fit for the model are to incorporate rates from our experimental observations and to incorporate a multiplier to account for the biological implications of confluency in the cells.

Having established a mathematical model that predicts cell cycle phase distribution in a convenient experimental system, we anticipate future examinations of toxicant impact on cell cycle inhibition and cell death can be quantified via specific mechanism. For example, we and others have determined that while MeHg induces a G2/M phase specific accumulation of cells, arsenic treatment results in G0/G1 accumulation. As these effects are concentration specific and intimately related to induction of cell death, we anticipate our model can be utilized to test hypotheses about mechanisms of toxicants across dose response relationships. Through the experimental use of p53 null fibroblasts, it may be possible to partition the myriad of p53 signaling responses into the rate parameters in our model. This should promote a more quantitative understanding of the relationship between p53, apoptosis, and cell cycle kinetics.

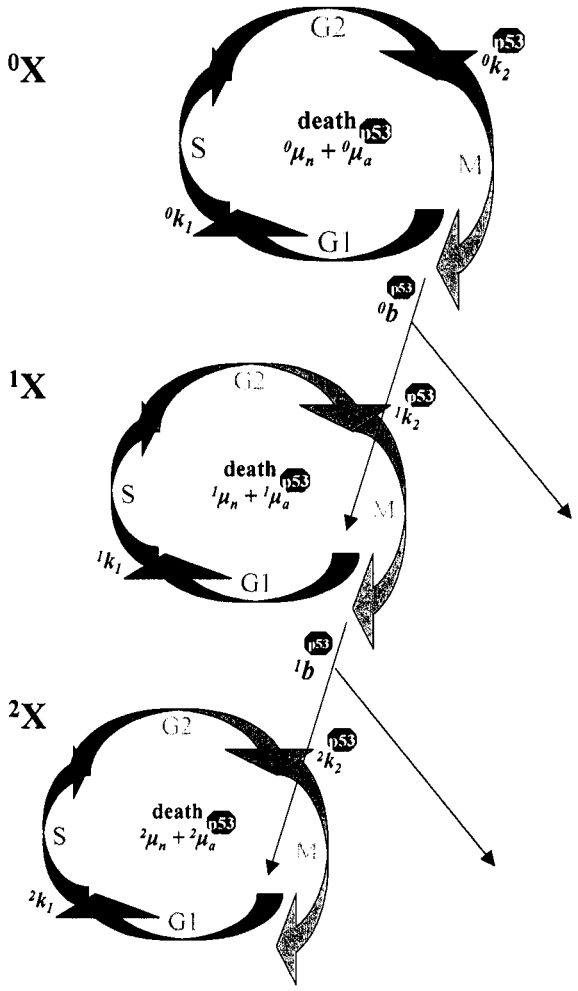

Figure 3.1. Model schematic. Mathematical model developed from Basse et al., 2003, "A mathematical model for analysis of the cell cycle in cell lines derived from human tumors," J. Math. Biol. 47:295-312. We have adapted the model to estimate and predict the role of p53 and impacts of toxicants on cell cycle phase distribution and cell death. Cells 'X' travel sequentially through each phase of the cell cycle. First order transition rates 'k_1' and 'k_2' reflect molecular checkpoints at the G1 to S and G2 to M phase boundaries, respectively. These checkpoints ensure optimal conditions and faithful DNA replication before allowing cell cycle progression. Following mitosis, two identical daughter cells are generated at rate 'b' divisions per unit time. Cells die at rates partitioned into to necrosis 'μ_n' and apoptosis 'μ_a.' As indicated in the figure, p53 signaling can critically impact several steps in the process.

Table 3.1. Parameters for model. Time spent in each phase of the cell cycle was first calculated from doubling time and percentage of cells in each cell cycle phase in asynchronous populations using formulas from Steel (1977). Previously published data from p53 wildtype and nullizygous MEFs from the same transgenic strain was utilized (Mendoza et al., 1999 and Harvey et al., 1993). Rates k_1, k_2, and b were calculated from time spent in each phase and the death rate as derived by Takahashi (1968).

Parameter	Description	p53+/+ value	p53-/- value
^iX	cell number		
t	time		
^it_s	time in S phase	10.7h	6.4h
$^ik_1$	transition rate from G_1 to S	0.06	.26
$^ik_2$	transition rate from G_2 to M	0.114	0.15
^ib	division rate	0.993	0.998
$^i\mu_n$	necrosis rate	0.0035	0.002
$^i\mu_a$	apoptosis rate	0.0035	0.0

i = generation number

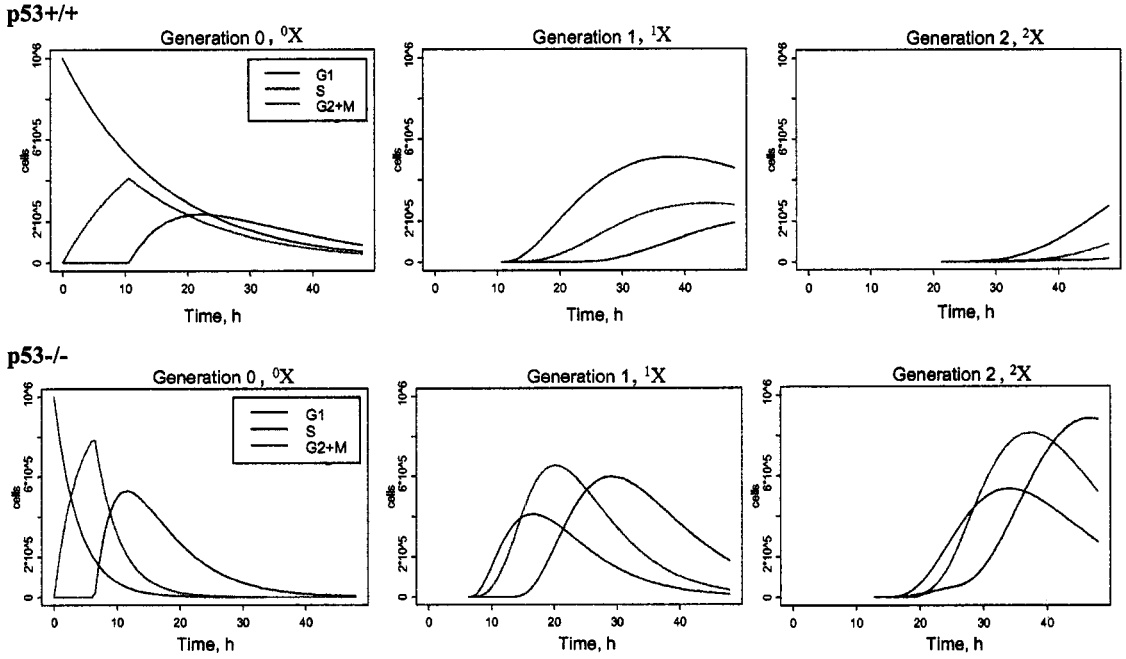

Figure 3.2. Model simulation of the percentage of cells in each cell cycle phase for three generations of cells. Generation 0 at time=0 represents a synchronized cell population following 24h of serum starvation. Cells from p53+/+ cells differ from p53-/- cells in several respects and are accurately predicted by the model. Doubling time is approximately 18h in the p53-/- as compared to 36h in the p53+/+ and is evidenced in the model output by earlier appearance of the first and second generation of cells in the p53-/-, ^1X and ^2X, as compared to the p53+/+ cells. G2 and M phase populations have been combined for this output in anticipation of comparing the model prediction with experimental data generated via flow cytometry where populations are defined via DNA staining and G2 and M phases are indistinguishable.

Genotype	Generation	Cell Cycle Phase	24h Predicted	24h Observed	48h Predicted	48h Observed
p53+/+	^{0}X	$\%G_0/G_1$	21.3	30.5	3.5	0.6
		%S	17.0	11.0	2.8	5.7
		$\%G_2/M$	21.7	46.4	5.8	10.1
	^{1}X	$\%G_0/G_1$	31.0	6.7	31.1	10.4
		%S	8.9	5.4	18.9	7.0
		$\%G_2/M$	0.1	15.8	13.0	48.8
	^{2}X	$\%G_0/G_1$	*	*	18.3	17.4
		%S	*	*	5.8	*
		$\%G_2/M$	*	*	0.8	*
p53-/-	^{0}X	$\%G_0/G_1$	0.1	5.2	*	*
		%S	0.4	4.5	*	*
		$\%G_2/M$	8.5	4.0	0.3	2.6
	^{1}X	$\%G_0/G_1$	14.3	47.0	0.6	3.2
		%S	30.1	10.7	1.7	3.2
		$\%G_2/M$	25.4	26.6	9.4	20.0
	^{2}X	$\%G_0/G_1$	12.5	2.2	14.3	55.1
		%S	6.5	*	27.4	15.4
		$\%G_2/M$	2.3	*	46.3	*

Figure 3.3. Comparison of predicted and observed cell cycle phase distribution. Model simulation was run under normal conditions and compared to experimental data. Observed data was collected following continuous exposure of cells to BrdU, a thymidine analog useful for tracking cells through progressive divisions, counterstained with propidium iodide, and analyzed via flow cytometry. Observed values are the average of at least three experiments. If no cells were predicted or observed, the particular cell cycle phase and timepoint is marked with an asterisk (*).

CHAPTER 4. DYNAMIC CHARACTERIZATION OF AN EMBRYONIC MESENCEPHALON NEURAL PRECURSOR CELL CULTURE SYSTEM

4.1 Introduction

Multipotent neural precursor cells (NPCs), capable of becoming neurons, astrocytes, and oligodendrocytes, are of great interest for their potential to treat neurodegenerative disorders and for understanding the mechanisms that regulate neuronal proliferation and differentiation in the central nervous system. The intensive study of these cell types is advantageous to the field of neurodevelopmental toxicology as disruption of these basic neurodevelopmental processes is the proposed mechanism of action for many toxicants. Alteration of proliferation is implicated in several neurodevelopmental disorders including spina bifida, exencephaly, anencephaly, and craniofacial defects such as cleft palate (Wlodarczyk et al., 1996; Sulik and Sadler, 1993; Rodier et al., 1979; Rodier et al., 1997). Furthermore, many environmental exposures that adversely affect neurodevelopment have been demonstrated to inhibit proliferation including metals (methylmercury, cadmium, and arsenic), valproic acid, rubella, heat stress, fungicides, and ionizing radiation (Gribble et al., 2005; Yu et al., 2005; Finnell et al., 2000; Wlodarczyk et al., 1996; Walsh and Morris, 1989; Rodier et al. 1984, Ponce et al, 1994). Because inhibition of proliferation can be a general, protective mechanism that gives the cell time to repair or wait for external conditions to improve, it is likely to be especially important for low-dose environmental exposures that do not cause outright cell death. While difficult to observe, more subtle structural or functional effects from developmental toxicants affecting neuronal proliferation are quite plausible.

Although mechanisms of neuronal differentiation and neurodevelopmental toxicants are often studied in established cell lines such as rat adrenal pheochromocytoma PC-12 or mouse embryonal carcinoma P-19 cells, primary culture systems are presumed to retain proliferative characteristics that more closely resemble those in the developing organism (Das et al., 2004). NPCs are defined by their ability

to form cellular aggregates in culture, to self-renew, and to potentially generate all neural cell lineages (Ostenfeld et al., 1999; Ostenfeld et al., 2002). The relative ease of manipulation and observation in vitro has fueled the establishment of numerous primary systems of NPCs that vary widely in isolation time and region (Storch, 2004). These culture systems range in utility for examining the development of specific neuroanatomical structures or cell types (ie. eye, oligodendrocytes), factors influencing self-renewal capacity, multipotency, and plasticity (ie. embryonic stem cells induced to a neural fate), mechanisms of acquiring specific neuronal phenotypes, and effects of toxicants on proliferation, cell cycle exit, and differentiation. NPCs originate from the epithelial or germinal layer of the neural tube and are thus most concentrated in numbers and region in the days following neural tube closure (ED10-14 in mice; ED11-15 in rat) (Temple, 2001). While neural progenitor cells are generally believed to become more restricted in developmental potential with developmental time, isolation protocols range from ED10 to PD3 depending on the specific region (Jori et al., 2003; Cai et al., 2004; Kintner, 2002). Table 4.1 lists several proteins that are commonly employed as markers of neuronal differentiation; these are shown in increasing neuronal maturation. For instance, nestin is predominantly expressed in immature progenitor cells and can be used to identify relatively immature, pluripotent cycling precursor cells (Park et al., 2004). Furthermore, NPCs grown in culture do appear to retain features of in vivo regionalization reflecting dorsal-ventral and anterior-posterior patterning that occurs much prior to isolation, simultaneously with neural induction (Storch et al., 2004). For example, Smith et al. (2003) observed different patterns of proliferation and differentiation in NPC neurosphere cultures derived from mouse and rat ED13-15 striatum, ventral mesencephalon, and cortex that were more dependent on species and tissue origin than culture conditions. Finally, while mouse and human embryonic stem cells have been manipulated into a dopaminergic phenotype (Lee et al., 2000; Chung et al., 2002; Yan et al., 2005), only progenitor cells isolated from the midbrain have been observed to develop into functional dopaminergic neurons (Storch et al., 2003). Recently, there has been an increased interest in mesencephalic NPCs as

they may be valuable in the understanding and treatment of Parkinson's disease (Vitalis et al., 2005).

The rat micromass culture system has been used extensively by our group and others to examine the effects of toxicants on proliferation and differentiation of neural precursor cells isolated from the embryonic midbrain on ED12 and plated in high density islands (Sidhu et al., 2005; Flint, 1983; Whittaker and Faustman, 1991; Whittaker and Faustman, 1992; Whittaker et al., 1993; Ribeiro and Faustman, 1990). Originally proposed as a screen for neurotoxicants, the rat micromass system has been used to evaluate the effects of chemicals on cell viability, [3H] γ-aminobutyric acid (GABA) uptake, and hematoxylin-stained neurites (Flint OP, 1984; Flint and Orton, 1984; Walum and Flint, 1990). Whittaker et al. characterized neuronal cells in these cultures that specifically stained for neuronal markers A2B5 (GQ ganglioside), γ-aminobutyric acid (GABA), microtubule-associated protein (MAP2), MAP5, neuron-specific enolase (NSE), neural cell adhesion molecule (N-CAM), and tau after 5 days in culture (1993). The cells were non-immunoreactive for glial fibrillary acidic protein (GFAP) (Whittaker et al., 1993). This system has also been successfully utilized to characterize changes in cell cycling in response to exogenous factors such as alkylating agents, albendazole, arsenic, methylmercury, chlorpyrifos, and serotonin (Menegola et al., 2004; Whittaker and Faustman, 1991; Seeley and Faustman, 1995; Ponce et al., 1994; Sidhu et al., 2005; Ribeiro and Faustman, 1990; Cosenza and Bidanset, 1995). Here, we establish a comparable mouse micromass system in order to access valuable mechanistic developmental information from transgenic mice and to allow for cross-species comparisons of neurodevelopmental toxicant impact. We compare the cycling and differentiating characteristics of midbrain cells from C57BL/6 mice and examine the temporal association of cell cycle regulatory proteins that may play an important role in the differentiation of these cells. Across 9 days in culture, we carefully characterize the culture kinetics of cell cycling and exit, neuronal differentiation and appearance of specific phenotypes in order to provide a battery of endpoints that can be examined for toxicant impact. This new culture system should expand possibilities for

studying molecular regulation of normal neuronal proliferation and differentiation and for identifying mechanisms of toxicant insult.

4.2 Methods

Cell culture. Micromass cultures were prepared according to the procedure by Flint (1983) with some modifications. Gravid uteri were removed from pregnant (11-day post-coitum) C57BL/6 mice. Embryonic midbrains were dissected and single cell suspensions were prepared in culture medium (Ham's F12 supplemented with 10% FBS, penicillin (50 U/mL), streptomycin (5 μg/mL) and L-glutamine (5.8 mg/mL) (Gibco, Grand Island NY) and adjusted to a concentration of 5 x 10^6 cells/mL. Five 10 μL aliquots were plated per 35mm culture dish (Falcon Primaria, Becton-Dickinson Labware, Lincoln Park, NJ) and the plates were incubated at 37° C in a 5% CO_2/95% air atmosphere with 100% relative humidity for 2.5 hours to allow for cell attachment before culture medium was added.

Assessment of viability. Cell viability was determined by the neutral red dye uptake assay. At appropriate timepoints, the medium was aspirated, cells were rinsed once with CMF-PBS and 2 mL of freshly prepared 0.05% (w/v) neutral red culture medium was added to each well for 3 hours in the incubator. The dishes were then rinsed once with CMF-PBS and the dye eluted with 2 mL 0.5% (v/v) acetic acid in ethanol for 1 hour. 200 μL of supernatent was transferred in triplicate to a 96 well plate and the optical density was read at 540 nm using a microplate reader (Molecular Devices Corp., Palo Alto, CA).

Assessment of proliferation via flow cytometry. BrdU-Hoechst analysis was performed as previously described (Rabinovitch et al., 1988). Cells were cultured with 60 μM bromo-deoxy-uridine (BrdU), a concentration determined to not affect viability, proliferation, or differentiation but allow identification of cells having undergone multiple cell cycles. At the appropriate time, cells were harvested by trypsinization and placed in Hoechst buffer (1.2 μg/ml Hoechst 33258 (Molecular Probes, Eugene OR), 0.146 M NaCl, 0.1 M TRIS Base, 0.5 mM $MgCl_2$, 0.2% BSA, 0.1% NP-40 (Sigma, St.

Louis, MO) in dd H_20)) with 10% NP40 (Sigma) and 10% DMSO and frozen at -20 °C until analysis. At time of analysis, cells were thawed on ice and 10 μg/mL propidium iodide was added. Flow cytometry was performed on a Coulter Elite flow cytometer.

Protein isolation. Cells were washed twice with 1 mL ice-cold CMF-PBS followed by the addition of 50 μL of cell lysis buffer containing additional phosphatase and protease inhibitor cocktails (Calbiochem). Cells were harvested by scraping in cell lysis buffer and then placed on ice. After storage at –80 °C, all extracts were homogenized by sonication and then centrifuged (16,000 x g, 10 min, 4 °C) to remove insoluble material. The resulting supernatant (cell extract) was gently removed, and total protein was determined using the BCA kit according to manufacturer's instructions (Pierce, IL).

Western Blotting. Equal quantities (10 μg) of protein were analyzed by SDS-Polyacrylamide gel electrophoresis. Briefly, proteins were separated on Criterion^{TM} 10-20% Tris-HCl precast gels (Bio-Rad) according to the manufacturer's protocol. Proteins were subsequently transferred onto PVDF nylon membranes (Bio-Rad) for immunoblot analyses. The membranes were probed (manufacturer's blotting instructions) with the following antibodies and concentrations: GAP-43, 1:2000; PCNA, 1:2500; ki-67, 1:500; p21, 1:200; p27 1:200; p53, 1:200. Secondary antibodies were used at a 1:5000 dilution as follows: goat anti-rabbit horseradish peroxidase (HRP) conjugated, anti-mouse-HRP, donkey anti-goat HRP. The ECL chemiluminescence system (Amersham Biosciences, Buckinghamshire, UK) was used to visualize specific immunoreactive proteins on Hyperfilm (Amersham Biosciences). The film was then analyzed using HP Scanjet 5400C scanner equipped with Precisionscan Pro 3.1 software and the bands of interest were selected and band density and area measured using ImageJ 1.30v software (NIH, USA).

Immunocytochemistry. Following culture for specific lengths of time, midbrain NPCs were washed twice with with ice-cold CMF-PBS and fixed with 4% paraformaldehyde for 20 minutes at room temperature. Following two more washes, cells were permeabilized and blocked with 1% BSA and 0.3% Triton X-100 in CMF-PBS. Cells

were then incubated with the appropriate primary antibody diluted in CMF-PBS with 1% BSA overnight at 4°C. Cells were washed three times and incubated with secondary antibody for 2 hours at room temperature. Following three final washes, cells were counterstained with Hoechst 33342 (2 μg/mL) for 20 minutes in the dark to determine nuclear staining. Assessment of staining was performed on a fluorescent laser microscope/image analysis system. At least 3 fields (containing approximately 500 neurons each) per island, 3-5 islands per dish, and 2 dishes per timepoint were counted in a blinded fashion. Results are reported as the mean ± SEM (n=3) and are representative of at least two independent experiments.

GABA uptake. At appropriate times in culture, 3H-labeled gamma-amino butyric acid ([3H]GABA) was added to culture media at a final concentration of 2 μCi/culture dish for 1h. Culture dishes were washed 3 times for 10 minutes each with Earle's Balanced Salt Solution (EBSS) (Gibco Life Technologies, Inc., Grand Island, NY) until radioactivity in the washes was less than 100 cpm. Cells were scraped in CMF-PBS and transferred to glass, screw-top vials with 500 μL hyamine hydroxide overnight. The next day, 500 μL cell digest, 40 μL glacial acetic acid, and 5 mL scintillation cocktail were read on a Beckman scintillation counter. To account for differences in growth across time in culture, GABA uptake was standardized to total protein content.

Acetylcholinesterase activity. Activity was measured according to Ellman et al. (1961) with slight modifications as described by Cole et al., 2005. Cells were washed in ice-cold CMF-PBS and then scraped in phosphate buffer with 1% triton X-100, pH 8.0, into microcentrifuge tubes and frozen at -80°C until analysis. At time of assay, 1 mL of 10 mM DTNB was mixed with 30 mL 100mM sodium phosphate buffer, pH 8.0 and placed in a 30 °C water bath. Cell lysates were thawed, sonicated, centrifuged at 13,000 x g, and the supernatant transferred to new tubes. Aliquots were removed for quantification of protein content and then 10 μL were added in triplicate to wells of a microtiter plate containing 180 μL of the buffered DTNB solution. Plates were incubated for 10 minutes then the kinetic assay was initialized by the addition of 10 μL of 20 mM acetylthiocholine iodide. Absorbance was measured at 412 nm continuously

for 10 minutes to measure the formation of 5-thio-2-nitrobenzoate. Rates of product formed during the assay were calculated by standardizing the microgram protein and expressed as U/μg of protein where U = μmol of acetylthiocholine hydrolyzed per minute.

Statistical Analysis. Intercooled Stata 7.0 for Windows (StataCorp, College Station, TX) was used to perform all statistical tests. Analysis of variance (ANOVA) and oneway ANOVA using Bonferroni's test for multiple comparisons were used to determine changes across time. A p value ≤ 0.05 was considered statistically significant.

4.3 Results

Method development

As one of our aims was to develop a correlate system to an existing rat midbrain culture, we first determined an equivalent embryonic stage for neurodevelopment in the mouse. Gestational day 12 in the rat, two days past closure of the neural tube and a time of rapid neurogenesis in the ventral epithelium, most closely corresponds to neural developmental landmarks happening on gestational day 11 in the mouse. For our first experiments, we performed simultaneous rat isolations and cultures as a control. Using the existing rat protocol, the mouse cells exhibited poor attachment to culture plates and relatively lower proliferation (data not shown). We thus explored optimizing several culture parameters in order to achieve equivalent proliferation and differentiation of the mouse NPCs. Optimization of media composition, plate coating, isolation on gestational day 10.5, and trypsinization conditions were analyzed. Ultimately, coating plates with poly-d-lysine was sufficient to promote the desired characteristics. Cell morphology using this optimized mouse protocol is shown in Figure 4.1.

Proliferation

To quantify proliferation in these cultures, we measured both cell counts and cell cycling rates over nine days in culture. As indicated in Figure 4.2, cell number for

both rat and mouse NPCs increases over seven days in culture and then plateaus. The mouse cells undergo approximately three divisions between D1 and D7 with an increase from 200,000 cells to nearly 2 million. In comparison to the rat, mouse cells appear to undergo less proliferation at early days in culture, ultimately leading to approximately 1 million fewer cells. As tested by ANOVA, proliferation patterns over time are different between mouse and rat ($p = 0.00$), although final cell number on day 9 in culture between species is only moderately significantly different using Bonferroni's test of multiple comparisons ($p = 0.06$).

We also examined cell proliferation by culturing the cells for 24 hour periods with bromo-deoxyuridine (BrdU), a thymidine analog incorporated into the DNA of cycling cells during S-phase, staining with Hoechst and propidium iodide, and analyzing cells by flow cytometry. As Hoechst fluorescence is quenched in the presence of BrdU, successive generations of cycling cells can be distinguished from non-cycling cells by their lower Hoechst fluorescence. Counter-staining with propidium iodide allows for the determination of cell cycle phase as well. Figure 4.3 quantifies the proportion of cells that have or have not incorporated BrdU during a 24h period across days in culture. On day 1, cultures contain 29.4% ± 12.3% of non-cycling cells; this percentage gradually and significantly increases to 56.9% ± 9.5% on day 7 ($p = 0.01$). By day 9, 96.1% ± 5.5% of cells have failed to incorporate BrdU ($p = 0.00$). To examine whether these proliferative characteristics could be confirmed through expression of protein markers of proliferation, we probed Western blots with antibodies to PCNA and ki-67, proteins only expressed in S phase of cycling cells. As indicated in Figure 4.4, PCNA expression was detectable at day 1, strongly increased with a peak at days 3 and 4, then declined and disappeared by day 9. Detection of ki-67 protein showed a similar pattern but expression was low at day 1, highest on day 3, and then slowly declined as well.

Differentiation

We next characterized the temporal expression of a battery of markers for neuronal differentiation (Figure 4.5). Nestin, an intermediate filament protein expressed in relatively undifferentiated, stem-cell like cells, was highest on day 1, decreased, and then appeared again at day 9. Interestingly, when we probed extracts from cells cultured for 15 days, nestin expression was twice that of day 1 (data not shown). Gap-43, a structural protein expressed concurrent with neurite outgrowth, was expressed at detectable levels on day 1 and increased to day 9. Finally, NF-L, a protein reported to be expressed in mature neurons, appeared at fairly constant levels across time in culture.

We identified specific types of neurons that were present in our cultures by assaying for GABAergic, cholinergic, and dopaminergic neurons. Figure 4.6 indicates the presence of tyrosine hydroxylase (TH), a critical enzyme in dopamine synthesis, through western blotting and a representative image of immunocytochemical staining. TH staining is visible as early as day 2 in a few isolated neurons (Figure 4.6B). Following time in culture, TH expression patterns changed such that large clusters of cells stained positive for TH. At later days, this was the predominant pattern of expression whereby some fields of view would contain hundreds of tightly packed dopaminergic neurons but some contain none. As the three dimensional nature of the midbrain NPC cultures make accurate quantitation problematic, we probed Western blots of total protein lysates from the cultures with an antibody to TH. Figure 4.6B indicates that TH expression in the cultures actually peaks around day 3 to day 5 and then decreases at days 7 and 9, indicating that this dopaminergic phenotype is lost with time in culture. Figure 4.7 shows neuronal uptake of tritiated GABA ([3H]) standardized to total protein content. GABA uptake was observed on the first day in culture and remained slightly variable but steady until day 5. From day 5 to day 9, [3H]GABA uptake triples from 256.2 ± 60.3 CPM/μg protein (D5) to 664.4 ± 57.3 CPM/μg protein ($p = 0.0$). Figure 4.8 quantifies acetylcholinesterase (AchE) activity in the midbrain NPC cultures. AchE activity was detectable at day 1 (1.07 ± 0.2 U/μg

protein) and increased slightly to D5 (1.2 ± 0.16 U/μg protein). A modest and non-significant increase in activity was measured on day 9 (1.4 ± 0.04 U/μg protein).

Cell cycle regulatory proteins

Following toxicant exposure, upregulation of cell cycle inhibitory proteins is a commonly employed defense mechanism in order to arrest the cell cycle, thus allowing for repair of macromolecular damage to DNA and protein. During neuronal differentiation, these same cell cycle regulatory proteins are employed to facilitate cell cycle exit. In order to determine which cell cycle regulatory proteins might be associated with cell cycle exit in midbrains NPCs, we probed Western blots for cell cycle inhibitory proteins p21, p27, and p53 (Figure 4.9). p27 and p53 protein levels increased with time in culture, parallel to increases in differentiation markers and the exit of cells from the cell cycle. In contrast, p21 protein levels mimicked the pattern of tyrosine hydroxylase expression (Fig 4.6B) and increased to days 3 and 4, then sharply fell, indicating this protein likely plays a different role than p27 and p53 in these cells.

In vivo comparisons

To begin to investigate whether the behavior of midbrain NPCs under our culture conditions resembles the developing midbrain in vivo, we dissected midbrain tissues from embryonic mice on days 11, 16, and PND1; these days approximately correspond to the isolation day in our cultures, D5 in vitro (i.v.), and D9 i.v. Figure 4.10 shows representative Western blots of changes in protein expression for PCNA, Gap-43, p21, p27, and p53 in vivo. The pattern of in vivo expression for all of these proteins was comparable to in vitro expression except that we did not detect any measurable p21 protein in vivo. Figure 11 makes direct comparisons of in vitro and in vivo expression of Western blots quantified by densitometry in an attempt to summarize the dynamic relationship of proliferation (PCNA), general differentiation (Gap-43), and cell cycle regulatory proteins. A slight temporal lag in the transition from proliferation to differentiation was observed in the cultured cells: whereas PCNA

expression was very low by ED16 in vivo, expression was still high on the approximate corresponding date in vitro (D5). Accordingly, Gap-43 expression was low on D5 in vitro, but high on ED16 in vivo. Importantly, the same temporal association of increased p27 and p53 protein concurrent with differentiation and declining proliferation was observed both in vitro and in vivo.

4.4 Discussion

In vitro primary neural precursor cell cultures can be of great utility as a model for understanding normal or perturbed neurodevelopment. Here, we report methods and characterization of a mouse midbrain neural precursor cell (NPC) culture system that closely resembles a previously established and commonly used rat midbrain culture system. Our principle purpose for extending the micromass to the mouse was two-fold: to use transgenic mouse models for in vitro examination of mechanisms of neurodevelopmental toxicants and to make cross species comparisons of toxicant effects as a way to inform risk assessment. Through careful characterization of the dynamic behavior of these cells in culture, we attempted to establish several parameters that could potentially be monitored to reveal mechanisms of neurodevelopmental toxicity.

We first attempted to establish a mouse system comparable to the rat by employing the original rat isolation protocol, modified for an equivalent embryonic day in the mouse. However, under these conditions, mouse midbrain NPCs had initial low attachment and formed clusters of cells that would detach and float off the culture plates after two or three of days in culture. We determined attachment was best facilitated by pre-coating the plates with poly-d-lysine. However, culture morphology still differed slightly between the mouse and the rat: while rat cells proliferated rapidly from day 1, mouse NPCs formed visible clusters and proliferation was slightly lower than the rat. Density dependent proliferation of neuronal precursor cells has been widely described as has the species-dependent tendency of mouse cells to form aggregates, perhaps due to different expression of cell surface adhesion proteins.

Indeed, whether mouse NPCs can be cultivated as attached or floating neurosphere cultures varies by brain region and time of isolation. It has been proposed that fibroblast growth factor (FGF)-dependent NPCs can be grown as either adherent or floating cultures while epidermal growth factor (EGF)-dependent cultures will not attach (Zuccato et al., 2005). After coating the plates, we achieved 80 ± 15% plating efficiency with the mouse NPCs, slightly greater than rat cell plating efficiency (76 ± 12%).

Previous rat micromass investigations into proliferation had reported approximately three cell population doublings over five days in culture (Flint, 1983; Ribeiro and Faustman, 1990). Our results were quite similar: on day 5, we estimated approximately 3.25 cell doublings in the rat NPCs and 2.9 in the mouse NPCs indicating cell cycle length is comparable between mouse and rat between days 1 and 5 in culture. Because we wanted to observe differentiation of the entire culture, we carried our cultures to nine days in the mouse and rat and counted total cell number. Again, mouse and rat NPCs exited the cell cycle similarly, with small increases in cell number between day 5 and day 9 representing a total of 3.1 population doublings in the mouse and 3.4 in the rat. Cell counts in the mouse were confirmed by flow cytometric analysis of BrdU uptake indicating an increase in the non-cycling population from 43.4 ± 5.0% on day 5 to 96.1 ± 5.5% on day 9.

Neuronal differentiation in the rat micromass has previously been determined by hemetoxylin staining of sulfated proteoglycans, acetylcholinesterase cytochemical staining, [3H]GABA uptake, and immunocytochemical staining for a variety of neuronal markers although only the first endpoint was observed across time (day 1, day 2, and day 5) while the rest were only documented on day 5 in culture (Flint, 1983; 1986, Flint et al., 1984; Ribeiro and Faustman; 1990; Whittaker et al., 1993). As indicated by cell count, cell cycle withdrawal as measured by BrdU uptake, and expression of proliferative and differentiation markers, mouse NPCs undergo dynamic changes well past five days in culture. Gap-43, an axonal protein expressed concomitant with neurite outgrowth, was determined to be a good marker for

differentiating neurons in our culture: expression increased steadily from day 1 to day 9. Other investigators have also determined Gap-43 to be a sensitive, responsive marker for perturbations to differentiation (Das et al., 2004). As neuronal differentiation can be thought of as a temporal spectrum with cell cycle exit preceding neurite outgrowth followed by acquisition of functional characteristics and electrical activity, Gap-43 should serve in our cultures as an early marker of differentiation, appearing just after cell cycle exit and maintained in mature, differentiated neurons.

The rat and mouse midbrain NPC culture systems resemble in vivo midbrain neurodevelopment in several aspects. The embryonic midbrain structure isolated on gestational day 11 for our cultures develops into several structures in the adult brain including the substantia nigra, the tectum, and the tegmentum, regions composed of principally GABAergic and dopaminergic neurons; this region sources the largest amount of dopamine to the CNS (Nelson et al., 1996). In the developing embryo, early midbrain patterning is achieved just after neural tube closure on GD 9.5 – 10.5 through spatiotemporally defined gene expression, notably Otx2, Gbx2, fibroblast growth factor 8 (Fgf8), Wnt 1, and sonic hedgehog (Shh) (Prakash and Wurst, 2004). While by no means thoroughly characterized, the generation of dopaminergic neurons has received special attention because of the critical role of dopamine in many physiological processes (ie. mood regulation, sleep, addiction) and disease states (ie. Parkinson's disease, schizophrenia). Studies using tritiated thymidine incorporation indicate the majority of midbrain dopaminergic neurons leave the cell cycle around GD12 to GD14 in the mouse and begin expressing tyrosine hydroxylase shortly thereafter (Altman and Bayer, 1981; Foster, 1988). Similarly, examining ontogeny of TH gene expression in the rat mesencephalon, Solberg et al. (1993) observed fluctuations in gene expression GD13 to GD15 (GD12 to GD14 mouse equivalent) that stabilized in later development (GD18-GD21) as the presumed dopaminergic neurons concluded migration at their final anatomical position. This temporally corresponds to our culture observations of differentiation and TH expression. Ex vivo, immunocytochemical and Western blot examination of our mesencephalic NPCs revealed a similar pattern with a small

percentage of the cell population expressing TH protein at D1 in culture that increased substantially to days 3 through 5. However, by day 7 and day 9, expression declined indicating the dopminergic phenotype is lost in these cultures. This has been observed by other researchers and addition of factors to promote and support dopaminergic neurons in vitro as discussed below is often necessary.

Determining which factors control differentiation into particular neuronal subtypes is an area of intense investigation. In contrast to many studies using exogenous factors to enhance dopaminergic neuron production from stem cells or midbrain NPCs, our culture method refrains from artificial induction of differentiation. Generating enriched cultures of dopaminergic neurons for treatment of neurodegenerative diseases has proven difficult: the most commonly employed cell system for studying mechanisms of Parkinson's, SH-SY5Y cells, contains only 5 – 15% dopaminergic neurons (Hu et al., 2005). More recently, differentiation of dopaminergic neurons has been successfully directed from human and mouse embryonic stem cells by specific treatment with FGF8 and Shh, two transcription factors with important midbrain patterning roles in vivo, (Yan et al., 2005; Bibel et al., 2004) or enhanced in rat ventral mesencephalon cultures through the addition of GSK-3B inhibitors or glial growth factor-2 (GGF2) (Zhang, 2004; Castelo-Branco et al., 2004). As the brain region isolated in the rat mesencephalon protocols is very similar to the region in the mouse described herein, it is reasonable to assume these factors may produce similar dopaminergic enhancement of our NPCs. Furthermore, we have not established whether differentiation in our cultures occurs through simple mitogen depletion over time (as media is not replenished) or whether the NPCs at time of isolation have been imparted, via transcription factors mentioned above, with instructions for differentiation. This kind of intrinsic program is akin to reports by Miyazawa et al. that cerebellar NPCs undergo cell cycle exit and differentiation even in the presence of saturating concentrations of Shh, a potent mitogen (2000). While our NPC cultures are certainly appropriate for investigations of mechanisms of neuronal phenotype specification via treatment with such factors, the conditions described here

produce a differentiation program uncomplicated by additional artificial perturbations. This should allow for a somewhat less complicated interpretation of mechanisms of normal or toxicant-impacted proliferation and differentiation.

We have reported here a culture of embryonic mesencephalon neuronal precursor cells, a mouse equivalent to the rat micromass system. This system should be considered exceptional as compared to other in vitro methods for studying neurodevelopment for the following characteristics: its three-dimensional properties more closely recapitulate the developing brain and timing of cell cycle exit and differentiation appear to closely reflect in vivo properties. Exogenous factors to stimulate differentiation are not employed, thus giving a less work intensive protocol that facilitates simpler interpretation of experimental results. We are currently exploring whether cell cycle regulatory proteins that are temporally associated with neuronal differentiation in our in vitro cultures are also employed in vivo. A better understanding of the interaction of extrinsic and intrinsic signaling during NPC proliferation and differentiation will largely inform investigations of neurodevelopmental toxicity and pathogenesis and treatment of neurodegenerative disease.

Table 4.1 Markers of neuronal differentiation. Commonly used markers of neuronal differentiation are listed below in order of increasing neuronal maturation.

Marker	Type	Description	Specificity	Reference
Nestin	Molecular	Intermediate filament protein	Undifferentiated. Expressed in neural stem cells and progenitors	Lendahl et al., 1990 Park et al., 2004
Sox1	Molecular	HMG-box protein	Expressed at neural induction and downregulated in post-mitotic, mature neurons	Pevny et al., 1998 Cai et al., 2004
GAP-43	Molecular	Axonal growth associated protein	Expressed coincident with the beginning of neurite outgrowth	Das et al., 2004
MAP2	Molecular	Microtubule-associated protein	Neurons. Expressed in neurites	Whittaker et al., 1993 Kim et al., 2004
Nurr1	Molecular	Orphan nuclear receptor-related factor 1	Expressed only in post-mitotic ventral mesencephalon. Necessary for full differentiation of dopaminergic phenotype	Saucedo-Cardenas et al., 1998 Roussa and Krieglstein, 2003
Ptx3	Molecular	Bicoid-related homeobox gene	Expressed only in post-mitotic ventral mesencephalon pre-dopaminergic neurons	Smidt et al., 1997 Farkas et al., 2003
NF-L	Molecular	Neuron specific intermediate filaments	Expressed in mature neurons	Paterno et al., 1997
Synapsin I	Molecular	Regulates synaptic vesicle fusion and neurotransmitter release	Expressed at presynaptic membrane in mature neurons	Thiel, 1993 Das et al., 2004

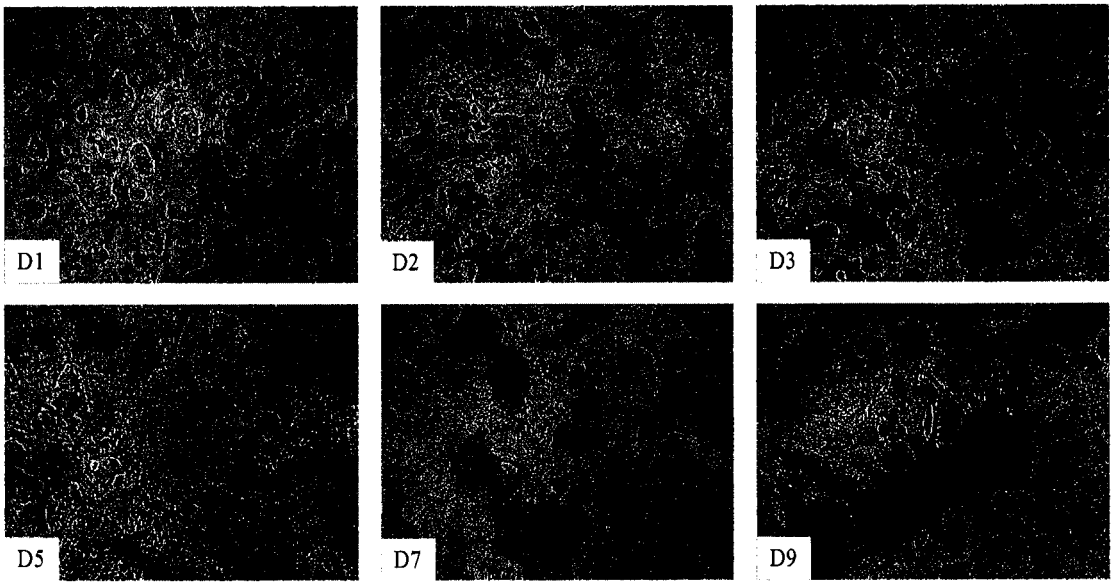

Figure 4.1. Morphology of mesencephalon cells from C57BL/6 mouse embryos across time in culture. Midbrain neuronal progenitor cells differentiate over 9 days in culture. Neuronal morphology as observed by neurite outgrowth is apparent as early as D3 in culture, but cells appear to continue to proliferate and increase in number and density until approximately D7.

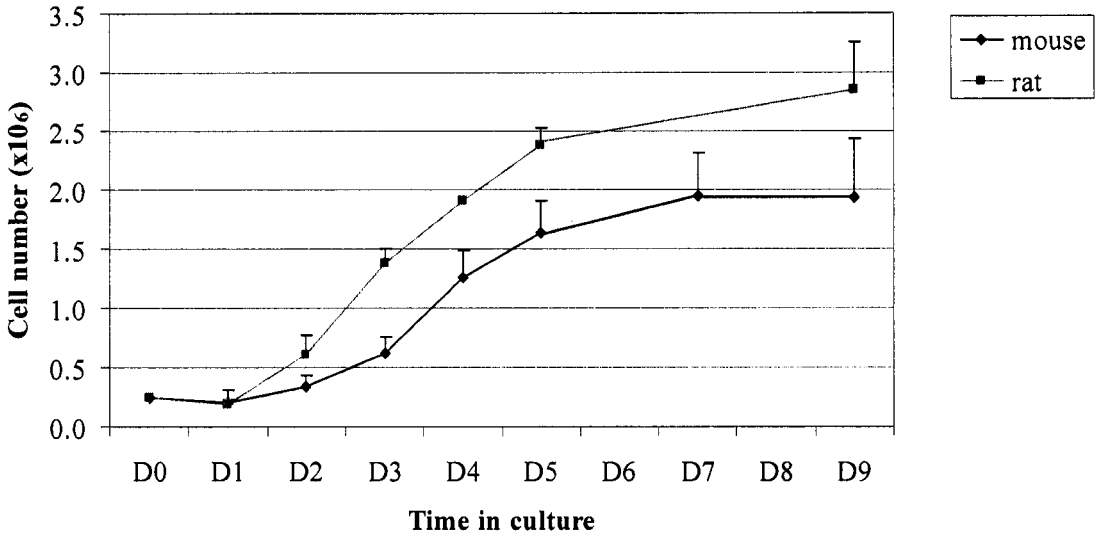

Figure 4.2. Examination of proliferation: cell counts. After an initial slight decline in cell number during the first 24h of culture, cell proliferation increases through approximately 7 days in culture. Proliferation patterns over time in the mouse and rat cultures are statistically significantly different as measured by ANOVA. The mouse cells undergo approximately three cellular divisions between D1 and D7 with an increase from 200,000 cells to nearly 2 million while the rat cells increase to approximately 2.8 million cells on D9. Data points are the average of three independent experiments ± SD.

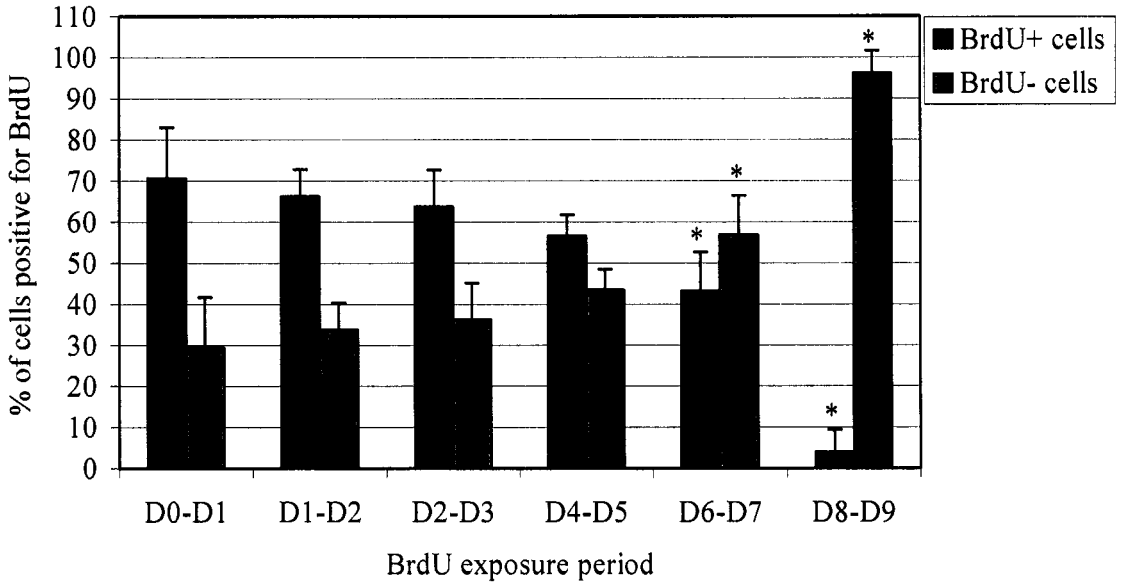

Figure 4.3. Characterization of cell cycle kinetics: BrdU uptake. Cells were cultured in the presence of BrdU, a thymidine analog, for 24h periods across time in culture to examine the percentage of the cycling cell population. Cells were stained with propidium iodide and Hoechst and analyzed by flow cytometry. Hoechst fluorescence is quenched in the presence of BrdU thus cycling cells can be differentiated from non-cycling. Cells that do not incorporate BrdU are presumed to have exited the cell cycle and differentiated into neurons. After eight days in culture, nearly 100% of the culture has exited the cell cycle. Bars represent the average of three independent experiments ± SD. Days that are statistically significantly different ($p \leq 0.05$) from D0-D1 are denoted with an asterisk (*).

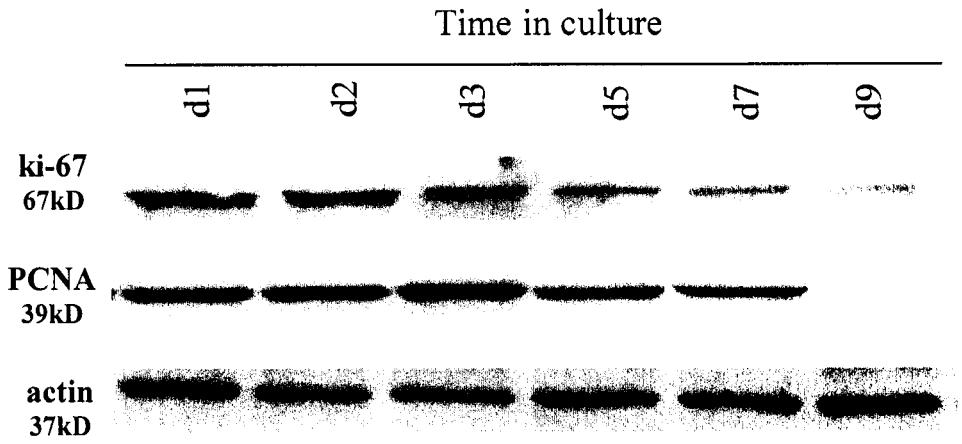

Figure 4.4 Western blot analysis of proliferation markers. Proliferation of cells was examined via expression of ki-67 and PCNA, two commonly used markers of actively cycling cells. Expression of these markers peaked at day 3 and declined with further time in culture. Blots shown are representative of results from at least three independent experiments.

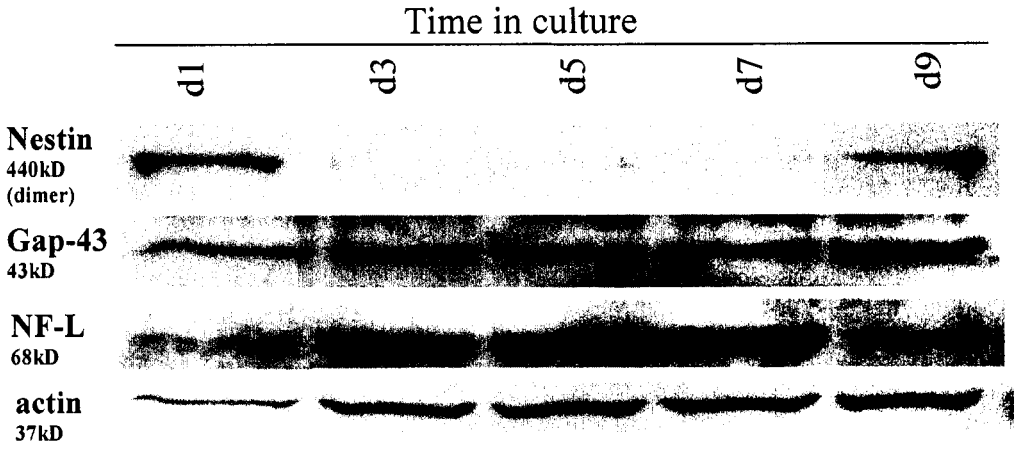

Figure 4.5. Western blot analysis of neuronal differentiation markers. Differentiation was characterized by the presence of nestin, a marker of relatively undifferentiated NPCs, GAP-43, expressed concurrent with neurite outgrowth, and NF-L, a marker of post-mitotic, differentiated neurons. Blots shown are representative of results from at least three independent experiments. Quantification by densitometry is contained in the Appendix.

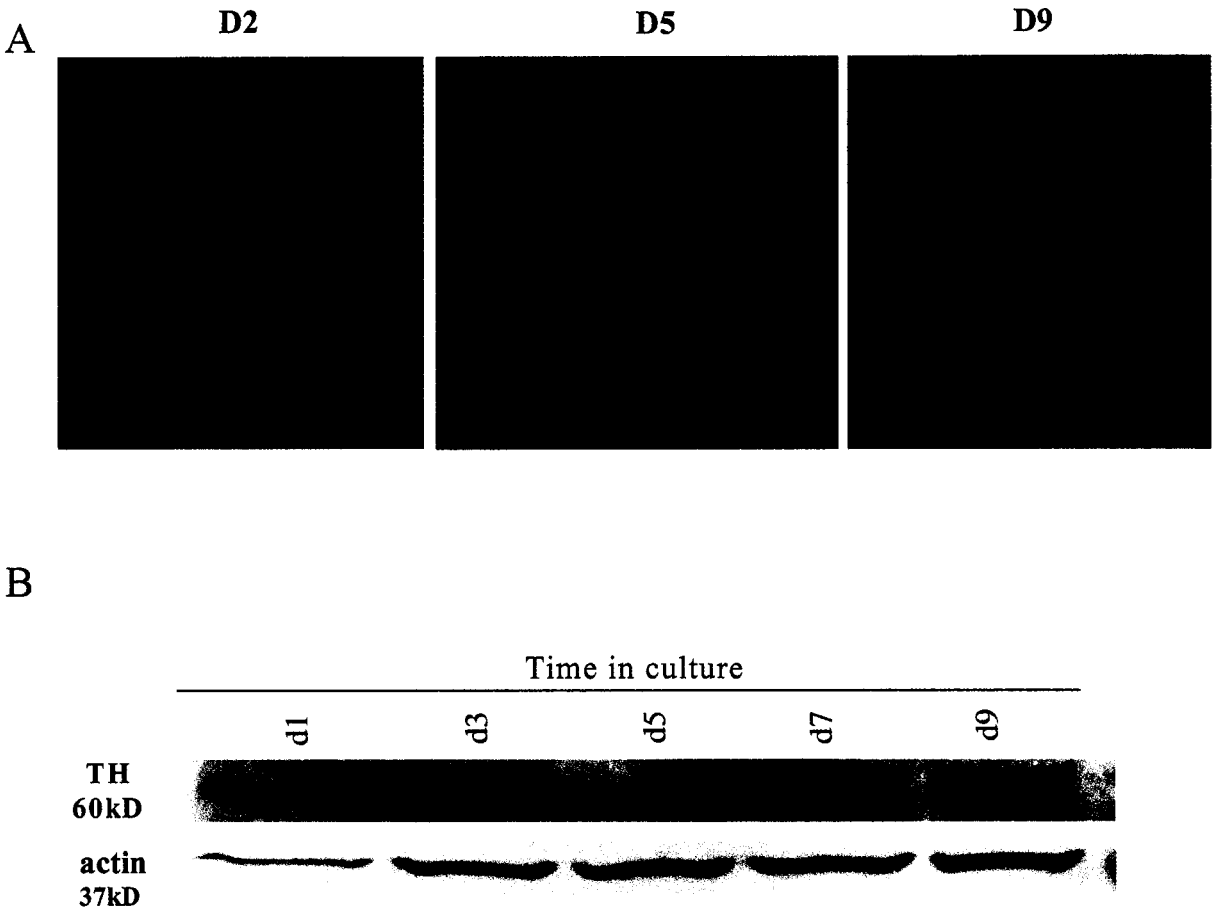

Figure 4.6. Assessment of dopaminergic neuronal phenotype by immunocytochemical staining for tyrosine hydroxylase (TH) (A) and Western blot (B). (A) After two days of culture, TH staining is observed in isolated neurons or small groups of neurons. By day 5 and on day 9, large clusters of TH-expressing cells are found throughout the culture. Nuclei are stained with Hoechst. (B) Western blot of average protein expression in the cultures indicates that TH expression actually appears to peak on D3 and D5 then decrease. Quantification of Western blots by densitometry in included in the Appendix. Images and blots shown are representative of at least three independent experiments.

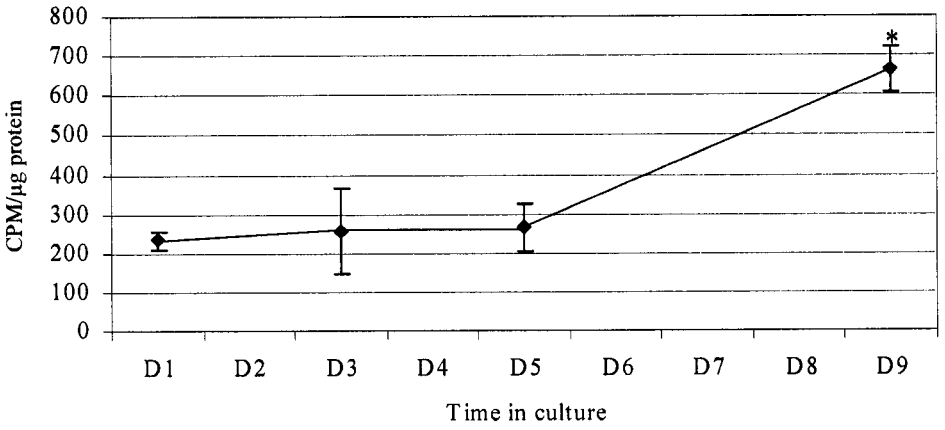

Figure 4.7. Assessment of GABAergic neuronal phenotype and functionality through tritiated GABA ([3H]GABA) uptake in cultured NPCs. GABA uptake remains steady but somewhat variable across the first five days of culture, but has tripled by day 9. Counts are expressed per microgram protein in order to account for proliferation across time in the cultures. Data points represent at least 3 independent experiments ± SE and days that are statistically significantly different ($p \leq 0.05$) from D1 are denoted with an asterisk (*).

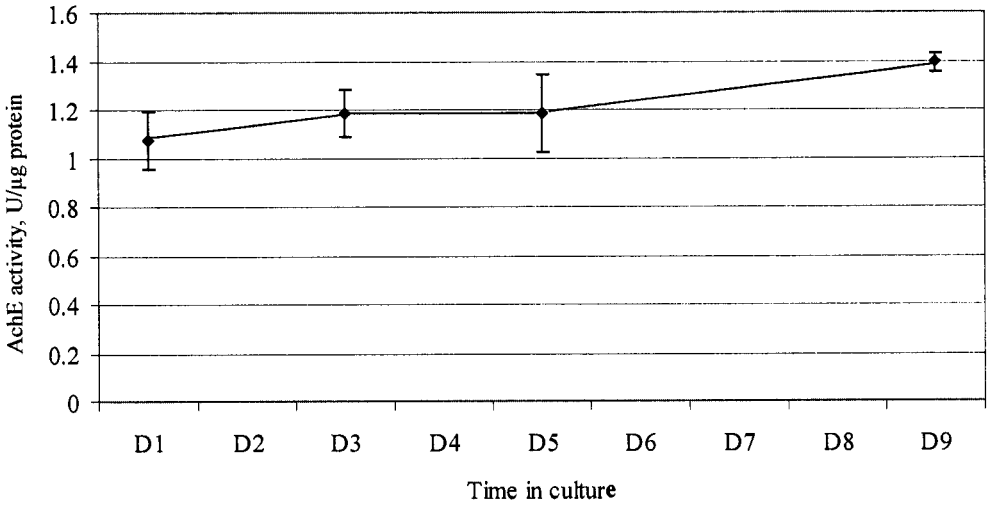

Figure 4.8. Assessment of cholinergic neuronal phenotype by acetylcholinesterase (AchE) activity measurement. To determine whether our cultures contained acetylcholinergic neurons, we assayed cell lysates for AchE activity and standardized the results to protein content. AchE activity increases slightly but non-significantly ($p = 0.3$) from day 1 to day 3 then to day 9. Data points represent at least 3 independent experiments ± SE.

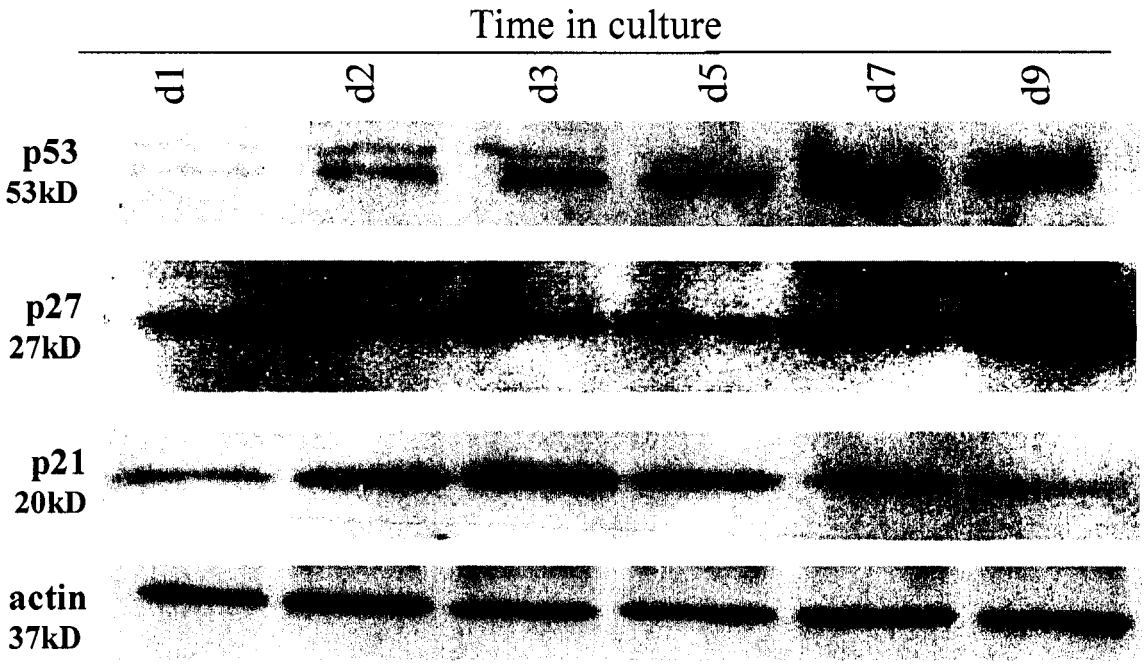

Figure 4.9. Cell cycle regulatory protein expression. p27 and p53 protein expression increase concurrent with the appearance of differentiated morphology and markers and exit from the cell cycle. P21 protein expression increases from day 1 to day 3 and then decreases. Blots shown are representative of results from at least three independent experiments.

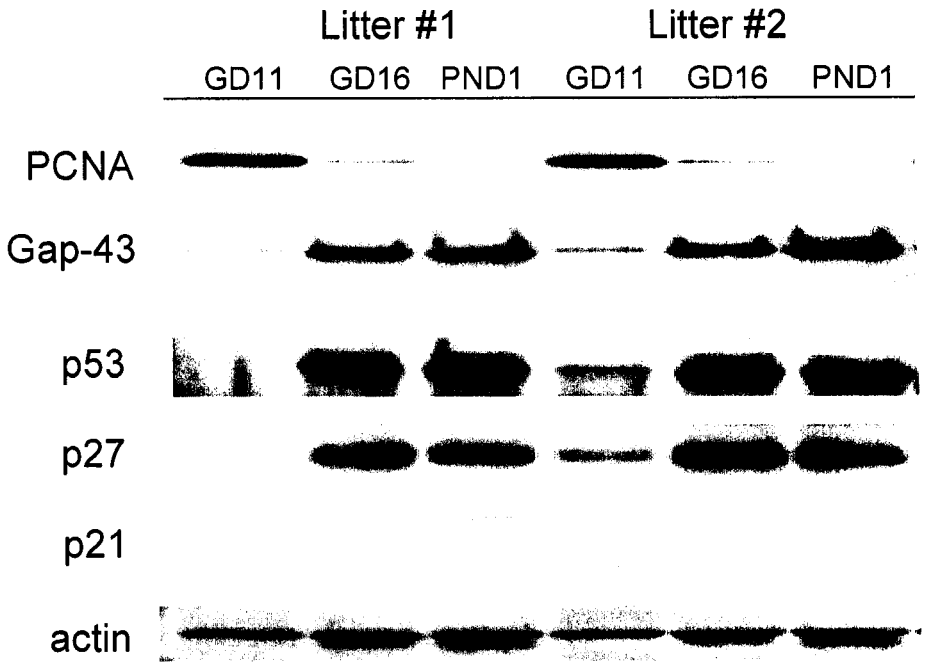

Figure 4.10. Protein expression from mouse embryonic midbrain tissue isolated on gestational days 11, 16, and 20 (PND1). These gestational days correspond approximately to the isolation day of the in vitro cultures (GD11), D5 in vitro (GD16), and D9 in vitro (PND1). PCNA expression, a marker of proliferation, decreases across time as Gap-43 expression increases, indicative of neurite outgrowth and differentiation. Cell cycle proteins p27 and p53 show strong expression on GD16 that is sustained at PND1 in the midbrain. No p21 expression was observed. Bands shown are representative isolations from 2 litters; at least 2 midbrains were pooled from each litter.

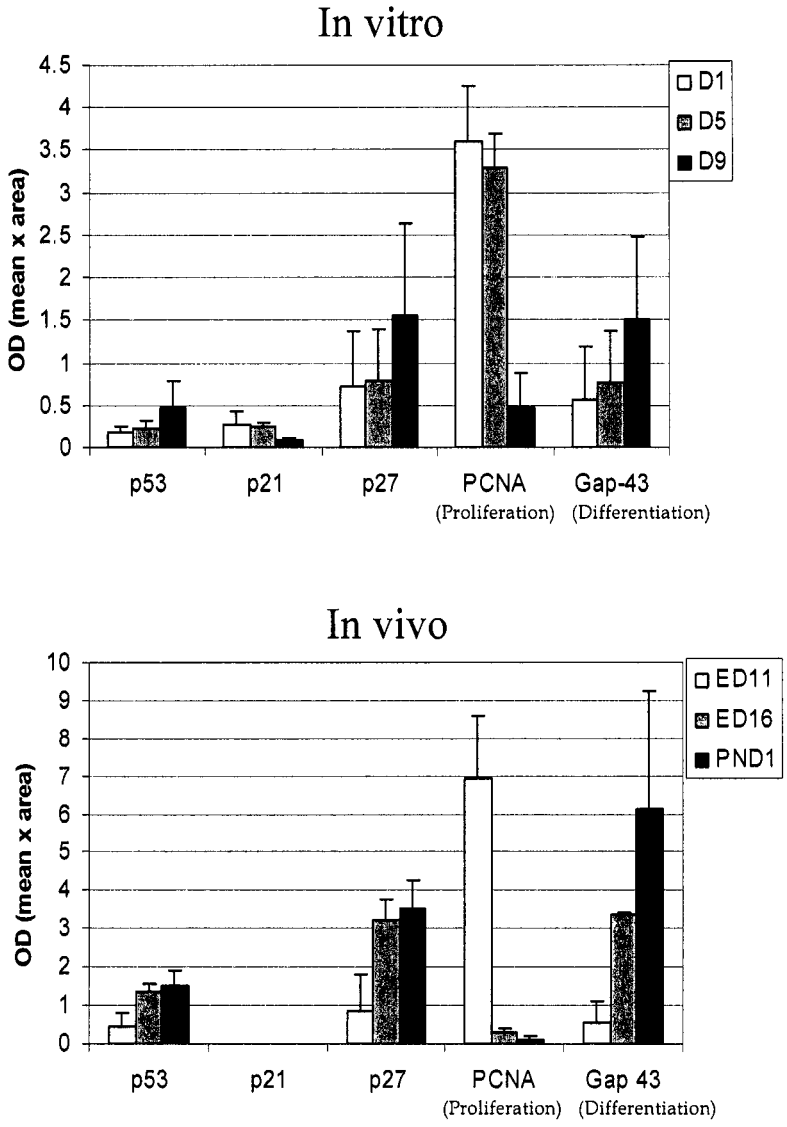

Figure 4.11 Summary and comparison of protein expression in vitro and in vivo. Densitometry of Western blotting for p21, p27, and p53 is compared to expression of PCNA, a marker of proliferation, and Gap-43, a marker of differentiation. In vitro and in vivo, a temporal correlation of increases in p27 and p53 protein is observed with increases in differentiation and the decline of proliferation. Histograms are summaries of densitometry of Western blots from at least three independent experiments.

CHAPTER 5. A ROLE FOR P53 AND P27 IN NORMAL AND PERTURBED MIDBRAIN DEVELOPMENT

5.1 Introduction

The embryonic midbrain is first morphologically defined shortly after neural tube closure through diffusible sonic hedgehog (Shh) signals from the floor plate, and fibroblast growth factor 8 (fgf8) and Wnt1 signals originating from the isthmic organizer at the midbrain hindbrain boundary (Prakash and Wurst, 2004). Midbrain neural precursor cells (NPCs) proliferate along the sagittal midline of the ventral epithelium and then migrate dorso-laterally away from the germinal zone. Mature brain structures derived from the embryonic midbrain function to process and modulate response to sensory and motor information. In addition, structures developing from this region, principally the substantia nigra, ventral tegmentum, and retrorubral field, are the primary source of dopamine for the CNS (Vitalis et al., 2005). Loss of dopaminergic neurons is associated with Parkinson's disease and its hallmark symptoms of lack of voluntary motor control including rigidity, tremor, and akinesia (Grunblatt et al., 2000). As midbrain NPCs can differentiate into mature, functional dopaminergic neurons in vitro and in vivo, they thus hold great potential for therapeutic uses (Sullivan and O'Keefe, 2005; Storch et al., 2004; Gribble et al., 2005). Understanding the mechanisms that facilitate proliferation and differentiation of midbrain NPCs are paramount to the two most promising therapeutic strategies: supporting existing dopaminergic neurons with neurotrophic factors, and culturing and transplanting new neurons (Collier and Sortwell, 1999).

Differentiation of most cell types requires cell cycle arrest in G1 phase and subsequent exit from the cell cycle. Often, cell cycle regulatory proteins are employed to effect this arrest prior to differentiation in response to extrinsic signaling by determination factors (for review see Ohnuma et al., 2003; Galderisi et al., 2003; Ohnuma and Harris, 2003). While the complex interactions that direct the balance of NPC proliferation and neuronal differentiation appear to be cell type specific, the cyclin kinase protein inhibitors (CKIs), p19, p21, and p27 and the tumor suppressor protein

p53 have been demonstrated to play important roles in the differentiation of several neuronal cell types including oligodendrocytes, cerebellar granule precursor cells, and cortical precursor cells (Miyazawa et al., 2000; Durand et al., 1997; Delalle et al., 1999; Billon et al., 2004). These same proteins are often upregulated in the stress response, although the distinction or overlap of these two uses of the same set of proteins during brain development remains poorly explored.

We have previously characterized a mouse midbrain neural precursor cell culture system where immature cells proliferate and then progressively differentiate over 9 days in culture (Gribble et al., 2005). In these cells and in midbrain tissues isolated at comparable gestational timepoints, the p27 and p53 proteins were temporally associated with cell cycle exit and differentiation. To examine whether protein expression was evident prior to differentiation in cycling cells and/or maintained in differentiated neurons in vivo, we examined midbrain expression of p27 and p53 across development. To explore the dual role of p53 in facilitating cell cycle exit in normal neuronal differentiation and following toxicant response, we compared cycling properties and differentiation of midbrain NPCs from mice wildtype or null for p53 in culture. We furthermore explored MeHg induced cell cycle arrest as a possible mechanism of premature differentiation and determined a role for p53 in this potential mode of abnormal neurodevelopment.

5.2 Methods

Cell culture. Midbrain NPCs were prepared as reported by Flint (1983) modified according to Gribble et al., 2005. Gravid uteri were removed from pregnant (11-day post-coitum) C57BL/6 mice, hereafter referred to as p53+/+, or p53-/- mice (originally generated in 129/sv x C57BL/6, then outcrossed to C57BL/6 for 6 generations and maintained through heterozygote matings) where the morning of plug detection was counted as day 0. Following dissection and trypsinization of embryonic midbrains, single cell suspensions were prepared in culture medium (Ham's F12 supplemented with 10% FBS, penicillin (50 U/mL), streptomycin (5 μg/mL) and L-glutamine (5.8

mg/mL) (Gibco, Grand Island NY) and adjusted to a concentration of 5 x 10^6 cells/mL. Five microislands of 10 μL aliquots were plated per 35mm culture dish (Falcon Primaria, Becton-Dickinson labware, Lincoln Park, NJ). A 2.5 hour incubation period at 37° C in a 5% CO_2/95% air atmosphere with 100% relative humidity was performed to allow for cell attachment before culture medium was added.

Immunohistochemistry. Following timed matings, gravid uteri were removed from pregnant p53+/+ or p53-/- mice in accordance with IACUC protocols. Embryos were washed thoroughly in CMF-EBSS and fixed in 10% neutral-buffered formalin for 6-48h depending on developmental age. Embryos were processed according to a standard protocol of dehydration and fixation steps and embedded in paraffin blocks. Serial five micron, perisaggital sections of were obtained with a microtome and baked onto glass slides. For immunolabeling, slides were deparaffinized and rehydrated through graded ethanol baths, followed by incubation with 3.0% hydrogen peroxide for 5 minutes to block endogenous peroxide activity. Antigen retrival was performed by placing slides in citrate buffer (pH 6.0) and heating to 95 °C for 20 minutes followed by a 20 minute cooling step. Slides were washed in PBS and incubated with primary antibody (rabbit anti-p27 or rat anti-PCNA) overnight at 4 °C. The following morning, slides were washed twice (10 minutes) with PBS and incubated sequentially with biotinylated secondary antibody (bio anti-rabbit or bio anti-rat), avidin-biotin complex (ABC) with horse radish peroxidase (HRP), and finally diaminobenzidine (DAB) with nickel chloride to produce a black reaction product. The slides were then dehydrated and coverslipped for inspection by microscope and image capture.

MeHg treatment. A 10^3-fold dilution of a 1 M methylmercury(II) hydroxide stock solution (Alfa Aesar, Ward Hill, MA) in sterile water was performed to obtain a working solution for MeHg treatments (0, 0.1, 0.5, 1.0 μM). For flow cytometric analysis of cell cycle progression, 5-bromo-2'-deoxyuridine (BrdU, Sigma) was also added to cultures with treatment at a final concentration of 60 μM. MeHg treated cells were placed in a plexiglass chamber in order to minimize MeHg exposure with water to

maintain humidity, gassed for 5 minutes with 5% CO_2/95% air, and placed in a 37 °C incubator.

Assessment of viability. The neutral red assay was used to determine changes in cell viability following 24h of MeHg treatment. Briefly, medium was aspirated, cells were washed with CMF-PBS and 2 mL of freshly prepared 0.05% (w/v) neutral red culture medium was added to each dish and incubated at 37 °C for 3 hours. The dishes were then rinsed once with CMF-PBS and the dye eluted with 2 mL 0.5% (v/v) acetic acid in ethanol for 1 hour. Then, 200 µL of supernatent were transferred in triplicate to a 96 well plate and the optical density was read at 540 nm using a microplate reader (Molecular Devices Corp., Palo Alto, CA).

Assessment of proliferation via flow cytometry. BrdU-Hoechst analysis was performed as previously described (Rabinovitch et al., 1988). Cells were cultured with 60 µM bromo-deoxy-uridine (BrdU), a concentration determined to not affect viability, proliferation, or differentiation but allow identification of cells having undergone multiple cell cycles. At the appropriate time, cells were harvested by trypsinization and placed in Hoechst buffer (1.2 µg/mL Hoechst 33258 (Molecular Probes, Eugene OR), 0.146 M NaCl, 0.1 M TRIS Base, 0.5 mM $MgCl_2$, 0.2% BSA, 0.1% Nonidet P-40 (NP-40; Sigma, St. Louis, MO) in dd H_20)) with 10% NP40 (Sigma) and frozen at -20 °C until analysis. At time of analysis, cells were thawed on ice and 10 µg/mL propidium iodide was added. Flow cytometry was performed on a Coulter Elite flow cytometer with excitation at 351-360 nm and emission 420-450 nm (Hoechst) and >620 nm (PI). MPLUS 5.0 software (Phoenix Flow Systems) was used to analyze data.

Protein isolation. Cells were washed twice with 1 mL ice-cold CMF-PBS followed by the addition of 50 µL of cell lysis buffer containing additional phosphatase and protease inhibitor cocktails (Calbiochem). Cells were harvested by scraping in cell lysis buffer and then placed on ice. After storage at –80 °C, all extracts were homogenized by sonication and then centrifuged (16,000 x g, 10 min, 4 °C) to remove insoluble material. The resulting supernatant (cell extract) was gently removed, and total protein

was determined using the BCA kit according to manufacturer's instructions (Pierce, IL).

Nuclear and cytosolic fractioning. Cellular fractioning was performed according to Woods et al. (1999). Briefly, following treatment, cells were washed and scraped in ice-cold CMF-PBS and pelleted at 14,000 x g at 4 °C. All further steps and centrifuge spins were carried out on ice with cold reagents or at 4 °C. The cell pellet was resuspended and vortexed in Buffer A (an aqueous stock of 10mM HEPES, 1.5 mM MgCl2, and 10mM KCL to which 0.5mM DTT, 0.5mM PMSF, and 10μg/mL leupeptin hydrogen sulfate (Boehringer Mannheim, Indianapolis, IN) and 0.1% NP-40 (Boehringer Mannheim) were added just before use), incubated for 10 minutes on ice, vortexed again, and centrifuged for 10 minutes at 14,000 x g. The supernatant containing the cytosolic fraction was collected while the remaining pellet was resuspended and vortexed in Buffer C (a stock of 20mM HEPES, 1.5 mM MgCl2, 0.42 NaCl, 0.2 mM EDTA, and 25% glycerol further supplemented as described for Buffer A above), incubated on ice for 10 minutes, vortexed again, and centrifuged at 4 °C at 14,000 x g. The supernatant was collected as the crude nuclear fraction. Aliquots of each fraction were taken for protein quantification before storing the extracts at -80 °C before Western blot analysis.

Western Blotting. Equal quantities (10 μg) of protein were analyzed by SDS-polyacrylamide gel electrophoresis. Briefly, proteins were separated on Criterion^{TM} 10-20% Tris-HCl precast gels (Bio-Rad) according to the manufacturer's protocol. Proteins were subsequently transferred onto PVDF nylon membranes (Bio-Rad) for immunoblot analyses. The membranes were probed (manufacturer's blotting instructions) with the following antibodies and concentrations: GAP-43, 1:2000; PCNA, 1:2500; p21, 1:200; p27 1:200; p53, 1:200. Secondary antibodies were used at a 1:5000 dilution as follows: goat anti-rabbit horseradish peroxidase (HRP) conjugated, anti-mouse-HRP, rabbit anti-goat HRP. The ECL chemiluminescence system (Amersham Biosciences, Buckinghamshire, UK) was used to visualize specific immunoreactive proteins on Hyperfilm (Amersham Biosciences). The films were

scanned using HP Scanjet 5400C scanner equipped with Precisionscan Pro 3.1 software and the bands of interest were selected and band density and area measured using ImageJ 1.30v software (NIH, USA).

GABA uptake. At appropriate times in culture, 3H-labeled gamma-amino butyric acid ([3H]GABA) was added to culture media at a final concentration of 2 μCi/culture dish for 1h. Culture dishes were washed 3 times for 10 minutes each with Earle's Balanced Salt Solution (EBSS) (Gibco Life Technologies, Inc., Grand Island, NY) until radioactivity in the washes was less than 100 cpm. Cells were scraped in CMF-PBS and transferred to glass, screw-top vials with 500 μL hyamine hydroxide overnight. The next day, 500 μL cell solution, 40 μL glacial acetic acid, and 5 mL scintillation cocktail were read on the Beckman Scintillation Counter. To account for differences across time in culture, GABA uptake was standardized to total protein content.

Acetylcholinesterase activity. Activity was measured according to Ellman et al. (1961) with slight modifications as described by Cole et al., 2005. Cells were washed in ice-cold CMF-PBS and then scraped in phosphate buffer with 1% triton X-100, pH 8.0, into microcentrifuge tubes and frozen at -80°C until analysis. At time of assay, 1 mL of 10 mM DTNB was mixed with 30 mL 100mM sodium phosphate buffer, pH 8.0 and placed in a 30 °C water bath. Cell lysates were thawed, sonicated, centrifuged at 13,000 x g, and the supernatant transferred to new tubes. Aliquots were removed for quantification of protein content and then 10 μL were added in triplicate to wells of a microtiter plate containing 180 μL of the buffered DTNB solution. Plates were incubated for 10 minutes then the kinetic assay was initialized by the addition of 10 μL of 20 mM acetylthiocholine iodide. Absorbance was measured at 412 nm continuously for 10 minutes to measure the formation of 5-thio-2-nitrobenzoate. Rates of product formed during the assay were calculated by standardizing the microgram protein and expressed as U/μg of protein where U = μmol of acetylthiocholine hydrolyzed per minute.

Statistical analysis. Intercooled Stata8 (StataCorp LP, College Station, TX) was used to perform all statistical tests. Analysis of variance (ANOVA) and linear regression

were used to determine differences in genotype response to toxicant treatment and temporal differences within genotype. Bonferroni's multiple comparisons procedure was used to compare MeHg doses to control or timepoints to eachother.

5.3 Results

Expression of p27 and PCNA in the midbrain

We had previously observed increases in p27 protein concurrent with increasing neuronal differentiation and decreasing proliferation in cultured midbrain NPCs. To determine if the same p27 expression patterns we observed in vitro paralleled in vivo developmental expression, we isolated embryos at GD11 and GD16 (approximately corresponding to our culture times of D0 and D5) and compared staining patterns of PCNA, a marker of proliferating cells, and p27 in perisaggital sections of the brain (Figure 5.1). On ED11, we observed strong PCNA staining throughout the epithelial lining of the entire midbrain region (Figure 5.1A). In contrast, no cells in the midbrain region stained positive for p27. By ED16, the pattern was reversed: PCNA expression was observed in a small percentage of the cell population distributed diffusively throughout the developing tectum and tegmentum. In contrast, p27 expression was observed in a majority of the cells throughout the tectum and tegmentum (Figure 5.1B) in a gradient of low to high expression from the ventral to dorsal portions of the midbrain.

Proliferation of p53-/- cultured midbrain NPCs

To further elucidate the importance of p53 in midbrain NPC differentiation, we examined the proliferative properties of NPCs from p53-/- mice. Compared to wildtype cells, cultured p53-/- NPCs underwent more rounds of cell division and proliferated longer. As measured by ANOVA, the genotypes proliferate significantly differently across time. Plating efficiency and cell counts were similar on D1 and D2 but by day 3, p53-/- cultures had $0.82 \times 10^6 \pm 0.1 \times 10^6$ cells compared to $0.62 \times 10^6 \pm 0.13 \times 10^6$ cells in the wildtype (Figure 5.2). The p53+/+ and p53-/- cultures also proliferate

significantly differently as measured by BrdU uptake. As indicated in Figure 5.3, at all timepoints after D1, more p53-/- NPCs were incorporating BrdU than the p53+/+ cells. In the p53-/- cells on D3, 76.9% ± 1.6% of the population had incorporated BrdU compared to 63.8% ± 8.9% in the wildtype. While basically no wildtype cells were proliferating on D9 (3.9% ± 5.5%), when we continued to culture p53-/- NPCs with BrdU for 11 days, 36.6% ± 4.0% of the population was still cycling (data not shown).

Effect of p53 gene inactivation on differentiation

Over 9 days in culture, we previously observed p53+/+ midbrain NPCs to generate GABAergic, dopaminergic, and cholinergic neurons. After observing altered proliferation in p53-/- midbrain NPCs in vitro and in vivo, we compared a battery of neuronal markers in p53+/+ and p53-/- NPCs and also asked whether differentiation of a specific neuronal subtype was particularly altered or if the observed delay of cell cycle exit corresponded to a general delay of overall differentiation. Western blot analysis of nestin, NF-L, and Gap-43 indicated some similar patterns of differentiation markers in the p53-/- and p53+/+ NPCs (Figure 5.4A). Nestin, a marker of relatively undifferentiated cells, was expressed much longer in the p53-/- cultures: immunoblotting demonstrated detectable protein at D7 while expression disappears in the p53+/+ by D3. Gap-43, a protein expressed concurrent with neurite outgrowth and used as a marker of general early neuronal differentiation, increases steadily in p53+/+ cultures; in the p53-/- cells, it is detectable and mostly constant across all days in culture. We measured NF-L, a neurofilament protein cited in the literature as expressed in mature neurons, and saw increases in expression from D1 to D3 and D5, then a decline to D9 in both p53+/+ and p53-/-.

Tyrosine hydroxylase expression was used as an indicator of dopaminergic phenotype. As indicated in Figure 5.4A, TH expression is highest on days 3 and 5 in culture in both wildtype and null cells and then declines to day 9. No significant difference in TH expression between genotypes was observed. We compared tritiated GABA uptake at days 1, 5, and 9 in culture and observed sustained increases from D1

to D9 in the p53-/- cells in contrast to no increase in the p53+/+ cells until D9 (Figure 5.4B). Acetylcholinesterase activity in the p53+/+ cells increased steadily across culture time (Figure 5.4C). In dramatic contrast, p53-/- cells appeared to lose cholinergic phenotype under our culture conditions. Analysis by ANOVA indicates that 3[H]GABA uptake and AchE activity across time in culture are both significantly different between p53+/+ and p53-/- NPCs. These results suggest that p53-/- NPCs do exhibit different differentiation profiles in culture rather than a general delay.

Effect of toxicant exposure on differentiation of wildtype and p53-/- NPCs.

Our evidence suggests that p53 and p27 play a role in facilitating cell cycle exit prior to differentiation in midbrain neuronal precursor cells and that p53 may be especially important for cholinergic neurons. Following toxicant exposure or DNA damage, these proteins also facilitate cell cycle arrest. Our lab has previously characterized a role for p21, another CKI, and p53 in cell cycle arrest following MeHg exposure at doses that cause small changes in cell viability in mouse embryonal fibroblasts. To test the hypothesis that p53 was not only important for differentiation but also in toxicant response, we exposed wildtype and p53-/- NPCs on Day 3 in culture to a range of MeHg concentrations and examined cell viability and cell cycle inhibition after 24h (Figures 5.6 and 5.7). At D3, the majority of wildtype NPCs are still cycling but are already expressing measurable levels of p27 and p53 protein, and also markers of differentiation correlated with cell cycle exit and differentiation. Therefore, we chose this timepoint to examine the effects of sublethal MeHg treatment on proliferation and differentiation. Similar to our observations in MEFs following MeHg treatment, p53-/- NPCs were significantly less sensitive to higher concentrations of MeHg with regard to reduction in cell viability and cell cycle inhibition ($p \leq 0.01$). While wildtype NPC viability was reduced to 19.8% ± 7.8% following exposure to 1.0 μM, p53-/- NPC viability was 48.8% ± 12.5% (Figure 5.6). At lower concentrations of MeHg (0.1 μM, 0.5 μM), cell viability was not significantly different between genotypes. Cell cycle inhibition following MeHg exposure was observed as a general

delay in transit through all phases of the cell cycle. Treatment induced changes in cell cycle kinetics were quantified as the percentage of the cell population reaching a new G0/G1 in 24h of treatment and is illustrated in Figure 5.7. In the p53+/+ NPCs, concentrations as low as 0.1 μM MeHg caused significant cell cycle delay as evidenced by a 21% decrease in the population reaching a new round of cycling compared to the control population. In contrast, cell cycle delay was only observed in the p53-/- population at concentrations of MeHg that caused a significant reduction in cell viability (1.0 μM).

We chose two concentrations of MeHg for further investigations in the wildtype cells: one that caused significant cell cycle inhibition but not significant reduction in viability (0.1 μM) and another that reduced cell cycle progression approximately 50% (0.5 μM). We hypothesized that the p53 protein was involved in cell cycle inhibition following MeHg exposure in NPC cells as had been observed in the MEFs. However, we also wanted to know whether the observed increased level of cell cycle arrest induced by MeHg exposure (over that occurring simultaneously with normal differentiation) would lead to premature differentiation. We again treated D3 p53+/+ NPC cultures with MeHg and assessed changes in nuclear and cytoplasmic levels of p53 protein at 20 minutes, 1h, 4h, and 24h. Figure 5.8A (quantified in 5.8B) shows upregulation and increased nuclear localization of p53 protein that was evident at 20 minutes and became statistically significant at 4h and 24h in cells treated with 0.5 μM MeHg as compared to untreated cells. We also probed for p27 and p21 to determine if they were involved in cellular toxicant response to MeHg. Both p21 and p27 expression were exclusively found in the cytoplasmic fraction and no significant changes in protein levels or distribution were observed following treatment (5.8A).

MeHg is a known neurodevelopmental toxicant but a definite mechanism of action remains elusive. To explore whether p53 upregulation and cell cycle inhibition following our low dose exposures could lead to inappropriate differentiation, we examined a longer time course of effects on differentiation endpoints following the same treatment design. Cells were treated for 24h on D3 with 0.1 μM or 0.5 μM MeHg

and examined at D4, D5, and D9. We first probed Western blot extracts of whole cell lysates for p53 expression (Figure 5.9A) and confirmed that upregulation of p53 protein is observed in response to MeHg treatment (0.1 μM, 0.5 μM) on D4 and D5. As quantified in Figures 5.9B and 5.9C, p53 upregulation in whole cell lysates was observed at 0.1 μM and 0.5 μM MeHg in two independent experiments in contrast to changes observed only at 0.5 μM MeHg in the nuclear fraction in the shorter timecourse. Figure 5.10A indicates that differentiation of GABAergic neurons as measured by [3H]GABA uptake was unchanged with treatment on D4; however, on D5, treated cultures (0.5μM) showed significant increases in [3H]GABA uptake. On D9, this trend toward increased uptake was observed in cultures treated with 0.1 μM MeHg and 0.5 μM MeHg, but statistical significance was not achieved. Acetylcholinesterase activity was significantly increased over control cells by 0.5 μM but not 0.1 μM MeHg treatment on all days (Figure 5.10B). Dopaminergic differentiation as measured by tyrosine hydroxylase expression appeared slightly but insignificantly transiently upregulated by 0.1 μM and 0.5 μM MeHg on D4 with no differences between treated and control cultures on D5 and D9 (Figure 5.10C). No changes were observed in Gap-43 expression (Figure 5.10C). These results indicated that MeHg treatment resulted in concurrent cell cycle inhibition, upregulation of p53 protein, and increased differentiation of GABAergic and cholinergic midbrain neuronal precursor cells.

To determine whether p53 was necessary for this observed premature differentiation, we treated p53-/- NPCs according to the same design and observed differentiation characteristics on D5 (Figure 5.11A, B, C). As p53-/- cells were less sensitive to cell cycle inhibition by MeHg, we treated with a higher concentration (1.0 μM) that produced a 26% increase in cell cycle inhibition over control cells, comparable to the cell cycle effects of 0.1 μM MeHg in wildtype cells. In contrast to the wildtype cells, no significant changes in any differentiation measures were observed, and the genotypes respond differently to MeHg treatment on D5 for all endpoints as determined by ANOVA. This suggests that the MeHg-induced

upregulation of p53 protein observed following treatment influences the subsequent premature differentiation of NPCs.

5.4 Discussion

Cell cycle regulatory proteins are utilized in brain development to control cell number and facilitate cell cycle exit and differentiation in a cell and brain-region specific manner. While this has been examined in the development of the cerebral cortex, the retina, the cerebellum, and in oligodendrocytes in some detail, we demonstrate herein for the first time an examination of the cell cycle regulatory proteins active in differentiation in the embryonic midbrain. We show that p27 and p53 are expressed in increasing levels from GD11 to PND1 in the embryonic midbrain, corresponding to cells that have left the cell cycle and do not express PCNA and that this expression pattern is conserved in cultured midbrain precursor cells. We demonstrate that midbrain NPCs from mice null for p53 proliferate longer in culture and differentiate with a different neuronal phenotypic pattern as compared to NPCs from cells wildtype for p53: while cholinergic phenotype is lost in culture, GABAergic differentiation is enhanced. In addition to a normal physiological role in midbrain NPC differentiation, the p53 protein is also responsive to low-dose chemical stress (MeHg, 0.1 μM, 0.5 μM), facilitates cell cycle arrest, and subsequent premature neuronal differentiation in our experiments. These observations contribute to the growing body of knowledge concerning molecular control in neuronal proliferation and cell fate determination, and the multiplicity of roles for which the cell cycle regulatory proteins are responsible.

What are the plausible extrinsic signals that direct the cell cycle regulatory proteins to commence cell cycle arrest in the midbrain? Nearly all studies to date have focused exclusively on the differentiation of midbrain dopaminergic neurons. In cultured cells from the ED 14.5 rat ventral midbrain, Castelo-Branco et al. (2004) explored the role of the Wnt family in the generation of dopaminergic neurons. They demonstrated a direct connection between extrinsic Wnt signaling and cell cycle

regulation: Wnt1 increased proliferation of Nurr1 positive precursor cells concurrent with increases in cyclinD1 and D3 and downregulation of p27 and p57 mRNAs. Recently, Farkas et al. treated ED14 rat midbrain NPCs with various factors and have shown that TGF-β, along with Shh and Fgf8, may be a critical factor for determination and survival of dopaminergic neurons (Farkas et al., 2003; Roussa et al., 2004). Adding to multiple reports on the specific capacity of growth factors to enhance dopaminergic phenotype (Lin et al., 1993; Krieglstein et al., 1995; O'Keeffe et al., 2004; Zhang et al., 2004), this same group determined no additional effect of BDNF, NT-3, or GDNF (Roussa and Krieglstein, 2004a; 2004b). TGF-β has been shown to promote differentiation in cerebellar precursor cells through cooperative signaling with BDNF that resulted in nuclear translocation of the transcription factors SMAD2 and SMAD4 and increases in p21 and p27 protein (Lu et al., 2005). Several excellent reviews describing the molecular coordination of neuronal proliferation and differentiation have recently been published and provide insight regarding possible upstream signals that produce the changes in p27 and p53 we observed in midbrain development (Ohnuma et al., 2001; Galderisi et al., 2003; Cunningham and Roussel, 2001; Ohnuma and Harris, 2003; Nakayama and Nakayama, 1998; Bally-Cuif and Hammerschmidt, 2003; Cremisi et al., 2003).

In our experiments, we observed cell cycle arrest that resulted in premature differentiation of NPCs into cholinergic and GABAergic neurons. Is the observed early differentiation in our cultures a specific effect of MeHg or rather, can toxicant induced cell cycle inhibition that mimics normal physiological cell cycle exit prior to differentiation be considered a general mode of neurodevelopmental toxicity? While relatively few studies have explored this mode of neurodevelopmental toxicity, especially in primary cultures, premature differentiation of immature neuronal cells following exposure to sub-lethal concentrations of toxicants has been documented in the PC-12 cell line. In a characterization of compounds for the potential treatment of neurodegenerative diseases, Parker et al. (2000) determined that rapamycin, flavopiridol, and ciclopirox all increased neurite outgrowth in PC-12 cells with co-

treatment of low concentrations of NGF. The distinct capacity of these particular compounds to promote differentiation was determined to correspond to an observed increase in cell cycle arrest, although the previously determined mechanism of this arrest differs between all three compounds (Dumont and Su, 1996; Hoffman et al., 1991; Carlson et al., 1996). Liu et al. (2005) also documented cell cycle arrest, increased AchE activity, and increased neurite outgrowth in PC-12 cells in response to *Nardostachys chinensis* glycoside, a component of a traditional Chinese analgesic. These results strongly suggest that cell cycle arrest is a downstream response mechanism common to many stressors that may be sufficient to promote differentiation. However, in a carefully designed study by Parran et al. (2000), the effects of sub-lethal concentrations of MeHg on PC-12 cell differentiation were examined in cells that had either been primed to differentiate via NGF treatment or had not been primed and were cycling at the time of exposure. While cell cycle arrest was not measured, in the undifferentiated cells, sub-lethal concentrations of MeHg had no effect on neurite outgrowth with or without co-exposure to NGF; in contrast, they observed inhibition of neurite outgrowth in the previously differentiated PC-12 cells. They concluded that low dose MeHg exposure does not specifically affect early differentiation but that dendritic elaboration of differentiated cells may be selectively sensitive to its effects. In contrast to MeHg, exposure of undifferentiated PC-12 cells to mercuric chloride ($HgCl_2$) did result in induction of neurite outgrowth, results which have also been observed with lead acetate in this same assay and cell system (Williams et al., 2000). Our results demonstrating sustained increases in differentiation following sub-lethal MeHg exposure as measured by increases in acetylcholinesterase activity and [3H]GABA uptake may differ from Parran et al. because their doses did not cause cell cycle arrest; because of cell type specific responses from the PC-12 cells and midbrain precursor cells; or because of the differences in endpoints measured. Because of the tightly packed three-dimensional growth properties of our cultures, careful quantification of neurite outgrowth as performed by Parran et al. is not possible. However, Gap-43 expression is perhaps a surrogate as it is expressed in the neurites,

concurrent with outgrowth and appears to be sustained in mature neurons. While we did not observe statistically significant increases in Gap-43 expression, this perhaps demonstrates that this marker is not as sensitive to detect changes in a mixed neuronal culture as our functional assays. Alternatively, we may have observed functional changes relating to neuronal differentiation although neurite outgrowth was not affected. In primary neurosphere cultures of fetal rat cerebral cortical NPCs, a recent study found that ethanol, when applied at doses lower than that which produced apoptosis, increased progression from stem to neuroblast cell maturation, as indicated by a transient increase in proliferation and a decrease in stem cell markers. This transition was followed by a decreased sensitivity to retinoic acid-induced differentiation into mature neurons suggesting a different cellular response than observed in our midbrain NPC cultures (Santillano et al., 2005). In cerebellar granule precursor cells, ethanol has been shown to cause downregulation of CDK2 and cyclin A concurrent with cell cycle arrest; however, the concentrations of ethanol used in this study were slightly higher resulting in apoptosis, and differentiation endpoints were not examined (Li et al., 2001). The complex behavior and composition of neuroepithelial precursor cell cultures highlights the importance of attempting to monitor proliferation and differentiation in specific cell subtypes when determining toxicant impact. Our group has previously compared the dose-response of three metals, cadmium chloride, sodium arsenite, and methylmercury across endpoints for cell viability, apoptosis, cell cycle kinetics, and gene expression in mouse embryonal fibroblasts (manuscript in preparation). While some unique patterns of response were observed for each metal, many commonalities in gene expression changes resulting in cell cycle arrest confirm that this is a common cellular defense mechanism to stress. Similar studies with carefully determined sub-lethal concentrations of toxicants resulting in equivalent cell cycle arrest in neuronal precursor cells could assist our understanding of the uniqueness or ubiquity of premature neuronal differentiation as observed in this study.

In midbrain NPCs, it appears that the p53 protein is dispensable for normal midbrain neuronal differentiation although we observed distinctly different behavior

between null and wildtype cells in culture. Early indications that p53 might function as a differentiation factor were obtained following the observation that gamma radiation increased p53 protein levels in pre-B 70Z/3 cells and subsequently induced their differentiation (Aloni-Grinstein et al., 1995). Other studies in both lymphoid and myeloid lineages helped determine that differentiation was facilitated either through stabilization of the p53 protein, as in gamma radiation treated pre-B cells, or through transcriptional activation by p53 through manipulations of a pre-erythroid cell line null for p53 (Almog and Rotter, 1997). In PC-12 cells and oligodendrocyte precursors, transient nuclear expression of p53 has been associated with the process of cell cycle withdrawal and early differentiation; p53 expression is significantly lower in fully differentiated neurons and oligodendrocytes (Hughes et al., 2000; Tokumoto et al., 2001; Eizenberg et al., 1996). Furthermore, a dominant negative form of p53 can block differentiation of cultured oligodendrocyte precurosor following thyroid hormone treatment (Billon et al., 2004). We observed a significantly greater proportion of midbrain NPCs from mice null for p53 proliferating at all timepoints in culture as compared to wildtype NPCs. This was dually reflected in a decrease in differentiation markers: nestin expression remained high across seven days in culture, Gap-43 expression did not increase across time in culture, and acetylcholinesterase activity was lower. These results support the idea that the p53 protein is important, but not essential for providing conditions (G1 arrest) that favor differentiation. However, compared to the wildtype cells, the pattern of tyrosine hydroxylase expression was unchanged and [3H]GABA uptake was increased in the null cells. A recent study characterizing an immortalized cell line from a cerebellar neoplasm in a p53 null mouse determined that following culture in serum-free media, the cells differentiated into oligodendrocytes and neurons: the neuronal cells were predominantly GABAergic (Tominaga et al., 2005). The results from the Tominaga study and ours suggest that increases in p53 protein during neuronal differentiation shift cells away from a GABAergic default program. Mice null for p53 have demonstrated a strain and sex specific increased incidence (3%-16%) of exencephaly, principally occurring in the fore- and midbrain

region (Donehower et al., 1992; Jacks et al., 1994; Purdie et al., 1994; Tsukada et al., 1993; Gondo et al., 1994). Exencephaly, a result of neural tissue overgrowth following failure of the neural tube to close, was reported at 3% in the mouse strain used in our study (Choi and Donehower, 1993). In our p53-/- NPC isolations on GD11, we observed similar rates (3-5%) of open neural tubes: these mice were excluded from cultures. With the exception of exencephaly, no other midbrain abnormalities in p53 null mice have been reported. This suggests compensatory or redundant pathways are active to facilitate cell cycle arrest or that structural or functional changes are subtle and midbrain development in these mice has not been evaluated at the necessary level of detail.

In our experiments, sub-lethal cell cycle inhibition by MeHg and subsequent differentiation in midbrain NPCs are dependent on the p53 protein. This is consistent with many reports of p53 responsivity to toxicant exposure including metals, ethanol, benzo[a]pyrene, and radiation in neurodevelopment (Limoli et al., 2004, Komarova et al., 1997; Frenkel et al., 1999; Nicol et al., 1995). However, little is known about the specific regulation of p53 in neuronal differentiation versus following toxicant exposure. Most often, acute p53 responsiveness to stress is achieved via post-translational modifications, principally, phosphorylation that prevents binding of Mdm2, a ubiquitin ligase, and thereby prevents proteasomal degredation of the protein (Ito et al., 2001). Recently, Vaghefi and Neet (2004) thoroughly demonstrated that NGF treatment of PC12 cells resulted in MAP kinase-induced deacetylation of lysine 382 on p53. Deacetylation of lys382 was not observed following treatment with EGF, FGF, or TNF-α, factors promoting proliferation, differentiation, and apoptosis, respectively, although FGF is able to induce differentiation through MAPK signaling as well. Deacetylation is suggested to render p53 more likely to interact with several cofactors necessary for transactivation of genes promoting differentiation; however, the lysine 382 specific modification may only be specific to NGF treatment of PC-12 cells and remains to be further explored in other cell types.

In our study, we hypothesized that toxicant induced cell cycle arrest in cycling midbrain neuronal precursor cells would result in premature differentiation and assayed for responses in GABAergic, dopaminergic, and cholinergic neurons across several days. Our observation of p53 dependent increases in GABAergic and cholinergic but not dopaminergic neurons support a mechanism of neuronal subtype-specific sensitivity and specificity of response to this toxicant. However, we suspect future comparisons in this and other NPC culture systems of other compounds that cause cell cycle inhibition will result in a similar outcome of premature differentiation. While different types of NPCs appear to utilize different cell cycle regulatory molecules to effect arrest prior to differentiation, we hypothesize that toxicant induced cell cycle inhibition is a common convergence effect of many different upstream pathways that may lead to early differentiation. Our results provide support for a possible mode of abnormal neurodevelopment following low dose chemical exposures and stress.

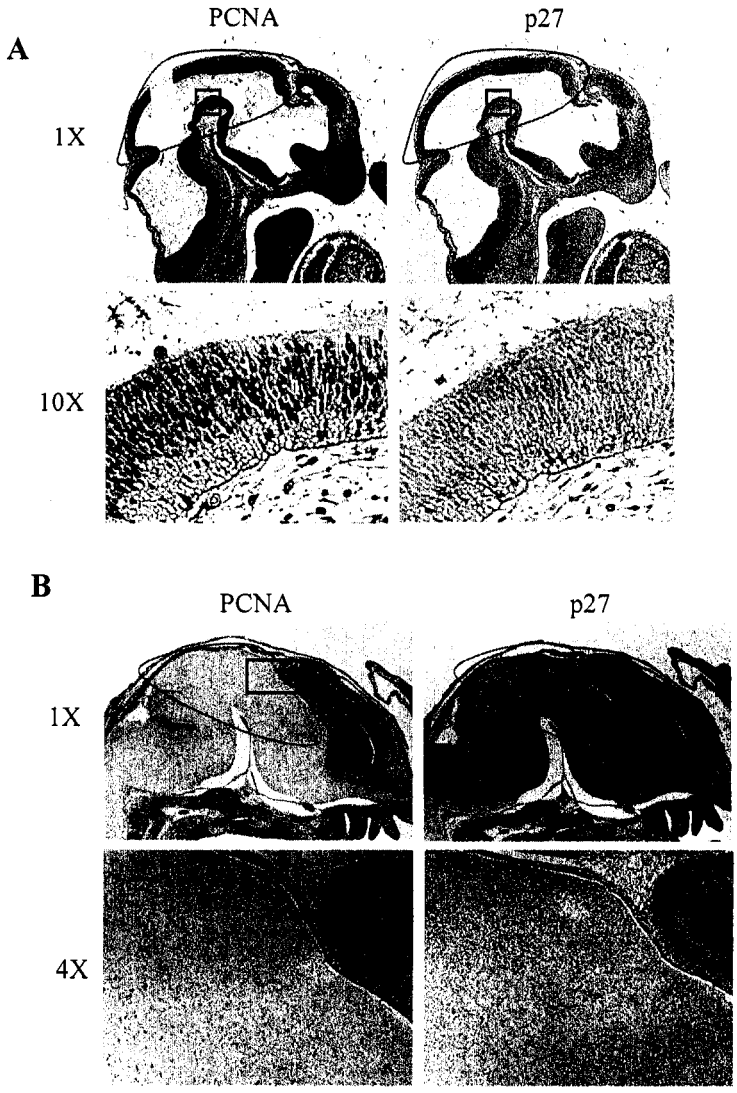

Figure 5.1. Expression of p27 and PCNA in p53+/+ mouse midbrain. Mouse embryos from mice wildtype for p53 were harvested on ED11 (A) and ED16 (B) (approximately corresponding to D0 and D5 of culture), fixed, paraffin embedded, and sectioned. Perisagittal sections were immunostained for p27 and PCNA to determine the relationship between neuronal precursor cell proliferation and cell cycle regulatory protein expression in the embryonic midbrain (circled). Strong PCNA staining was observed on ED11 throughout the midbrain epithelium; no p27 staining was noted. On ED16 (B), midbrain cells occasionally stain positive for PCNA, as observed via higher magnification of the boxed region. In contrast, p27 expression is high on ED16 and staining is observed in gradient of lower to higher expression from ventral to dorsal midbrain. Images are representative of at least two embryos examined from three different litters at both timepoints.

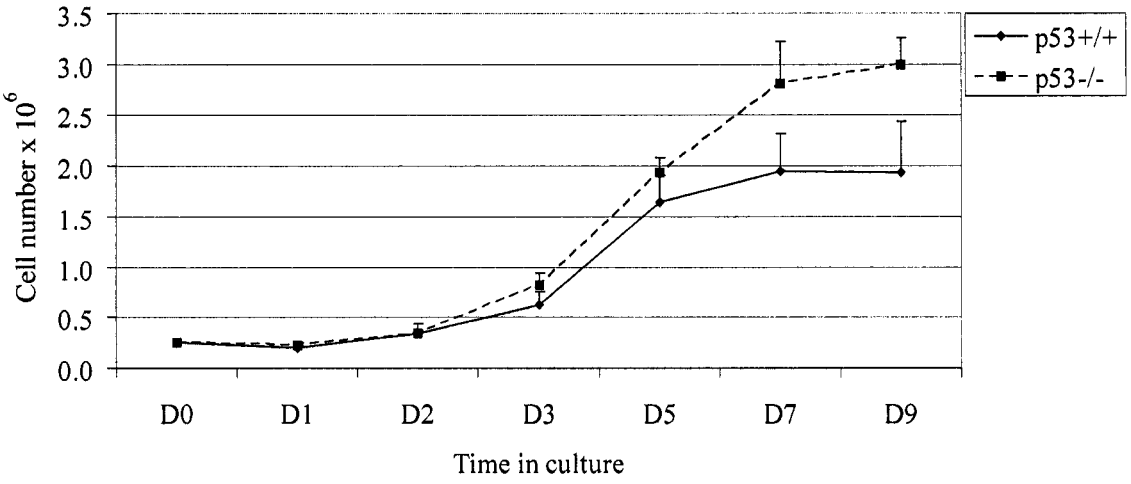

Figure 5.2. Cell counts of p53+/+ and p53-/- neuronal precursor cells across time. At the indicated timepoints, NPCs were trypsinized and counted. Changes in cell number over time are significantly different by genotype as measured by ANOVA ($p=0.00$). Each data point represents at least two counts from three independent experiments.

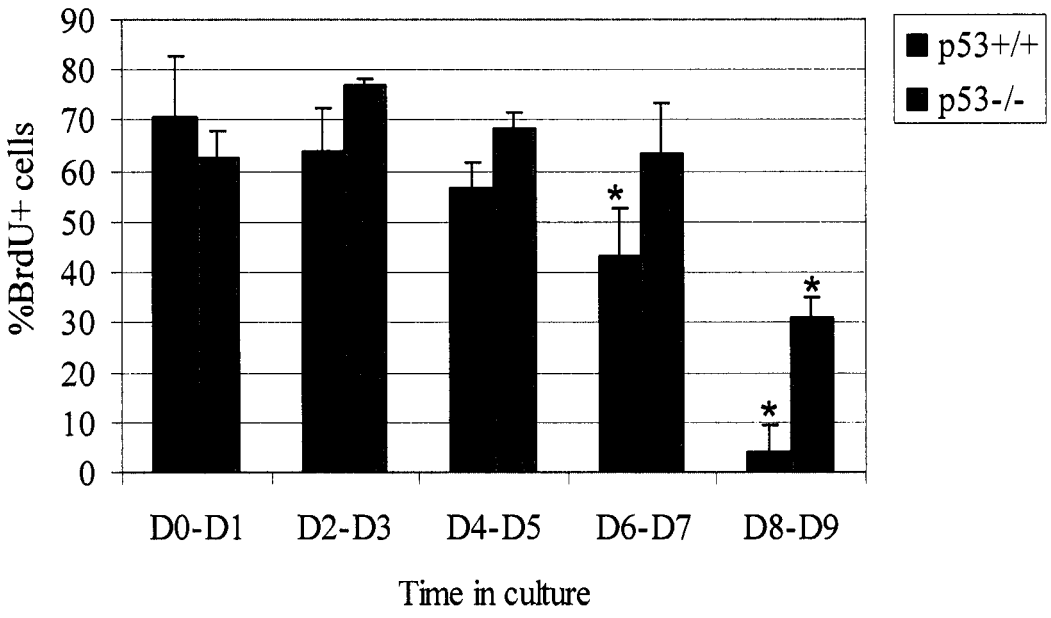

Figure 5.3. Flow cytometric analysis of BrdU uptake in p53+/+ and p53-/- midbrain NPCs. Cells were cultured with BrdU, a thymidine analog, for 24h periods as indicated in the figure then harvested and placed in a buffer containing Hoechst dye and propidium iodide for flow cytometric analysis. As Hoechst fluorescence is quenched in the presence of BrdU, BrdU uptake was quantified as a measure of proliferating cells. Incorporation of BrdU is significantly different between genotypes over time as tested by ANOVA. Each point represents the mean ($n \geq 3$) ± SD and days that are statistically significantly different ($p \leq 0.05$) from D0-D1 are denoted with an asterisk (*).

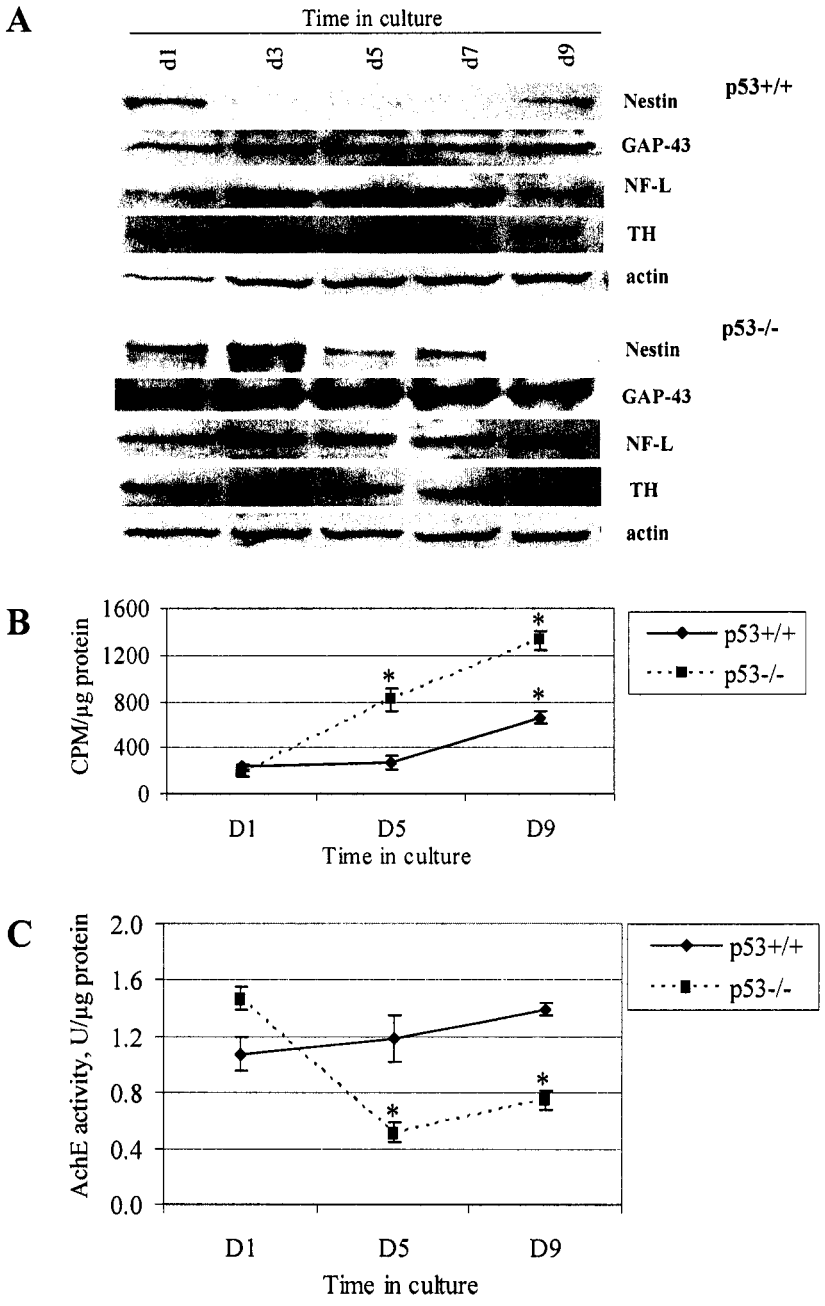

Figure 5.4. Comparison of differentiation characteristics of p53+/+ and p53-/- NPCs across time in culture. (A) Western blot analysis of differentiation markers nestin, Gap-43, and NF-L and tyrosine hydroxylase. NPCs from p53-/- midbrains retain nestin expression longer in culture than p53+/+ NPCs while expressing steady levels of Gap-43 across time. Gap-43 expression increases steadily in the p53+/+ NPCs. Patterns of NF-L expression are similar. Quantification of protein expression by densitometry can be found in the Appendix. (B) [3H] GABA uptake. NPCs null for p53 demonstrate greater [3H]GABA uptake at D5 and D9 than the p53+/+ cells. (C) Acetylcholinesterase activity. In contrast, p53-/- cells have higher AchE activity on D1 that significantly decreases on D5 and D9. Changes in [3H]GABA uptake and AchE activity across time significantly differ between genotypes as measured by ANOVA ($p \leq 0.05$). Blots shown are representative of three independent experiments while data points (B,C) represent the mean ($n \geq 3$) ± SD. Days with values that are statistically significantly different ($p \leq 0.05$) from D1 are denoted with an asterisk (*).

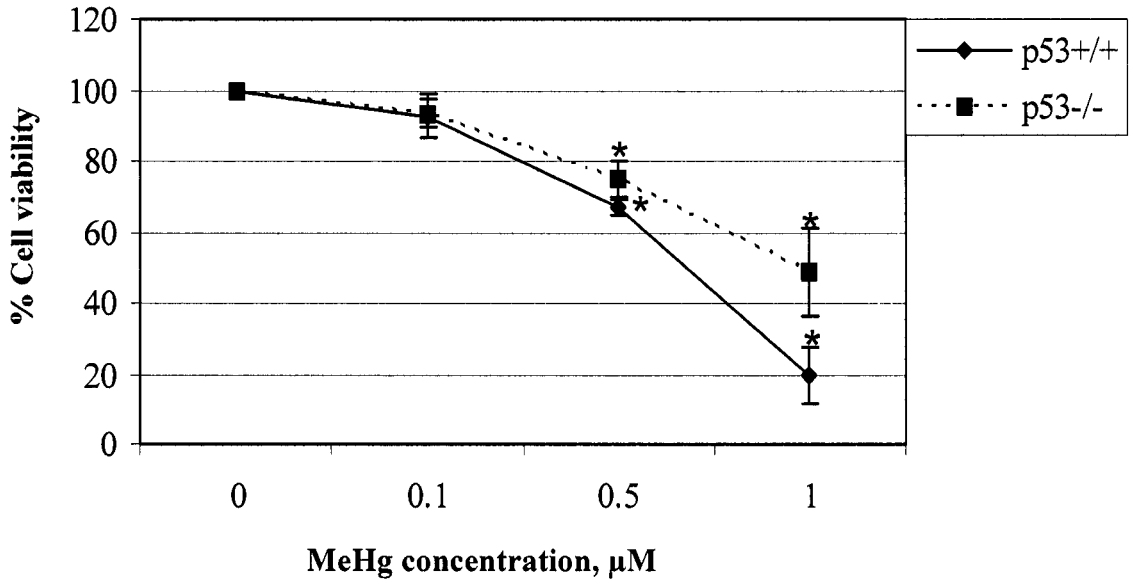

Figure 5.5. Cell viability following MeHg exposure in p53+/+ and p53-/- cells. On D3 of culture, cells were exposed to a range of MeHg concentrations for 24h and assessed for changes in viability by the neutral red assay. While changes in cell viability are similar at lower doses (0.1 μM, 0.5 μM), the overall dose response is significantly different between the genotypes as measured by ANOVA ($p \leq 0.05$). Data points represent the average of three independent experiments ± SD and MeHg concentrations producing a statistically significant change ($p \leq 0.05$) from untreated controls are indicated with an asterisk (*).

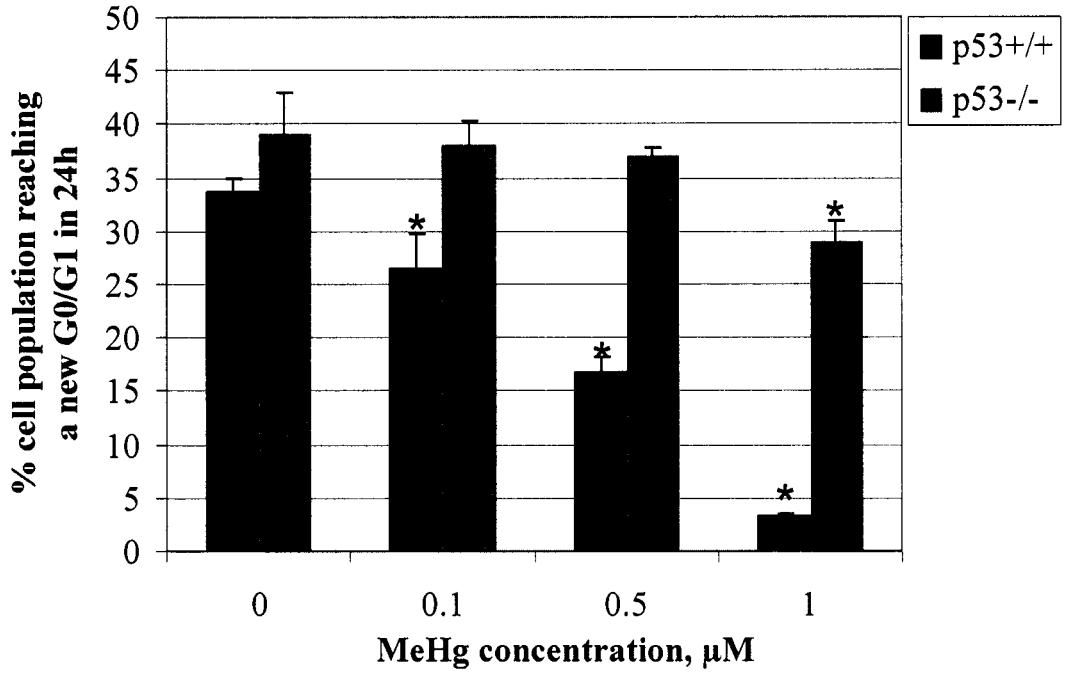

Figure 5.6. Cell cycle inhibition following MeHg exposure in p53+/+ and p53-/- NPCs. NPCs were cultured with BrdU and treated with a range of MeHg concentrations on D3 of culture and examined 24h later. Cell cycle progression was measured by flow cytometric analysis of quenched Hoechst fluorescence and propidium iodide staining allowing differentiation of cell cycle phase distribution over multiple cycles of cells. Cell cycle inhibition in response to treatment was significantly different between genotypes as measured by ANOVA ($p \leq 0.05$). Data points represent the average of three independent experiments ± SD and MeHg concentrations producing a statistically significant change ($p \leq 0.05$) from untreated controls are indicated with an asterisk (*).

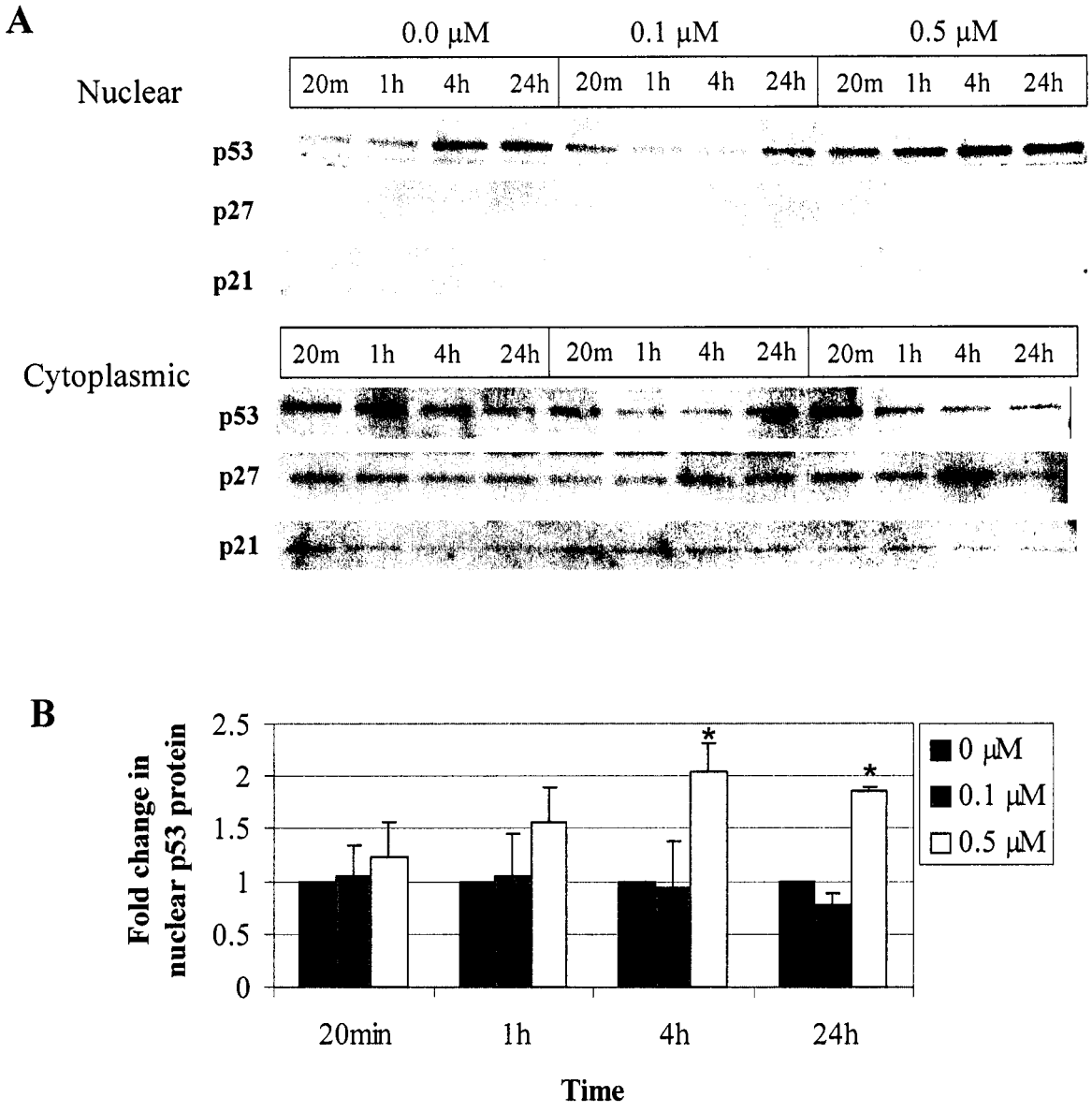

Figure 5.7. Effect of MeHg on nuclear and cytoplasmic distribution of p53, p21, and p27 protein in p53+/+ NPCs. Following MeHg treatment (0.5 μM), p53 protein increases in the nuclear fraction as early as 20 minutes and becomes statistically significant (*, $p \leq 0.05$) at 4h and 24h for an approximate 2-fold change over untreated cells (A, B). The p27 and p21 proteins remain in the cytosol and not significantly changed by treatment (A). Blots shown are representative of three independent experiments that are quantified by densitometry and expressed as average fold change ± SD over untreated NPCs in B.

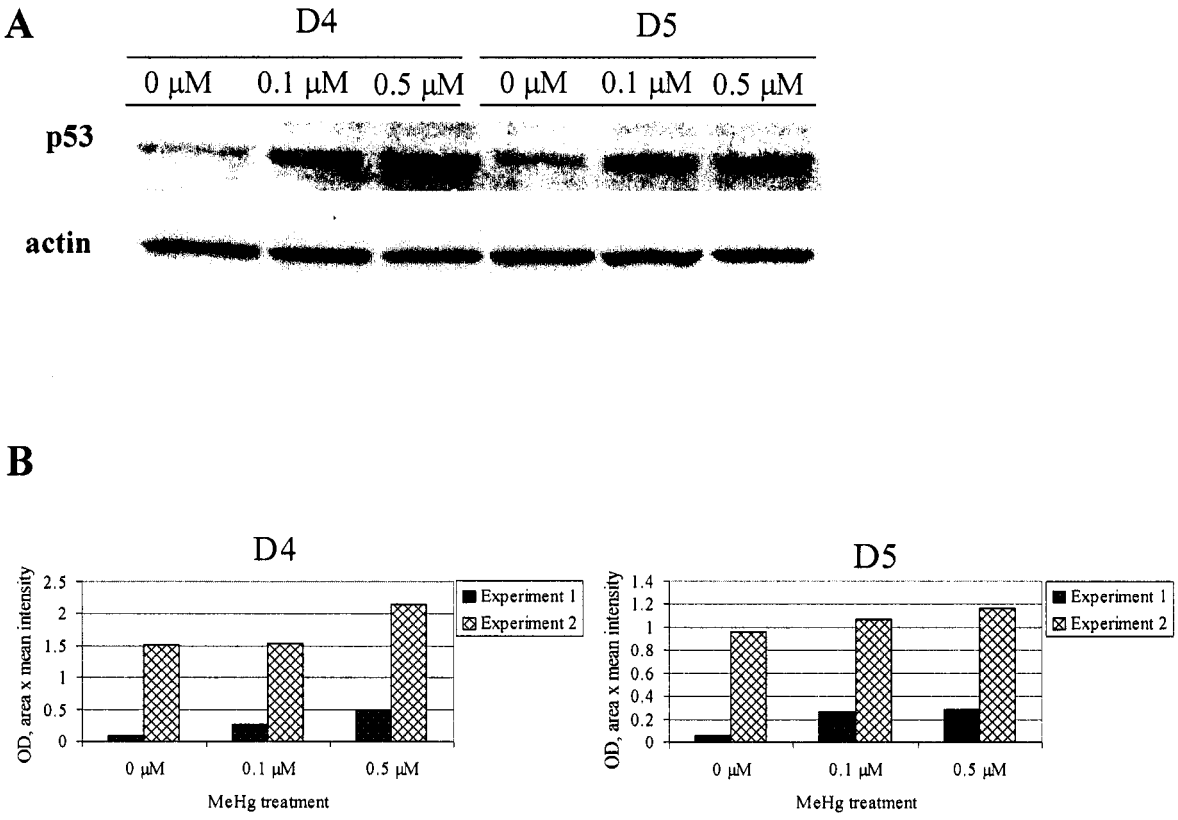

Figure 5.8. Upregulation of p53 protein is observed in whole cell lysates following MeHg exposure. Midbrain NPC cultures were treated with MeHg (0, 0.1 μM, 0.5 μM) for 24h on D3 of culture. On D4, treatment was removed and whole cell lysates were collected and probed on D4 and D5. MeHg treatment results in increases in p53 protein (0.1 μM, 0.5 μM) on D4 and D5. Western blots shown are representative of results from two independent experiments (A). Bands from each of the experiments are quantified via densitometry and expressed as raw optical density values in B.

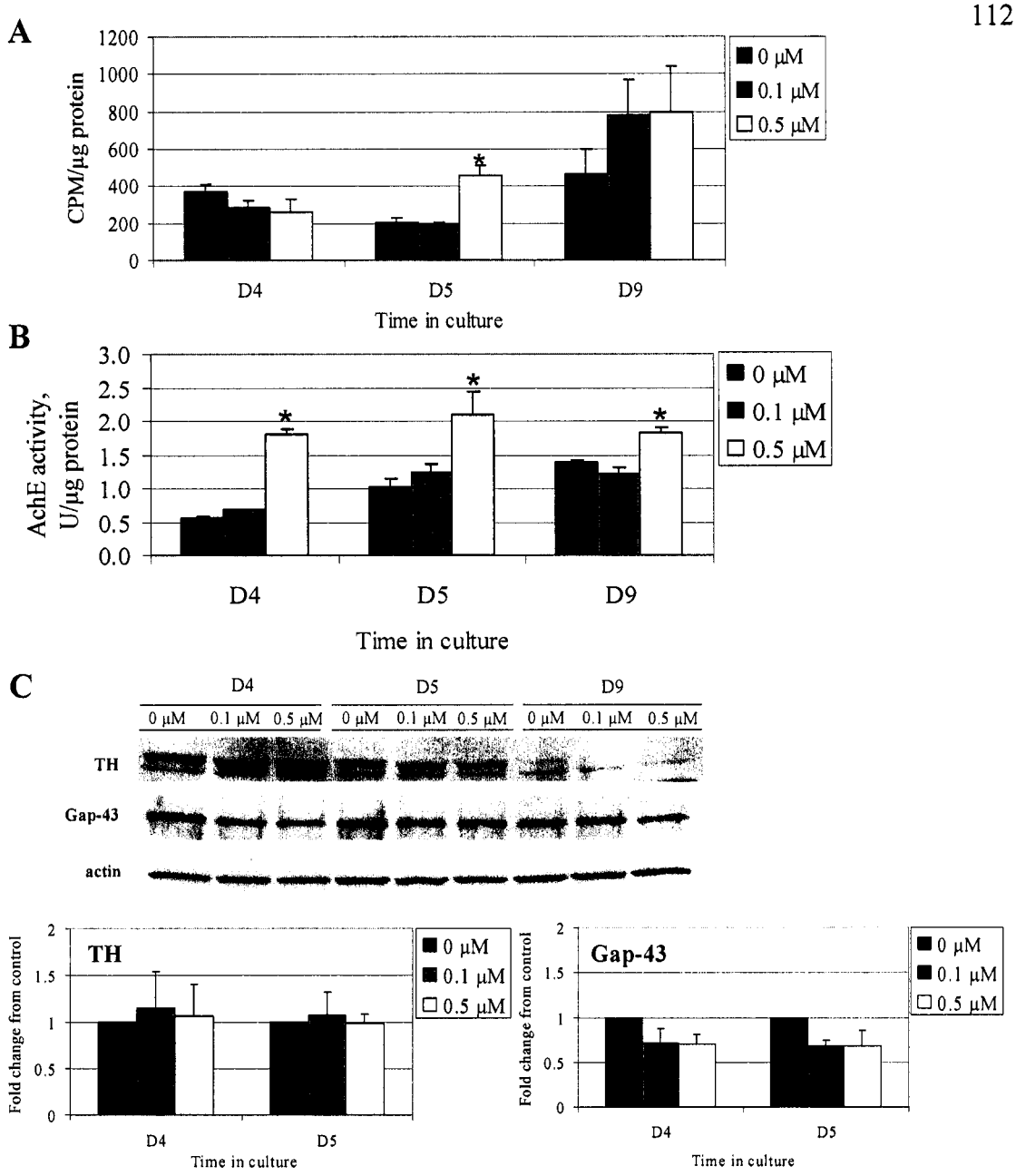

Figure 5.9. Effect of MeHg on differentiation of p53+/+ NPCs. Midbrain NPC cultures were treated with MeHg (0, 0.1 µM, 0.5 µM) for 24h on D3 of culture. On D4, treatment was removed, and NPCs were assayed for differentiation characteristics on D4, D5, and D9. (A) [3H] GABA uptake. MeHg treatment caused increases in tritiated GABA uptake on D5 and D9. (B) AchE activity. MeHg treatment (0.5 µM) caused significant increases in acetylcholinesterase activity on D4, D5, and D9. (C) TH and Gap-43 expression. Western blot analysis of TH, a marker of dopaminergic neurons showed slight but insignificant increases in expression on D4 but not D5 or D9 following MeHg treatment (0.5 µM). Gap-43 expression, a general marker of early differentiation, declined slightly with treatment. Data points (A, B) represent the mean of three independent experiments ± SD and values significantly different from untreated controls are marked with an asterisk (*). Western blots are representative of two independent experiments.

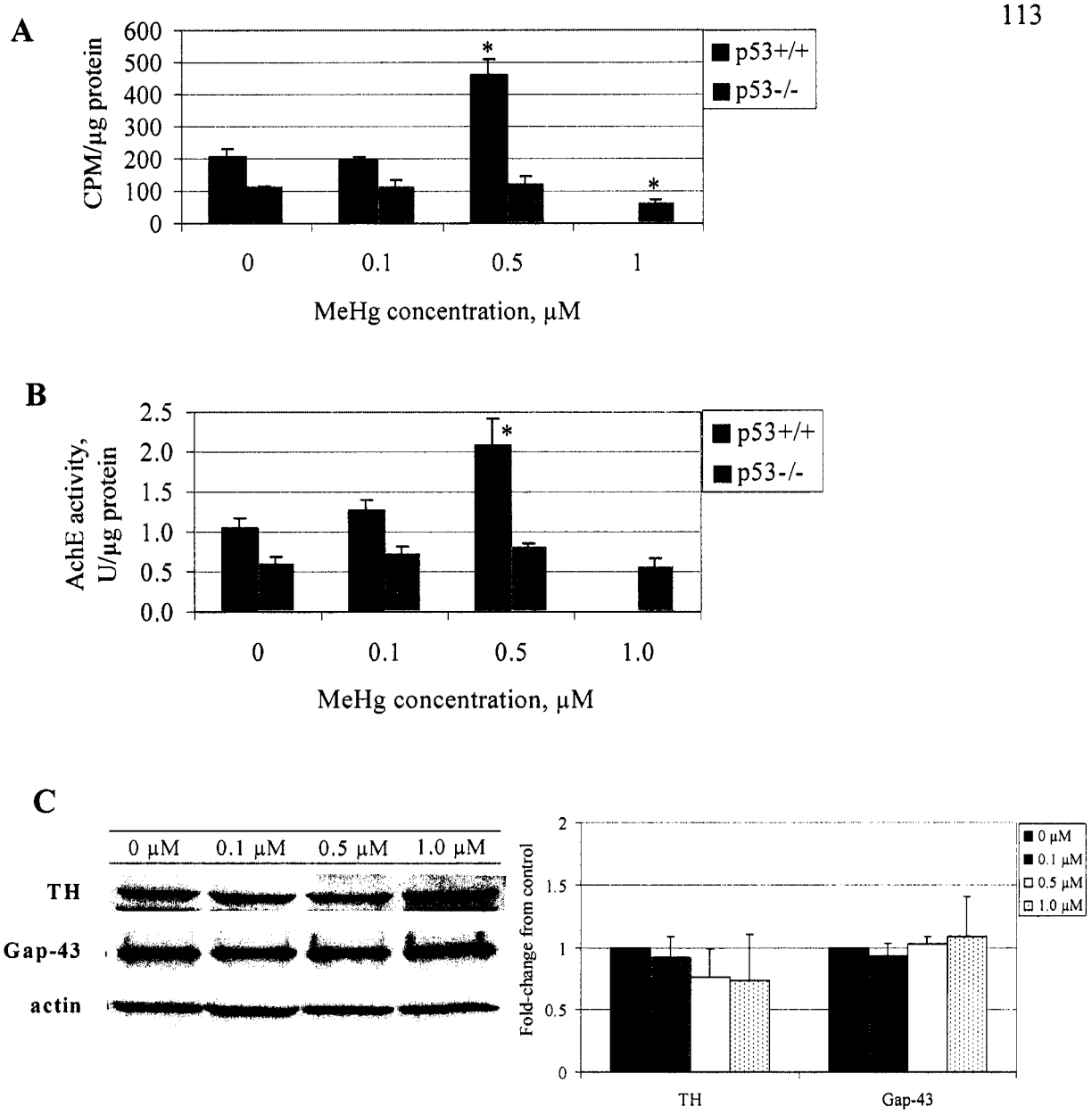

Figure 5.10. Comparison of differentiation on D5 in p53+/+ and p53-/- midbrain NPCs following MeHg treatment. (A) [3H] GABA uptake, (B) Acetylcholinesterase activity, (C) Western blot analysis of TH, a marker of dopaminergic neurons, and Gap-43, a general marker of differentiation (p53-/- NPCs only). In contrast to p53+/+ NPCs, p53-/- cells do not show an increase in any marker of differentiation following 24h of MeHg treatment and genotypes respond significantly differently to MeHg treatment as measured by ANOVA (A, B). Data points (A, B) represent the mean of three independent experiments ± SD and values significantly different from untreated controls are marked with an asterisk (*). Blots are representative of three independent experiments.

CHAPTER 6. SUMMARY AND CONCLUSIONS

The work contained in this dissertation has addressed the role of cell cycle regulatory proteins, principally p53, in normal midbrain neuronal precursor cell differentiation and following toxicant exposure. Cell cycle regulatory proteins are most frequently studied in the field of cancer biology where unregulated growth and differentiation lead to pathology. However, perturbations to proliferation and differentiation, two key dynamic processes during development, may underlie many neurodevelopmental pathologies as well. As cell cycle inhibition is a front-line defense mechanism of the cell, the premise that cell cycle inhibition following sub-lethal toxicant exposure may be a ubiquitous and sensitive endpoint calls for a better understanding of the specific contributions of these signaling pathways in neurodevelopmental toxicity. Furthermore, as observed in Chapter 5, cell cycle inhibition may lead to premature neuronal differentiation that depletes proliferating progenitor cell populations resulting in too few mature neurons in the developed organism. Experimentally, examining these hypotheses translates into careful comparisons of dose responsivity across endpoints for cell viability, cell cycle kinetics, and differentiation. A summary and integration of the important achievements, findings, and limitations of this work follows.

The p53 protein confers sensitivity to MeHg exposure with regards to cell cycle inhibition and cell death. A shift in the dose response curve for wildtype and null mouse embryonal fibroblasts and midbrain neural precursor cells was observed such that decreases in cell viability and increases in cell cycle inhibition were observed in p53 null cells, but at higher concentrations than wildtype cells. This is slightly counterintuitive: we think of p53 as a cellular defense protein yet its presence leads to greater death in these cells. The assumption is that p53-/- cells are less sensitive to cell cycle inhibition and cell death from toxicant exposure at the expense of incurring genetic damage. While not readily observable in our short time course of several days in culture, the accumulative damage incurred in p53-/- cells makes knockout mice highly prone to cancer at a much earlier age than their wildtype counterparts. For our

studies, the difference in response to MeHg exposure between genotypes demonstrates the critical role of p53 signaling in neurodevelopmental toxicant defense. As reviewed by Brash (1996), in whole animal studies of pregnant p53 wildtype and null mice exposed to radiation or benzo[a]pyrene, embryos from the p53 null mice exhibit a higher incidence of malformations as compared to wildtype embryos. Following radiation, increased teratogenicity in the absence of fetal resorption was documented while benzo[a]pyrene treated dams had higher teratogenicity and resorptions as compared to wildtype mice (Nicol et al., 1995; Norimura et al., 1996). This evidence corroborates that p53 is critical in toxicant defense during development, especially for apoptotic signaling in damaged cells, and suggests it may further participate to abort embryos damaged by radiation. Our in vitro work suggests differential sensitivity of p53+/+ and p53-/- embryos to brain malformations induced by higher dose in utero exposure to MeHg would likely be observed.

I established and characterized a mouse midbrain neural precursor cell system for the evaluation of mechanisms of normal and perturbed NPC proliferation and differentiation. I demonstrated the utility of these cultures for examining the role of specific signaling pathways in neurodevelopment through comparisons of cultures from p53+/+ and p53-/- mice, and assessed several assays and endpoints for monitoring proliferation and differentiation for future characterization of other genetically modified mouse cultures. Most informative to this work was the use of BrdU incorporation to track proliferation although cell counts and monitoring PCNA expression provided an accurate, if more gross assessment. Following MeHg exposure, we assayed for changes in differentiation via Western blotting for Gap-43 as a marker of general neuronal differentiation, measurement of acetylcholinesterase activity and 3[H]GABA uptake as indicators of functional cholinergic and GABAergic neurons, repectively, and Western blotting for tyrosine hydroxlase, an enzyme present in dopaminergic neurons. Increases in cholinergic and GABAergic neurons were observed with the functional assays while no changes in Gap-43 were measured with Western blotting. This indicates the functional assays may provide a more sensitive and more

speicifically informative measure of differentiation than Western blotting of general differentiation markers such as Gap-43 and nestin. Accordingly, an assay for [3H]dopamine uptake should be fairly straightforward to set up and may be a better assessment for dopaminergic differentiation than Western blotting of tyrosine hydroxylase. Furthermore, a functional assay for serotonergic neurons should be adopted to monitor their presence in these cultures: the mature midbrain in the mouse and humans contain serotenergic neurons although the developmental ontogeny of their appearance has not been documented in vivo.

I demonstrated a role for p27 and p53 in midbrain NPC differentiation in vitro and in vivo. While p27 has been shown to be important for differentiation of other neuronal precursor populations (i.e. cerebellar granule cells) and p53 for neuronal cell lines (i.e. PC-12 cells), this was the first examination of the midbrain NPC population. Iincreases in the p27 and p53 proteins were observed in our midbrain NPC cultures, in isolated midbrain tissue, and in sections from fixed midbrains (only examined for p27) concurrent with neuronal differentiation and decreased precursor cell proliferation. We furthermore utilized midbrain NPC cultures from p53+/+ and p53-/- mice and demonstrated greater proliferation and a different differentiation profile in cells from null mice: this demonstrates a role for p53 in the differention of these cells. We were unable to establish in vitro cultures from the p27 mice due to technical difficulties: knockouts can only be obtained through heterozygous matings, but there is not sufficient time to genotype or readily sort embryos at the time of midbrain isolation without excessively stressing the tissues. In our experiments, p27 was not responsive to MeHg treatment, indicating the utility of the p27-/- model may be optimized with examinations of other toxicants or hypotheses such as discerning whether p27 expression contributes to acquisition of a specific neuronal phenotype by using our functional assays. Culturing stem cells and neural stem cells, with special attention for the generation of dopaminergic neurons, has become an extremely popular area of research in the last several years. Certainly our midbrain NPC cultures could be exploited to pursue this research avenue and I expect that media manipulation as

discussed in Chapter 5 would enrich our dopaminergic population. Cell cycle control of differentiation in each of the specific neuronal phenotypes observed in our cultures should be an especially fruitful area of research.

In Chapter 5, I reported observations of increases in acetylcholinesterase activity and [3H]GABA uptake in midbrain NPCs following MeHg treatment that resulted in cell cycle inhibition and upregulation of the p53 protein. It appears that the toxicant induced state of cell cycle arrest biologically mimicked physiological NPC cell cycle exit and initiated differentiation of GABAergic and cholinergic neurons. Figure 6.1 shows a pictorial summary of this portion of my work. The potential consequences for the developing human nervous system of early neuronal differentiation in the absence of cell death following low dose exposures are somewhat difficult to predict. In Figure 6.2, I've listed three possible impacts: reduction in total cell number, an alteration in neuronal phenotypic composition of the brain, and altered migration and brain structure. Premature toxicant induced cell cycle arrest will deplete the proliferating progenitor population resulting in a reduced potential to generate all the cells necessary for the CNS. As discussed throughout this dissertation, reduction in brain cell number has been demonstrated to have significant functional consequences and has been observed in disorders such as schizophrenia and mental retardation (Brent, 2001). Beyond depletion of the progenitor population, what are the consequences of premature differentiation? Early appearance of GABAergic neurons, for example, could impact neurodevelopment in a time and brain region specific manner. GABA is the major inhibitory neurotransmitter in the CNS and is also the first developmentally expressed. Prior to being employed for cell-cell communication in the brain, GABA is neurotrophic. Experimentally, GABA has been shown to inhibit proliferation of cortical striatal NPCs but increase proliferation in cortical ventricular NPCs and cerebellar NPCs (Nguyen et al., 2003; Fiszman et al., 1999). GABA can influence neuronal migration as well: it increases random motility of more mature, post-mitotic (Tuj+) neurons from the cortical plate and can act as a chemoattractant to direct migration via radial glia of immature NPCs (nestin+) from cortical ventricular

zone (Haydar et al., 2000; Lopez-Bendito et al., 2003). While no in vivo studies have been undertaken, the aforementioned in vitro evidence strongly suggests that inappropriate differentiation of GABAergic neurons could severely disrupt proliferation and migration of a developing brain structure. Among many brain abnormalities observed in autistic spectrum disorders, overgrowth of GABAergic neurons has been characterized in a subset of patients indicating serious functional changes would likely be observed if our experimental predictions held true in vivo (Polleux and Lauder, 2004). Finally, it is worth noting that GABA receptor agonists including some sedatives, tranquilizers, and anti-epileptic drugs are somewhat controversially prescribed during pregnancy but may nonetheless subtly affect brain development.

Cell cycle inhibition following toxicant exposure has been observed in our laboratory and others in response to a spectrum of toxicants. However, induction of early differentiation following cell cycle inhibition in neural precursor cells has not been explored nearly so fully across agents. The comparison of several agents in the mouse midbrain NPC culture system for effects on viability, proliferation, and differentiation, will provide extremely valuable information regarding the specificity of our observations to MeHg and the utility of the cultures for neurodevelopmental toxicity screening. While we found good temporal correlation between markers of proliferation and differentiation in our cultures and in the developing midbrain, the ramification of in vitro observations of cell cycle delay for in vivo development remain difficult to examine experimentally. Control of dose at the target tissue, timing, and major physiological and structural changes between exposure and experimental observation are inherent to mammalian in vivo developmental toxicity testing. Nonetheless, the hypothesis that permanent structural and functional nervous system alterations can be induced by toxicant exposure resulting in cycle delay, can perhaps be best explored in detail in simpler organisms such as *Caenorhabditis elegans* or *Danio rerio* that can then direct experimental design for mammalian examinations. Another next step is to more carefully explore the specific regulation of the p53 protein under conditions promoting differentiation and following stress. Because of the complex

mixture of cells in our cultures and the anticipated difficulty of transfections in these primary cells, at this point, this research should probably be explored in a simpler in vitro model. As discussed in Chapter 5, deacetylation of lys382 is the only post-translational modification to date that has been specifically associated with induction of neuronal differentiation: this was observed in NGF treated PC-12 cells but could be examined in the midbrain NPC cultures without too much difficulty.

We suggest that cell cycle inhibition may be a common cellular response to many toxicant induced upstream signals and use MeHg as a model toxicant to explore potential low dose responses of cycling precursor cells to this inhibition. We observed significant cell cycle inhibition in the absence of cytotoxicity following treatment of midbrain NPCs to 0.1 μM MeHg. In order to compare media concentrations of in vitro studies to in vivo, and ultimately from animal to human models, Lewandowski et al. (2003) compared media and intracellular concentration of MeHg in order to develop a common dose metric for comparisons. In both rat (primary midbrain NPCs) and mouse (P-19 cells), an approximate 3-fold intracellular concentration of mercury was observed. If this is also true for mouse midbrain NPCs, we would expect 0.1 μM MeHg to result in 0.3 μg/g mercury in our cells. Figure 6.3 shows comparisons of lowest observed adverse effect levels (LOAEL) for cell cycle inhibition in vitro and in vivo for rats, mice, and humans (Lewandowski et al., 2003). Our current results present a new LOAEL in mice for MeHg that is a magnitude lower in concentration than previously observed in the literature. Furthermore, brain mercury concentrations determined at autopsy of "non-symptomatic" human populations from the Seychelles Islands (Laptham et al., 1995) and Japan (Nishimura et al., 1974) ranged from 0.16 - 0.3 μg/g brain tissue. Compared to the rat, the mouse appears to be more sensitive to MeHg and more closely resembles human susceptibility to MeHg neurodevelopmental toxicity. As indicated in Figure 6.5, the concentrations used in this study are comparable to common human dietary exposure and may represent experimental evidence to continue to question what constitutes a true NOAEL for human MeHg exposure.

We have addressed our research questions in mouse embryonal fibroblasts and midbrain neural precursor cells (NPCs) from mice wildtype and null for the p53 protein. The knockout mouse has become a valuable tool for several fields of biology and some strengths and limitations deserve mention. First, assuming a properly executed gene disruption or deletion, this is the only method capable of total ablation of functional mRNA and/or protein expression. Many proteins are known to operate on functional gradients such that low versus high levels lead to different outcomes. The knockout mouse model prevents this potential confounder that is often observed when utilizing pharmacological inhibitors, dominant negative and overexpression transfections, or RNA interference techniques. When inferring the role of the missing protein in a knockout model, it is essential to remember that the organism has developed in its absence, and other compensatory pathways, indeed, entire regulatory networks, may be altered to make up for lost function. This can often provide crucial and exciting insight about the overlap and redundancy of biological processes, such as discussed for the cell cycle in Chapter 1, but limits the extent of conclusions that may be drawn about a critical or specific role for the protein. Two structural homologues of the p53 protein have been identified and are described in Table 6.1. Despite good structural similarity among these proteins and some functional overlap with regards to cell cycle regulation and apoptosis, their physiological roles are apparently diverse as indicated by null mouse model phenotypes, human disease correlates, and mutations in human cancers (reviewed in Moll and Slade, 2004). As described previously, p53 null mice exhibit a low incidence of neural tube defects but otherwise lack a developmental phenotype. However, whether this is due to compensation by the p63 and p73 proteins has not directly been examined. Multiple promoters and alternative splicing for p63 and p73 generate several protein products; only one isoform of each contains the p53 transactivation domain (TA), and has been observed to mimic p53 function with regards to transcriptionally activating p53 target genes involved in cell cycle control and apoptosis (Yang et al. 1998; 2000). These TA isoforms, TAp63 and TAp73, do not appear to be predominantly expressed during development. Furthermore, the severe and

distinct phenotypes of p63 and p73 null mice indicate a specific developmental role for these proteins that cannot be substituted by p53 (Table 6.1) (Mills et al., 1999; Yang et al., 2000). Microarray analysis of differential gene expression across development between p53+/+ and p53-/- embryos should begin to answer how p53 null mice develop mostly normally. A simple experiment comparing gene expression of untreated midbrain p53+/+ and p53-/- NPCs and following MeHg treatment would greatly enhance our understanding of the contribution of p53 to normal midbrain NPC differentiation and following toxicant response. Ultimately, our observations of induced differentiation following MeHg treatment leading to upregulation of p53 and cell cycle arrest in p53+/+ but not p53-/- NPCs could also be confirmed via another experimental approach such as through the use of pifithrin-α, a pharmacological inhibitor of p53 (Gudkov and Komarova, 2005). Such direct comparisons of experimental strategies would further elucidate the specificity of p53 signaling in normal and toxicant induced neuronal differentiation.

Finally, the research contained within this dissertation utilized a variety of strategies and experimental systems to address mechanisms of normal and perturbed neurodevelopment. I first utilized a very simple in vitro model of mouse embryonal fibroblasts to investigate mechanisms of MeHg, a known human neurodevelopmental toxicant. Our observations in the MEFs regarding the role of p53 signaling pathways in MeHg induced changes in cell viability and cell cycle kinetics held true when we moved to a primary neuronal culture system. With the aim of beginning to assess the effects of a single gene knockout on cell cycle control, we developed a quantitative mathematical model for the cell cycle checkpoint pathways and cell death are conceptualized as rates using literature values. This model was validated through comparisons with our experimental data from the MEFs and predicts cell cycle phase populations across three generations of cells. It is anticipated that further development of this model will test hypotheses of mechanisms of toxicants across dose response relationships via perturbations to the model parameters. In Chapters 4 and 5, I characterized temporal proliferation, differentiation, and expression of p21, p27, and

p53 in cultured midbrain NPCs and compared this to the developing midbrain in vivo. Again, we saw surprisingly good temporal correlation of these dynamic processes and expression of specific proteins in our cultured cells and the developing mouse brain. The overall goal of neurodevelopmental toxicological research is to extrapolate findings to better understand and protect human neurodevelopment. To illustrate, Figure 6.4 outlines the types of information one can gather across experimental platforms and species. In general, moving left to right across Figure 6.4, meaningful context regarding toxicant impacts on whole systems is gained along with increasing complexity of interpretation of results, and decreased capability to manipulate your experimental system. Our results support the utility of investigating across systems of biological complexity in order to more fully inform human health risk assessment.

In summary, this work has explored the role of key cell cycle checkpoint pathways in normal neurodevelopment and following toxicant exposure from an experimental and quantitative modeling approach. Importantly, we showed p27 and p53 help facilitate normal midbrain NPC differentiation, and determined a role for the p53 protein in cell cycle inhibition and subsequent neuronal differentiation following MeHg exposure in these cells. In addition to contributions to the field of developmental toxicology, the careful characterization of the mouse midbrain NPC system for both wildtype and p53 null cells has provided valuable groundwork for ongoing use of this system in our laboratory for examinations of other toxicants, including domoic acid, arsenic, and cadmium, and transgenic mouse models such as the recently acquired ubiquitin-GFP mouse.

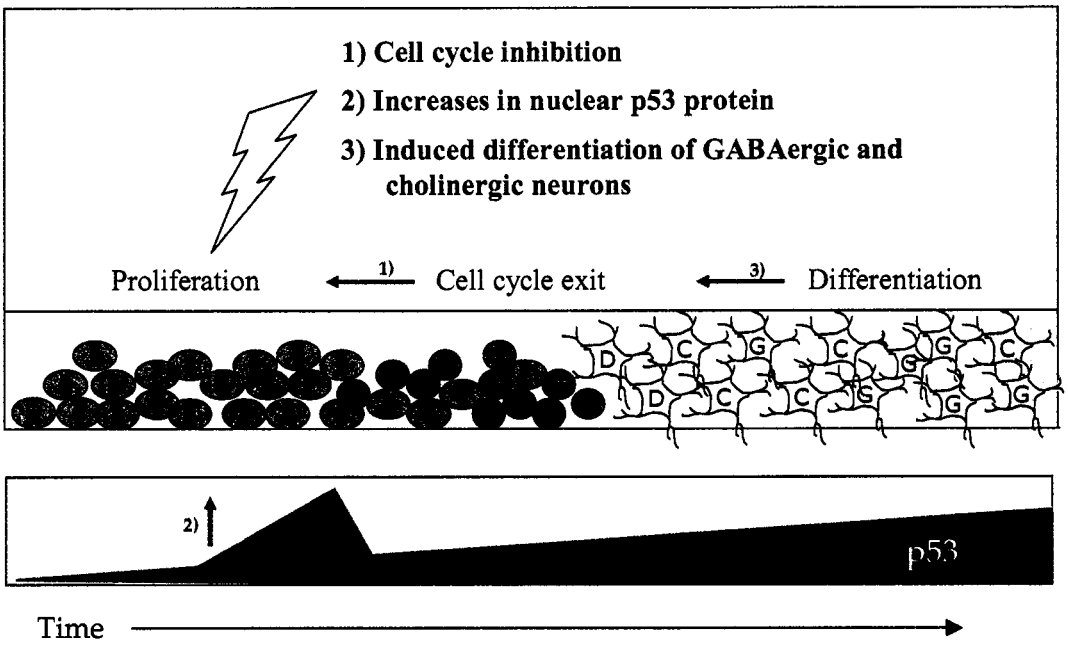

Figure 6.1 A role for p53 in early midbrain NPC differentiation following sublethal MeHg exposure. This figure summarizes the results from investigations in Chapter 5 where MeHg treatment (lightning bolt) on D3 in culture caused cell cycle inhibition, increases in p53 protein, and early differentiation of GABAergic (yellow, G) and cholinergic (orange, C), but not dopaminergic neurons (pink, D).

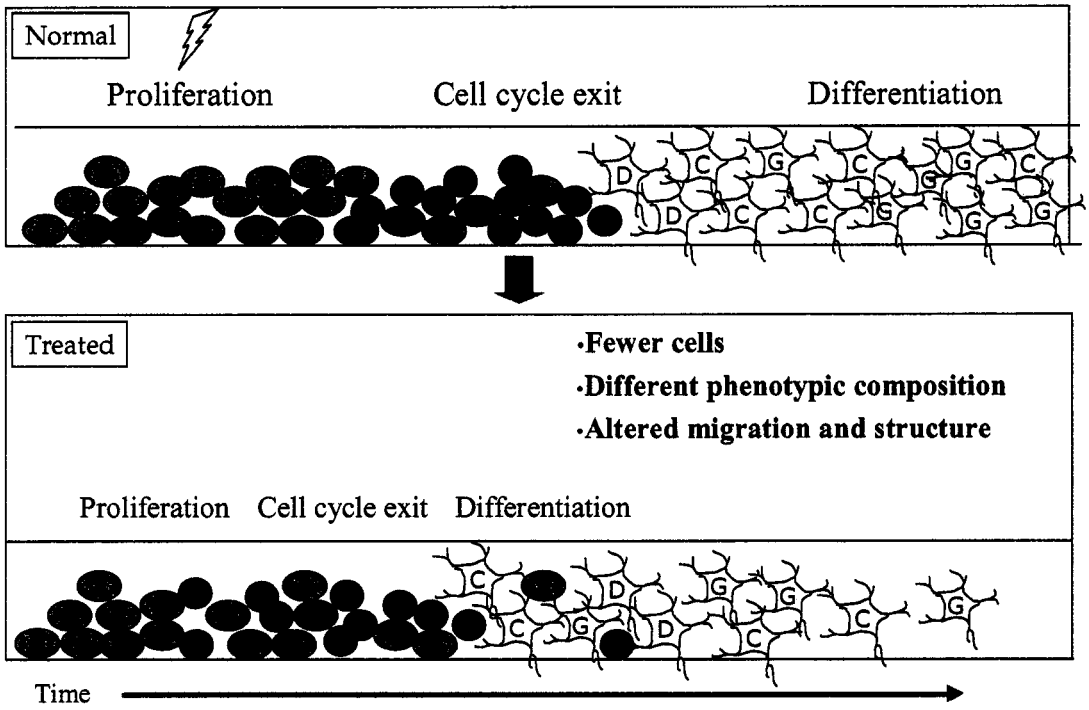

Figure 6.2 Implications of toxicant induced early differentiation. The "normal" panel demonstrates the time dependent progression of neuronal precursor cell proliferation, cell cycle exit, and differentiation. The potential impacts of toxicant treatment of cycling precursor cells (lightning bolt) for a cell population or developing brain region include a reduction in total cell number due to depletion of the precursor population by early cell cycle exit, an altered composition of mature differentiated neuron phenotypes, and changes in organization of brain structure.

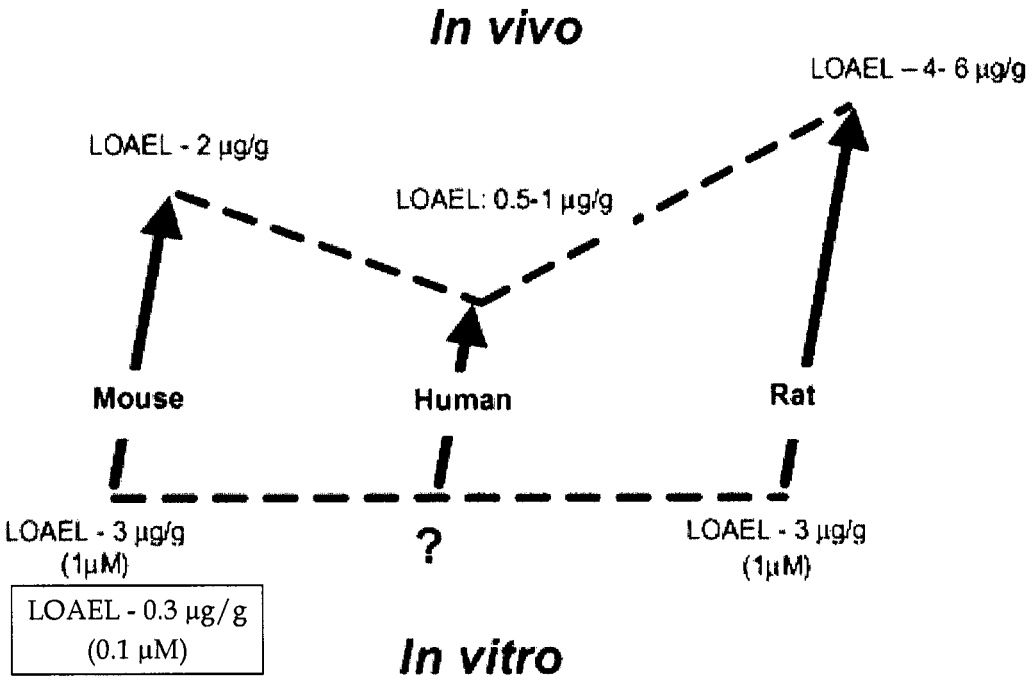

Figure 6.3 Use of the parallelogram approach to compare effects of MeHg across species and experimental system. Lewandowski et al. (2003) determined lowest observed adverse effect levels (LOAELs) for MeHg induced changes in proliferation for in vitro and in vivo experiments from the literature across species. Our observations of significant cell cycle inhibition following treatment with 0.1 µM MeHg in midbrain NPCs presents a new LOAEL for in vitro effects in mouse cells.

Table 6.1 Functional overlap of p53 structural homologues in neurodevelopment and cancer.

	Null mice		Human correlate	
	Neurodevelopment	Cancer	Neurodevelopment	Cancer
p53	Low incidence NTDs Altered neuronal phenotypes?	Highly prone Overexpression = enhanced aging	Li-Fraumini syndrome	Most frequently mutated protein
p63	Severe craniofacial defects but mostly limb and ectoderm complications	Dies shortly after birth	Ectrodactyly-Ectodermal dysplasia facial Clefts (EEC), Split-Hand/split-Foot Malformation-4 (SHFM-4)	Rarely mutated
p73	Hippocampal dysgenesis Altered behavior	No increased tumorigenesis	N/A	Rarely mutated

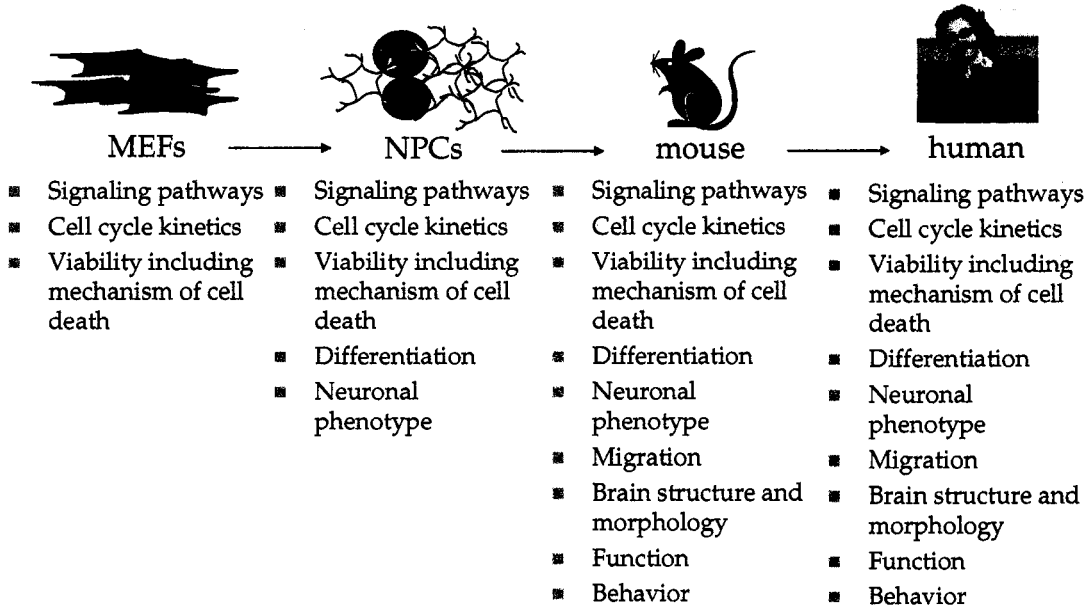

Figure 6.4 Ability of experimental systems to assess and predict neurodevelopmental toxicity across multiple levels of biological complexity. Our experimental questions were assessed in mouse embryonal fibroblasts (MEFs), a simple in vitro cell system, primary midbrain neuronal precursor cells (NPCs), and in isolated tissue from mouse midbrain. We observed good correlation of results across experimental systems. Listed in the figure are types of information one can gather across experimental platforms. In general, moving left to right will increase capacity to understand impacts on whole systems and complexity of interpretation of results. Additionally, the ability to specifically manipulate the experimental system is reduced left to right. Understanding and interpreting experimental results across biological systems and species should greatly assist our ability to predict and assess human health risk.

REFERENCES

Aarnaes, E. B. Kirkhus, O. P. Clausen (1990). "Mathematical model analysis of mouse epidermal cell kinetics measured by bivariate DNA/anti-bromodeoxyuridine flow cytometry and continuous [3H]-thymidine labeling." Cell Tissue Kinet 23(5):409-24.

Agarwal, M. L., W. R. Taylor, M. V. Chernov, O. B. Chernova and G. R. Stark (1998). "The p53 network." J Biol Chem 273(1): 1-4.

Alarcon-Vargas, D. and Z. Ronai (2002). "p53-Mdm2--the affair that never ends." Carcinogenesis 23(4): 541-7.

Alessandrini, A., D. S. Chiaur and M. Pagano (1997). "Regulation of the cyclin-dependent kinase inhibitor p27 by degradation and phosphorylation." Leukemia 11(3): 342-5.

Almog, N. and V. Rotter (1997). "Involvement of p53 in cell differentiation and development." Biochim Biophys Acta 1333(1): F1-27.

Aloni-Grinstein, R., D. Schwartz and V. Rotter (1995). "Accumulation of wild-type p53 protein upon gamma-irradiation induces a G2 arrest-dependent immunoglobulin kappa light chain gene expression." Embo J 14(7): 1392-401.

Altman, J. and S. A. Bayer (1981). "Time of origin of neurons of the rat superior colliculus in relation to other components of the visual and visuomotor pathways." Exp Brain Res 42(3-4): 424-34.

Appella, E. and C. W. Anderson (2001). "Post-translational modifications and activation of p53 by genotoxic stresses." Eur J Biochem 268(10): 2764-72.

Armstrong, J. F., M. H. Kaufman, D. J. Harrison and A. R. Clarke (1995). "High-frequency developmental abnormalities in p53-deficient mice." Curr Biol 5(8): 931-6.

Bally-Cuif, L. and M. Hammerschmidt (2003). "Induction and patterning of neuronal development, and its connection to cell cycle control." Curr Opin Neurobiol 13(1): 16-25.

Basse, B., B. C. Baguley, E. S. Marshall, W. R. Joseph, B. van Brunt, G. Wake and D. J. Wall (2003). "A mathematical model for analysis of the cell cycle in cell lines derived from human tumors." J Math Biol 47(4): 295-312.

Bennett, G. D., B. M. Amore, R. H. Finnell, B. Wlodarczyk, T. F. Kalhorn, G. L. Skiles, S. D. Nelson and J. T. Slattery (1996). "Teratogenicity of carbamazepine-10,

11-epoxide and oxcarbazepine in the SWV mouse." J Pharmacol Exp Ther 279(3): 1237-42.

Berthet, C., E. Aleem, V. Coppola, L. Tessarollo and P. Kaldis (2003). "Cdk2 knockout mice are viable." Curr Biol 13(20): 1775-85.

Betsholtz, C., L. Karlsson and P. Lindahl (2001). "Developmental roles of platelet-derived growth factors." Bioessays 23(6): 494-507.

Bibel, M., J. Richter, K. Schrenk, K. L. Tucker, V. Staiger, M. Korte, M. Goetz and Y. A. Barde (2004). "Differentiation of mouse embryonic stem cells into a defined neuronal lineage." Nat Neurosci 7(9): 1003-9.

Billon, N., A. Terrinoni, C. Jolicoeur, A. McCarthy, W. D. Richardson, G. Melino and M. Raff (2004). "Roles for p53 and p73 during oligodendrocyte development." Development 131(6): 1211-20.

Borisuk, M. T. and J. J. Tyson (1998). "Bifurcation analysis of a model of mitotic control in frog eggs." J Theor Biol 195(1): 69-85.

Borriello, A., V. D. Pietra, M. Criscuolo, A. Oliva, G. P. Tonini, A. Iolascon, V. Zappia and F. D. Ragione (2000). "p27Kip1 accumulation is associated with retinoic-induced neuroblastoma differentiation: evidence of a decreased proteasome-dependent degradation." Oncogene 19(1): 51-60.

Bossenmeyer-Pourie, C., V. Lievre, S. Grojean, V. Koziel, T. Pillot and J. L. Daval (2002). "Sequential expression patterns of apoptosis- and cell cycle-related proteins in neuronal response to severe or mild transient hypoxia." Neuroscience 114(4): 869-82.

Brandeis, M., I. Rosewell, M. Carrington, T. Crompton, M. A. Jacobs, J. Kirk, J. Gannon and T. Hunt (1998). "Cyclin B2-null mice develop normally and are fertile whereas cyclin B1-null mice die in utero." Proc Natl Acad Sci U S A 95(8): 4344-9.

Brash, B. E. (1996). "Cellular proofreading." Nature Med 2:525-6.

Brent, R. L. (2001). "Addressing environmentally caused human birth defects." Pediatr Rev 22(5): 153-65.

Brooks, C. L. and W. Gu (2003). "Ubiquitination, phosphorylation and acetylation: the molecular basis for p53 regulation." Curr Opin Cell Biol 15(2): 164-71.

Brooks, C. L. and W. Gu (2004). "Dynamics in the p53-Mdm2 ubiquitination pathway." Cell Cycle 3(7): 895-9.

Brugarolas, J., C. Chandrasekaran, J. I. Gordon, D. Beach, T. Jacks and G. J. Hannon (1995). "Radiation-induced cell cycle arrest compromised by p21 deficiency." Nature 377(6549): 552-7.

Burbacher, T. M., P. M. Rodier and B. Weiss (1990). "Methylmercury developmental neurotoxicity: a comparison of effects in humans and animals." Neurotoxicol Teratol 12(3): 191-202.

Cadwell, C. and G. P. Zambetti (2001). "The effects of wild-type p53 tumor suppressor activity and mutant p53 gain-of-function on cell growth." Gene 277(1-2): 15-30.

Cai, J., A. Cheng, Y. Luo, C. Lu, M. P. Mattson, M. S. Rao and K. Furukawa (2004). "Membrane properties of rat embryonic multipotent neural stem cells." J Neurochem 88(1): 212-26.

Calegari, F. and W. B. Huttner (2003). "An inhibition of cyclin-dependent kinases that lengthens, but does not arrest, neuroepithelial cell cycle induces premature neurogenesis." J Cell Sci 116(Pt 24): 4947-55.

Carlson, B. A., M. M. Dubay, E. A. Sausville, L. Brizuela and P. J. Worland (1996). "Flavopiridol induces G1 arrest with inhibition of cyclin-dependent kinase (CDK) 2 and CDK4 in human breast carcinoma cells." Cancer Res 56(13): 2973-8.

Castelo-Branco, G., N. Rawal and E. Arenas (2004). "GSK-3beta inhibition/beta-catenin stabilization in ventral midbrain precursors increases differentiation into dopamine neurons." J Cell Sci 117(Pt 24): 5731-7.

Castoldi, A. F., S. Barni, I. Turin, C. Gandini and L. Manzo (2000). "Early acute necrosis, delayed apoptosis and cytoskeletal breakdown in cultured cerebellar granule neurons exposed to methylmercury." J Neurosci Res 59(6): 775-87.

Chan, T. A., P. M. Hwang, H. Hermeking, K. W. Kinzler and B. Vogelstein (2000). "Cooperative effects of genes controlling the G(2)/M checkpoint." Genes Dev 14(13): 1584-8.

Chen M. S., J. Hurov, L. S. White, T. Woodford-Thomas, H. Pwnica-Worms (2001). "Absence of apparent phenotype in mice lacking Cdc25C protein phosphatase." Mol Cell Biol 21(12):3853-61.

Chen, P. and N. Segil (1999). "p27(Kip1) links cell proliferation to morphogenesis in the developing organ of Corti." Development 126(8): 1581-90.

Chernov, M. V., L. J. Bean, N. Lerner and G. R. Stark (2001). "Regulation of ubiquitination and degradation of p53 in unstressed cells through C-terminal phosphorylation." J Biol Chem 276(34): 31819-24.

Choi, B. H. (1991). "Effects of methylmercury on neuroepithelial germinal cells in the developing telencephalic vesicles of mice." Acta Neuropathol (Berl) 81(4): 359-65.

Choi, B. H., L. W. Lapham, L. Amin-Zaki and T. Saleem (1978). "Abnormal neuronal migration, deranged cerebral cortical organization, and diffuse white matter astrocytosis of human fetal brain: a major effect of methylmercury poisoning in utero." J Neuropathol Exp Neurol 37(6): 719-33.

Choi, B. H. and H. Simpkins (1986). "Changes in the molecular structure of mouse fetal astrocyte nucleosomes produced in vitro by methylmercuric chloride." Environ Res 39(2): 321-30.

Choi, J. and L. A. Donehower (1999). "p53 in embryonic development: maintaining a fine balance." Cell Mol Life Sci 55(1): 38-47.

Chung S., K. C. Sonntag, T. Andersson, L. M. Bjorklund, J. J. Park, D. W. Kim, U. J. Kang, O. Isacson, K. S. Kim (2002). "Genetic engineering of mouse embryonic stem cells by Nurr1 enhances differentiation and maturation into dopaminergic neurons." Eur J Neurosci 16(10):1829-38.

Chylicki, K., M. Ehinger, H. Svedberg, G. Bergh, I. Olsson and U. Gullberg (2000). "p53-mediated differentiation of the erythroleukemia cell line K562." Cell Growth Differ 11(6): 315-24.

Chylicki, K., M. Ehinger, H. Svedberg and U. Gullberg (2000). "Characterization of the molecular mechanisms for p53-mediated differentiation." Cell Growth Differ 11(11): 561-71.

Cole T. B., B. J. Walter, D. M. Shih, A. D. Tward, A. J. Lusis, C. Timchalk, R. J. Richter, L. G. Costa, C. E. Furlong (2005). "Toxicity of chlorpyrifos and chlorpyrifos oxon in transgenic mouse model of the human paraoxonase (PON1) Q192R polymorphism." Pharmacogenet Genomics 15(8): 589-98.

Coles, C. D., R. T. Brown, I. E. Smith, K. A. Platzman, S. Erickson and A. Falek (1991). "Effects of prenatal alcohol exposure at school age. I. Physical and cognitive development." Neurotoxicol Teratol 13(4): 357-67.

Collier, T. J. and C. E. Sortwell (1999). "Therapeutic potential of nerve growth factors in Parkinson's disease." Drugs Aging 14(4): 261-87.

Conlon, I. and M. Raff (1999). "Size control in animal development." Cell 96(2): 235-44.

Coqueret, O. (2003). "New roles for p21 and p27 cell-cycle inhibitors: a function for each cell compartment?" Trends Cell Biol 13(2): 65-70.

Cosenza, M. E. and J. Bidanset (1995). "Effects of chlorpyrifos on neuronal development in rat embryo midbrain micromass cultures." Vet Hum Toxicol 37(2): 118-21.

Cremisi, F., A. Philpott and S. Ohnuma (2003). "Cell cycle and cell fate interactions in neural development." Curr Opin Neurobiol 13(1): 26-33.

Cross, F. R., V. Archambault, M. Miller and M. Klovstad (2002). "Testing a mathematical model of the yeast cell cycle." Mol Biol Cell 13(1): 52-70.

Crump K. S., T. Kjellstrom, A. M. Shipp, A. Silvers, A. Stewart (1998). "Influence of prenatal mercury exposure upon scholastic and psychological test performance: benchmark analysis of a New Zealand cohort." Risk Anal 18(6):701-13.

Crumpton, T. L., F. J. Seidler and T. A. Slotkin (2000). "Developmental neurotoxicity of chlorpyrifos in vivo and in vitro: effects on nuclear transcription factors involved in cell replication and differentiation." Brain Res 857(1-2): 87-98.

Crumpton, T. L., F. J. Seidler and T. A. Slotkin (2000). "Is oxidative stress involved in the developmental neurotoxicity of chlorpyrifos?" Brain Res Dev Brain Res 121(2): 189-95.

Cunningham, J. J., E. M. Levine, F. Zindy, O. Goloubeva, M. F. Roussel and R. J. Smeyne (2002). "The cyclin-dependent kinase inhibitors p19(Ink4d) and p27(Kip1) are coexpressed in select retinal cells and act cooperatively to control cell cycle exit." Mol Cell Neurosci 19(3): 359-74.

Cunningham, J. J. and M. F. Roussel (2001). "Cyclin-dependent kinase inhibitors in the development of the central nervous system." Cell Growth Differ 12(8): 387-96.

Das, K. P., T. M. Freudenrich and W. R. Mundy (2004). "Assessment of PC12 cell differentiation and neurite growth: a comparison of morphological and neurochemical measures." Neurotoxicol Teratol 26(3): 397-406.

Davidson P. W., G. J. Myers, C. Cox, C. F. Shamlaye, D. O. Marsh, M. A. Tanner, M. Berlin, J. Sloane-Reeves, E. Cernichiari, O. Choisy, et al. (1995). "Longitudinal neurodevelopmental study of Seychellois children following in utero exposure to

methylmercury from maternal fish ingestion: outcomes at 19 and 29 months." Neurotoxicology 16(4): 677-88/

Davidson P. W., G. J. Myers, C. Cox, C. Axtell, C. Shamlaye, J. Sloane-Reeves, E. Cernichiari, L. Needham, A. Choi, Y. Wang, M. Berlin, T. W. Clarkson (1998). "Effects of prenatal and postnatal methylmercury exposure from fish consumption on neurodevelopment: outcomes at 66 months of age in the Seychelles Child Development Study." JAMA 280(8):701-7.

Delalle, I., T. Takahashi, R. S. Nowakowski, L. H. Tsai and V. S. Caviness, Jr. (1999). "Cyclin E-p27 opposition and regulation of the G1 phase of the cell cycle in the murine neocortical PVE: a quantitative analysis of mRNA in situ hybridization." Cereb Cortex 9(8): 824-32.

Deng C., P. Zhang, J. W. Harper, S. J. Elledge, P. Leder (1995). "Mice lacking p21CIP1/WAF1 undergo normal development, but are defective in G1 checkpoint control." 82(4):675-84.

Donehower, L. A., M. Harvey, B. L. Slagle, M. J. McArthur, C. A. Montgomery, Jr., J. S. Butel and A. Bradley (1992). "Mice deficient for p53 are developmentally normal but susceptible to spontaneous tumours." Nature 356(6366): 215-21.

Dumont, F. J. and Q. Su (1996). "Mechanism of action of the immunosuppressant rapamycin." Life Sci 58(5): 373-95.

Durand, B., F. B. Gao and M. Raff (1997). "Accumulation of the cyclin-dependent kinase inhibitor p27/Kip1 and the timing of oligodendrocyte differentiation." Embo J 16(2): 306-17.

Edlund, T. and T. M. Jessell (1999). "Progression from extrinsic to intrinsic signaling in cell fate specification: a view from the nervous system." Cell 96(2): 211-24.

Eguchi, Y., A. Srinivasan, K. J. Tomaselli, S. Shimizu and Y. Tsujimoto (1999). "ATP-dependent steps in apoptotic signal transduction." Cancer Res 59(9): 2174-81.

Eizenberg, O., A. Faber-Elman, E. Gottlieb, M. Oren, V. Rotter and M. Schwartz (1996). "p53 plays a regulatory role in differentiation and apoptosis of central nervous system-associated cells." Mol Cell Biol 16(9): 5178-85.

Ellman G. L., K. D. Courtney, V. Andres Jr., R. M. Feather-Stone (1961). "A new and rapid colorimetric determination of acetylcholinesterase activity." Biochem Pharmacol 7:88-95.

Eto, K., S. Oyanagi, Y. Itai, H. Tokunaga, Y. Takizawa and I. Suda (1992). "A fetal type of Minamata disease. An autopsy case report with special reference to the nervous system." Mol Chem Neuropathol 16(1-2): 171-86.

Eto, K. (1997). "Pathology of Minamata disease." Toxicol Pathol 25(6): 614-23.

Eto, K., A. Yasutake, K. Miyamoto, H. Tokunaga and Y. Otsuka (1997). "Chronic effects of methylmercury in rats. II. Pathological aspects." Tohoku J Exp Med 182(3): 197-205.

Eto, K., H. Tokunaga, K. Nagashima and T. Takeuchi (2002). "An autopsy case of minamata disease (methylmercury poisoning)-- pathological viewpoints of peripheral nerves." Toxicol Pathol 30(6): 714-22.

Farkas, L. M., N. Dunker, E. Roussa, K. Unsicker and K. Krieglstein (2003). "Transforming growth factor-beta(s) are essential for the development of midbrain dopaminergic neurons in vitro and in vivo." J Neurosci 23(12): 5178-86.

Faustman, E. M., R. A. Ponce, Y. C. Ou, M. A. Mendoza, T. Lewandowski and T. Kavanagh (2002). "Investigations of methylmercury-induced alterations in neurogenesis." Environ Health Perspect 110 Suppl 5: 859-64.

Feinstein, E., R. P. Gale, J. Reed and E. Canaani (1992). "Expression of the normal p53 gene induces differentiation of K562 cells." Oncogene 7(9): 1853-7.

Fero, M. L., M. Rivkin, M. Tasch, P. Porter, C. E. Carow, E. Firpo, K. Polyak, L. H. Tsai, V. Broudy, R. M. Perlmutter, K. Kaushansky and J. M. Roberts (1996). "A syndrome of multiorgan hyperplasia with features of gigantism, tumorigenesis, and female sterility in p27(Kip1)-deficient mice." Cell 85(5): 733-44.

Ferreira, A. and K. S. Kosik (1996). "Accelerated neuronal differentiation induced by p53 suppression." J Cell Sci 109 (Pt 6): 1509-16.

Field S. J., F. Y. Tsai, F. Kuo, A. M. Zubiaga, W. G. Kaelin, D. M. Livingston, S. H. Orkin, M. E. Greenberg (1996). "E2F-1 functions in mice to promote apoptosis and suppress proliferation." 85(4):549-61.

Finnell, R. H., J. Gelineau-van Waes, G. D. Bennett, R. C. Barber, B. Wlodarczyk, G. M. Shaw, E. J. Lammer, J. A. Piedrahita and J. H. Eberwine (2000). "Genetic basis of susceptibility to environmentally induced neural tube defects." Ann N Y Acad Sci 919: 261-77.

Fiszman, M. L., L. N. Borodinsky, J. H. Neale (1999). "GABA induces proliferation of immature cerebellar granule cells grown in vitro." Brain Res Dev Brain Res. 114(1): 1-8.

Flint, O. P. (1983). "A micromass culture method for rat embryonic neural cells." J Cell Sci 61: 247-62.

Flint, O. P. (1984). "Interactions between differentiating nerve and limb cells in vitro: implications for limb pattern formation." Prog Clin Biol Res 151: 399-408.

Flint, O. P. and T. C. Orton (1984). "An in vitro assay for teratogens with cultures of rat embryo midbrain and limb bud cells." Toxicol Appl Pharmacol 76(2): 383-95.

Foster, G. A., M. Schultzberg, T. Kokfelt, M. Goldstein, H. C. Hemmings, Jr., C. C. Ouimet, S. I. Walaas and P. Greengard (1988). "Ontogeny of the dopamine and cyclic adenosine-3':5'-monophosphate-regulated phosphoprotein (DARPP-32) in the pre- and postnatal mouse central nervous system." Int J Dev Neurosci 6(4): 367-86.

Frenkel, J., D. Sherman, A. Fein, D. Schwartz, N. Almog, A. Kapon, N. Goldfinger and V. Rotter (1999). "Accentuated apoptosis in normally developing p53 knockout mouse embryos following genotoxic stress." Oncogene 18(18): 2901-7.

Fuchs, S. Y., V. Adler, T. Buschmann, Z. Yin, X. Wu, S. N. Jones and Z. Ronai (1998). "JNK targets p53 ubiquitination and degradation in nonstressed cells." Genes Dev 12(17): 2658-63.

Galderisi, U., F. P. Jori and A. Giordano (2003). "Cell cycle regulation and neural differentiation." Oncogene 22(33): 5208-19.

Geelen, J. A., J. A. Dormans and A. Verhoef (1990). "The early effects of methylmercury on the developing rat brain." Acta Neuropathol 80(4): 432-8.

Geng Y., Q. Yu, E. Sicinska, M. Das, R. T. Bronson, P. Sicinski (2001). "Deletion of the p27Kip1 gene restores normal development in cyclin D1-deficient mice." Proc Natl Acad Sci U S A 98(1): 19409.

Geng Y., Q. Yu, E. Sicinska, M. Das, J. E. Schneider, S. Bhattacharya, W. M. Rideout, R. T. Bronson, H. Gardner, P. Sicinski (2003). "Cyclin E ablation in the mouse." Cell 114(4):431-43.

Giaccia, A. J. and M. B. Kastan (1998). "The complexity of p53 modulation: emerging patterns from divergent signals." Genes Dev 12(19): 2973-83.

Gilmore E. C., T. Ohshima, A. M. Goffinet, A. B. Kulkami, K. Herrup (1998). "Cyclin-dependent kinase 5-deficient mice demonstrate novel developmental arrest in cerebral cortex." 18(16):6370-7.

Gohlke, J. M., W. C. Griffith, S. M. Bartell, T. A. Lewandowski and E. M. Faustman (2002). "A computational model for neocortical neuronogenesis predicts ethanol-induced neocortical neuron number deficits." Dev Neurosci 24(6): 467-77.

Gohlke, J. M., W. C. Griffith and E. M. Faustman (2004). "The role of cell death during neocortical neurogenesis and synaptogenesis: implications from a computational model for the rat and mouse." Brain Res Dev Brain Res 151(1-2): 43-54.

Gondo, Y., K. Nakamura, K. Nakao, T. Sasaoka, K. Ito, M. Kimura and M. Katsuki (1994). "Gene replacement of the p53 gene with the lacZ gene in mouse embryonic stem cells and mice by using two steps of homologous recombination." Biochem Biophys Res Commun 202(2): 830-7.

Gottlieb, E., R. Haffner, A. King, G. Asher, P. Gruss, P. Lonai and M. Oren (1997). "Transgenic mouse model for studying the transcriptional activity of the p53 protein: age- and tissue-dependent changes in radiation-induced activation during embryogenesis." Embo J 16(6): 1381-90.

Grandjean P., P. Weihe, R. F. White, F. Debes, S. Araki, K. Yokoyama, K. Murata, N. Sorensen, R. Dahl, P. J. Jorgensen (1997). "Cognitive deficit in 7-year-old children with prenatal exposure to methylmercury." Neurotoxicol Teratol 19(6):417-28.

Gribble, E. J., S. W. Hong and E. M. Faustman (2005). "The magnitude of methylmercury-induced cytotoxicity and cell cycle arrest is p53-dependent." Birth Defects Res A Clin Mol Teratol 73(1): 29-38.

Grossman, S. R., M. E. Deato, C. Brignone, H. M. Chan, A. L. Kung, H. Tagami, Y. Nakatani and D. M. Livingston (2003). "Polyubiquitination of p53 by a ubiquitin ligase activity of p300." Science 300(5617): 342-4.

Grunblatt, E., S. Mandel and M. B. Youdim (2000). "MPTP and 6-hydroxydopamine-induced neurodegeneration as models for Parkinson's disease: neuroprotective strategies." J Neurol 247 Suppl 2: II95-102.

Gudkov, A. V. and E. A. Komarova (2005). "Prospective therapeutic applications of p53 inhibitors." Biochem Biophys Res Commun 331(3): 726-36.

Guerri, C. (1998). "Neuroanatomical and neurophysiological mechanisms involved in central nervous system dysfunctions induced by prenatal alcohol exposure." Alcohol Clin Exp Res 22(2): 304-12.

Harvey, M., A. T. Sands, R. S. Weiss, M. E. Hegi, R. W. Wiseman, P. Pantazis, B. C. Giovanella, M. A. Tainsky, A. Bradley and L. A. Donehower (1993). "In vitro growth characteristics of embryo fibroblasts isolated from p53-deficient mice." Oncogene 8(9): 2457-67.

Hatten, M. E., A. M. Francois, E. Napolitano and S. Roffler-Tarlov (1984). "Embryonic cerebellar neurons accumulate [3H]-gamma-aminobutyric acid: visualization of developing gamma-aminobutyric acid-utilizing neurons in vitro and in vivo." J Neurosci 4(5): 1343-53.

Haydar, T. F., F. Wang, M. L. Schwartz, P. Rakic (2000). "Differential modulation of proliferation in the neocortical ventricular and subventribular zones." J Neurosci 20(15): 5764-74.

Hengst, L., V. Dulic, J. M. Slingerland, E. Lees and S. I. Reed (1994). "A cell cycle-regulated inhibitor of cyclin-dependent kinases." Proc Natl Acad Sci U S A 91(12): 5291-5.

Hengst, L. and S. I. Reed (1996). "Translational control of p27Kip1 accumulation during the cell cycle." Science 271(5257): 1861-4.

Herzog, K. H., J. S. Braun, S. H. Han and J. I. Morgan (2002). "Differential post-transcriptional regulation of p21WAF1/Cip1 levels in the developing nervous system following gamma-irradiation." Eur J Neurosci 15(4): 627-36.

Hoch, R. V. and P. Soriano (2003). "Roles of PDGF in animal development." Development 130(20): 4769-84.

Hoffman, B. D., H. M. Hanauske-Abel, A. Flint and M. Lalande (1991). "A new class of reversible cell cycle inhibitors." Cytometry 12(1): 26-32.

Howard, J. D. and N. K. Mottet (1986). "Effects of methylmercury on the morphogenesis of the rat cerebellum." Teratology 34(1): 89-95.

Hu L. F., S. Wang, X. R. Shi, H. H. Yao, Y. H. Sun, J. H Ding, S. Y. Liu, G. Hu (2005). "ATP-sensitive potassium channel opener iptakalim protected against the cytotoxicity of MPP+ on SH-SY5Y cells by decreasing extracellular glutamate level." J Neurochem 94(6):1570-9.

Hughes, A. L., L. Gollapudi, T. L. Sladek and K. E. Neet (2000). "Mediation of nerve growth factor-driven cell cycle arrest in PC12 cells by p53. Simultaneous differentiation and proliferation subsequent to p53 functional inactivation." J Biol Chem 275(48): 37829-37.

Ito, A., C. H. Lai, X. Zhao, S. Saito, M. H. Hamilton, E. Appella, T. P. Yao (2001). "p300/CBP-mediated p53 acetylation is commonly induced by p53-activating agents and inhibited by MDM2." EMBO J 20(6):1331-40.

Jacks T., A. Fazeli, E. M. Schmitt, R. T. Bronson, M. A. Goodell, R. A. Weinberg (1992). "Effects of an Rb mutation in the mouse." 359(6393): 295-300.

Jacks, T., L. Remington, B. O. Williams, E. M. Schmitt, S. Halachmi, R. T. Bronson and R. A. Weinberg (1994). "Tumor spectrum analysis in p53-mutant mice." Curr Biol 4(1): 1-7.

Jones, S. N., A. E. Roe, L. A. Donehower, A. Bradley (1995). "Rescue of embryonic lethality in Mdm2-deficient mice by absence of p53." Nature 378(6553):206-8.

Jori, F. P., U. Galderisi, E. Piegari, M. Cipollaro, A. Cascino, G. Peluso, R. Cotrufo, A. Giordano and M. A. Melone (2003). "EGF-responsive rat neural stem cells: molecular follow-up of neuron and astrocyte differentiation in vitro." J Cell Physiol 195(2): 220-33.

Kakita, A., C. Inenaga, M. Sakamoto and H. Takahashi (2003). "Disruption of postnatal progenitor migration and consequent abnormal pattern of glial distribution in the cerebrum following administration of methylmercury." J Neuropathol Exp Neurol 62(8): 835-47.

Katayama, K., R. Ohtsuka, H. Takai, H. Nakayama and K. Doi (2002). "Expression of p53 and its transcriptional target genes mRNAs in the ethylnitrosourea-induced apoptosis and cell cycle arrest in the fetal central nervous system." Histol Histopathol 17(3): 715-20.

Kemp, C. J. (2005). "Multistep skin cancer in mice as a model to study the evolution of cancer cells." Semin Cancer Biol 15(6): 460-73.

Kintner, C. (2002). "Neurogenesis in embryos and in adult neural stem cells." J Neurosci 22(3): 639-43.

Kiyokawa, H., R. D. Kineman, K. O. Manova-Todorova, V. C. Soares, E. S. Hoffman, M. Ono, D. Khanam, A. C. Hayday, L. A. Frohman and A. Koff (1996). "Enhanced growth of mice lacking the cyclin-dependent kinase inhibitor function of p27(Kip1)." Cell 85(5): 721-32.

Komarova, E. A., M. V. Chernov, R. Franks, K. Wang, G. Armin, C. R. Zelnick, D. M. Chin, S. S. Bacus, G. R. Stark and A. V. Gudkov (1997). "Transgenic mice with p53-

responsive lacZ: p53 activity varies dramatically during normal development and determines radiation and drug sensitivity in vivo." Embo J 16(6): 1391-400.

Kramer, B. P. and M. Fussenegger (2005). "Hysteresis in a synthetic mammalian gene network." Proc Natl Acad Sci U S A 102(27): 9517-22.

Krieglstein, K., C. Suter-Crazzolara and K. Unsicker (1995). "Development of mesencephalic dopaminergic neurons and the transforming growth factor-beta superfamily." J Neural Transm Suppl 46: 209-16.

Kuo, M. L., E. J. Duncavage, R. Mathew, W. den Besten, D. Pei, D. Naeve, T. Yamamoto, C. Cheng, C. J. Sherr and M. F. Roussel (2003). "Arf induces p53-dependent and -independent antiproliferative genes." Cancer Res 63(5): 1046-53.

Lapham, L. W., E. Cernichiari, C. Cox, G. J. Myers, R. B. Baggs, R. Brewer, C. F. Shamlaye, P. W. Davidson and T. W. Clarkson (1995). "An analysis of autopsy brain tissue from infants prenatally exposed to methymercury." Neurotoxicology 16(4): 689-704.

Lee S. H., N. Lumelsky, L. Studer, J. M. Auerbach, R. D. McKay (2000). "Efficient generation of midbrain and hindbrain neurons from mouse embryonic stem cells." Nat Biotechnol 18(6):675-9.

Lendahl, U., L. B. Zimmerman and R. D. McKay (1990). "CNS stem cells express a new class of intermediate filament protein." Cell 60(4): 585-95.

Leng, R. P., Y. Lin, W. Ma, H. Wu, B. Lemmers, S. Chung, J. M. Parant, G. Lozano, R. Hakem and S. Benchimol (2003). "Pirh2, a p53-induced ubiquitin-protein ligase, promotes p53 degradation." Cell 112(6): 779-91.

Leroux, B., W. Leisenring, S. Moolgavkar and E.M. Faustman (1996). "A biologically-based dose–response model for developmental toxicology." Risk Analysis 16: 449–458.

Leveillard, T., P. Gorry, K. Niederreither and B. Wasylyk (1998). "MDM2 expression during mouse embryogenesis and the requirement of p53." Mech Dev 74(1-2): 189-93.

Lewandowski, T. A., R. A. Ponce, J. S. Charleston, S. Hong and E. M. Faustman (2003). "Changes in cell cycle parameters and cell number in the rat midbrain during organogenesis." Brain Res Dev Brain Res 141(1-2): 117-28.

Li, Z., H. Lin, Y. Zhu, M. Wang and J. Luo (2001). "Disruption of cell cycle kinetics and cyclin-dependent kinase system by ethanol in cultured cerebellar granule progenitors." Brain Res Dev Brain Res 132(1): 47-58.

Li, Z., M. W. Miller and J. Luo (2002). "Effects of prenatal exposure to ethanol on the cyclin-dependent kinase system in the developing rat cerebellum." Brain Res Dev Brain Res 139(2): 237-45.

Limke, T. L. and W. D. Atchison (2002). "Acute exposure to methylmercury opens the mitochondrial permeability transition pore in rat cerebellar granule cells." Toxicol Appl Pharmacol 178(1): 52-61.

Limoli, C. L., E. Giedzinski, R. Rola, S. Otsuka, T. D. Palmer and J. R. Fike (2004). "Radiation response of neural precursor cells: linking cellular sensitivity to cell cycle checkpoints, apoptosis and oxidative stress." Radiat Res 161(1): 17-27.

Lin, L. F., D. H. Doherty, J. D. Lile, S. Bektest, F. Collins (1993). "GDNF: a glial cell line-derived neurotrophic factor for midbrain dopaminergic neurons." Science 260(5111): 1130-2.

Little, J. (2000). "Epidemiology of neurodevelopmental disorders in children." Prostaglandins Leukot Essent Fatty Acids 63(1-2): 11-20.

Liu, D., M. M. Matzuk, W. K. Sung, Q. Guo, P. Wang, D. J. Wolgemuth (1998). "Cyclin A1 is required for meiosis in the male mouse." Nat Genet 20(4): 377-80.

Liu, J. H., F. Yin, X. X. Zheng (2005). "Nardostachys chinensis glycoside induces characteristics of neuronal differentiation in rat pheochromocytoma PC12 cells." Biol Pharm Bull 28(4): 769-71.

Louis, J. M., V. W. McFarland, P. May and P. T. Mora (1988). "The phosphoprotein p53 is down-regulated post-transcriptionally during embryogenesis in vertebrates." Biochim Biophys Acta 950(3): 395-402.

Lopez-Bendito, G., R. Lujan, R. Shigemoto, P. Ganter, O. Paulsen, Z. Molnar (2003). "Blockade of GABA(B) receptors alters the tangential migration of cortical neurons." Cereb Cortex 13(9): 932-42.

Lowenheim, H., D. N. Furness, J. Kil, C. Zinn, K. Gultig, M. L. Fero, D. Frost, A. W. Gummer, J. M. Roberts, E. W. Rubel, C. M. Hackney and H. P. Zenner (1999). "Gene disruption of p27(Kip1) allows cell proliferation in the postnatal and adult organ of corti." Proc Natl Acad Sci U S A 96(7): 4084-8.

Lu, J., Y. Wu, N. Sousa, O. F. Almeida (2005). "SMAD pathway mediation of BDNF and TGF beta 2 regulation of proliferation and differentiation of hippocampal granule neurons." Development 132(14): 3231-42.

MacCallum, D. E., T. R. Hupp, C. A. Midgley, D. Stuart, S. J. Campbell, A. Harper, F. S. Walsh, E. G. Wright, A. Balmain, D. P. Lane and P. A. Hall (1996). "The p53 response to ionising radiation in adult and developing murine tissues." Oncogene 13(12): 2575-87.

Mendoza, M. A., R. A. Ponce, Y. C. Ou and E. M. Faustman (2002). "p21(WAF1/CIP1) inhibits cell cycle progression but not G2/M-phase transition following methylmercury exposure." Toxicol Appl Pharmacol 178(2): 117-25.

Menegola, E., M. L. Broccia, F. Di Renzo, V. Massa and E. Giavini (2004). "Effects of excess and deprivation of serotonin on in vitro neuronal differentiation." In Vitro Cell Dev Biol Anim 40(1-2): 52-6.

Miller, M. W. (1986). "Effects of alcohol on the generation and migration of cerebral cortical neurons." Science 233(4770): 1308-11.

Miller, M. W., A. Peter, S. B. Wharton and A. H. Wyllie (2003). "Proliferation and death of conditionally immortalized neural cells from murine neocortex: p53 alters the ability of neuron-like cells to re-enter the cell cycle." Brain Res 965(1-2): 57-66.

Mills, A. A., B. Zheng, X. J. Wang, H. Vogel, D. R. Roop, A. Bradley (1999). "p63 is a p53 homologue required for limb and epidermal morphogenesis." Nature 398(6729): 708-13.

Mitsuhashi, T., Y. Aoki, Y. Z. Eksioglu, T. Takahashi, P. G. Bhide, S. A. Reeves and V. S. Caviness, Jr. (2001). "Overexpression of p27Kip1 lengthens the G1 phase in a mouse model that targets inducible gene expression to central nervous system progenitor cells." Proc Natl Acad Sci U S A 98(11): 6435-40.

Miura, K., K. Suzuki and N. Imura (1978). "Effects of methylmercury on mitotic mouse glioma cells." Environ Res 17(3): 453-71.

Miyazawa, K., T. Himi, V. Garcia, H. Yamagishi, S. Sato and Y. Ishizaki (2000). "A role for p27/Kip1 in the control of cerebellar granule cell precursor proliferation." J Neurosci 20(15): 5756-63.

Moll, U. M. and N. Slade (2004). "p63 and p73: roles in development and tumor formation." Mol Cancer Res 2(7): 371-86.

Morgan, D. O. (1997). "Cyclin-dependent kinases: engines, clocks, and microprocessors." Annu Rev Cell Dev Biol 13: 261-91.

Murphy M., M. G. Stinnakre, C. Senamaud-Beaufort, N. J. Winston, C. Sweeney, M. Kubelka, M. Carrington, C. Brechot, J. Sobczak-Thepot (1999). "Delayed early

embryonic lethality following disruption of the murine cyclin A2 gene." Nat Genet 15(1):83-6.

Nakamura, T., J. G. Pichel, L. Williams-Simons and H. Westphal (1995). "An apoptotic defect in lens differentiation caused by human p53 is rescued by a mutant allele." Proc Natl Acad Sci U S A 92(13): 6142-6.

Nakayama, K., N. Ishida, M. Shirane, A. Inomata, T. Inoue, N. Shishido, I. Horii and D. Y. Loh (1996). "Mice lacking p27(Kip1) display increased body size, multiple organ hyperplasia, retinal dysplasia, and pituitary tumors." Cell 85(5): 707-20.

Nakayama, K. (1998). "Cip/Kip cyclin-dependent kinase inhibitors: brakes of the cell cycle engine during development." Bioessays 20(12): 1020-9.

Nakayama, K. I., S. Hatakeyama and K. Nakayama (2001). "Regulation of the cell cycle at the G1-S transition by proteolysis of cyclin E and p27Kip1." Biochem Biophys Res Commun 282(4): 853-60.

National Research Council (2000). Scientific Frontiers in Risk Assessment and Developmental Toxicology. National Academy Press. Washington, D.C.

Nelson, E. L., C. L. Liang, C. M. Sinton, D. C. German (1996). "Midbrain dopaminergic neurons in the mouse: computer-assisted mapping." J Comp Neurol 369(3): 361-71.

Nguyen, L., B. Malgrange, I. Breuskin, L. Bettendorff, G. Moonen, S. Belachew, J. M. Rigo (2003). "Autocrine/paracrine activation of the GABA(A) receptor inhibits the proliferation of neurogenic polysialylated neural cell adhesion molecule-positive (PSA-NCAM+) precursor cells from postnatal striatum." J Neurosci 23(8): 3278-94.

Nicol, C. J., M. L. Harrison, R. R. Laposa, I. L. Gimelshtein and P. G. Wells (1995). "A teratologic suppressor role for p53 in benzo[a]pyrene-treated transgenic p53-deficient mice." Nat Genet 10(2): 181-7.

Nishimura, H., S. Hirota, O. Tanaka, M. Ueda and T. Uno (1974). "Normal mercury level in human embryos and fetuses." Biol Neonate 24(3): 197-205.

Norimura T., S. Nomoto, M. Katsuki, Y. Gondo, S. Kondo (1996). "p53-dependent apoptosis suppresses radiation-induced teratogenesis." 2(5): 577-80.

Novak, B., A. Csikasz-Nagy, B. Gyorffy, K. Chen and J. J. Tyson (1998). "Mathematical model of the fission yeast cell cycle with checkpoint controls at the G1/S, G2/M and metaphase/anaphase transitions." Biophys Chem 72(1-2): 185-200.

Novak, B., Z. Pataki, A. Ciliberto and J. J. Tyson (2001). "Mathematical model of the cell division cycle of fission yeast." Chaos 11(1): 277-286.

Ohnuma, S. and W. A. Harris (2003). "Neurogenesis and the cell cycle." Neuron 40(2): 199-208.

Ohnuma, S., A. Philpott and W. A. Harris (2001). "Cell cycle and cell fate in the nervous system." Curr Opin Neurobiol 11(1): 66-73.

Ohshima T., J. M. Ward, C. G. Huh, G. Longenecker, Veeranna, H. C. Pant, R. O. Brady, L. J. Martin, A. B. Kulkami (1996). "Targeted disruption of the cyclin-dependent kinase 5 gene results in abnormal corticogenesis, neuronal pathology and perinatal death." Proc Natl Acad Sci U S A 93(20):11173-8.

Olashaw, N. and W. J. Pledger (2002). "Paradigms of growth control: relation to Cdk activation." Sci STKE 2002(134): RE7.

Ostenfeld, T., P. Horn, C. Aardal, I. Orpen, M. A. Caldwell and C. N. Svendsen (1999). "Mouse epidermal growth factor-responsive neural precursor cells increase the survival and functional capacity of embryonic rat dopamine neurons in vitro." Neuroreport 10(9): 1985-92.

Ostenfeld, T., E. Joly, Y. T. Tai, A. Peters, M. Caldwell, E. Jauniaux and C. N. Svendsen (2002). "Regional specification of rodent and human neurospheres." Brain Res Dev Brain Res 134(1-2): 43-55.

Pagano, M., S. W. Tam, A. M. Theodoras, P. Beer-Romero, G. Del Sal, V. Chau, P. R. Yew, G. F. Draetta and M. Rolfe (1995). "Role of the ubiquitin-proteasome pathway in regulating abundance of the cyclin-dependent kinase inhibitor p27." Science 269(5224): 682-5.

Park, K. S., R. D. Lee, S. K. Kang, S. Y. Han, K. L. Park, K. H. Yang, Y. S. Song, H. J. Park, Y. M. Lee, Y. P. Yun, K. W. Oh, D. J. Kim, Y. W. Yun, S. J. Hwang, S. E. Lee and J. T. Hong (2004). "Neuronal differentiation of embryonic midbrain cells by upregulation of peroxisome proliferator-activated receptor-gamma via the JNK-dependent pathway." Exp Cell Res 297(2): 424-33.

Parker, E. M., A. Monopoli, E. Ongini, G. Lozza, C. M. Babij (2000). "Rapamycin, but not FK506 and GPI-1046, increases neurite outgrowth in PC12 cells by inhibiting cell cycle progression." Neurophamacology 39(10): 1913-9.

Parran, D. K., W. R. Mundy and S. Barone, Jr. (2001). "Effects of methylmercury and mercuric chloride on differentiation and cell viability in PC12 cells." Toxicol Sci 59(2): 278-90.

Paterno, G. D., L. L. Gillespie, J. P. Julien and D. Skup (1997). "Regulation of neurofilament L, M and H gene expression during retinoic acid-induced neural differentiation of P19 embryonal carcinoma cells." Brain Res Mol Brain Res 49(1-2): 247-54.

Pearce, A. K. and T. C. Humphrey (2001). "Integrating stress-response and cell-cycle checkpoint pathways." Trends Cell Biol 11(10): 426-33.

Pevny, L. H., S. Sockanathan, M. Placzek and R. Lovell-Badge (1998). "A role for SOX1 in neural determination." Development 125(10): 1967-78.

Philipp-Staheli, J., K. H. Kim, D. Liggitt, K. E. Gurley, G. Longton and C. J. Kemp (2004). "Distinct roles for p53, p27Kip1, and p21Cip1 during tumor development." Oncogene 23(4): 905-13.

Philipp-Staheli, J., K. H. Kim, S. R. Payne, K. E. Gurley, D. Liggitt, G. Longton and C. J. Kemp (2002). "Pathway-specific tumor suppression. Reduction of p27 accelerates gastrointestinal tumorigenesis in Apc mutant mice, but not in Smad3 mutant mice." Cancer Cell 1(4): 355-68.

Pietenpol, J. A. and Z. A. Stewart (2002). "Cell cycle checkpoint signaling: cell cycle arrest versus apoptosis." Toxicology 181-182: 475-81.

Polleux, F. and J. M. Lauder (2004). "Toward a developmental neurobiology of autism." Ment Retard Dev Disabil Res Rev 10(4): 303-17.

Ponce, R. A., T. J. Kavanagh, N. K. Mottet, S. G. Whittaker and E. M. Faustman (1994). "Effects of methyl mercury on the cell cycle of primary rat CNS cells in vitro." Toxicol Appl Pharmacol 127(1): 83-90.

Prakash, N. and W. Wurst (2004). "Specification of midbrain territory." Cell Tissue Res 318(1): 5-14.

Prives, C. (1998). "Signaling to p53: breaking the MDM2-p53 circuit." Cell 95(1): 5-8.

Purdie, C. A., D. J. Harrison, A. Peter, L. Dobbie, S. White, S. E. Howie, D. M. Salter, C. C. Bird, A. H. Wyllie, M. L. Hooper and et al. (1994). "Tumour incidence, spectrum and ploidy in mice with a large deletion in the p53 gene." Oncogene 9(2): 603-9.

Rabinovitch, P. S., M. Kubbies, Y. C. Chen, D. Schindler and H. Hoehn (1988). "BrdU-Hoechst flow cytometry: a unique tool for quantitative cell cycle analysis." Exp Cell Res 174(2): 309-18.

Raff, M. C., L. E. Lillien, W. D. Richardson, J. F. Burne, M. D. Noble (1988). "Platelet-derived growth factor from astrocytes drives the clock that times oligodendrocyte development in culture." Nature 333(6173):562-5.

Rane, S. G., P. Dubus, R. V. Mettus, E. J. Galbreath, G. Boden, E. P. Reddy, M. Barbacid (1999). "Loss of Cdk4 expression causes insulin-deficient diabetes and Cdk4 activation results in beta-islet cell hyperplasia." Nat Genet 22(1):44-52.

Ribeiro, P. L. and E. M. Faustman (1990). "Chemically induced growth inhibition and cell cycle perturbations in cultures of differentiating rodent embryonic cells." Toxicol Appl Pharmacol 104(2): 200-11.

Rice, D. and S. Barone, Jr. (2000). "Critical periods of vulnerability for the developing nervous system: evidence from humans and animal models." Environ Health Perspect 108 Suppl 3: 511-33.

Rodier, P. M. (1994). "Vulnerable periods and processes during central nervous system development." Environ Health Perspect 102 Suppl 2: 121-4.

Rodier, P. M. (1995). "Developing brain as a target of toxicity." Environ Health Perspect 103 Suppl 6: 73-6.

Rodier, P. M., M. Aschner and P. R. Sager (1984). "Mitotic arrest in the developing CNS after prenatal exposure to methylmercury." Neurobehav Toxicol Teratol 6(5): 379-85.

Rodier, P. M., J. L. Ingram, B. Tisdale and V. J. Croog (1997). "Linking etiologies in humans and animal models: studies of autism." Reprod Toxicol 11(2-3): 417-22.

Rodier, P. M., S. S. Reynolds and W. N. Roberts (1979). "Behavioral consequences of interference with CNS development in the early fetal period." Teratology 19(3): 327-36.

Rotter, V., D. Schwartz, E. Almon, N. Goldfinger, A. Kapon, A. Meshorer, L. A. Donehower and A. J. Levine (1993). "Mice with reduced levels of p53 protein exhibit the testicular giant-cell degenerative syndrome." Proc Natl Acad Sci U S A 90(19): 9075-9.

Roussa, E., L. M. Farkas and K. Krieglstein (2004). "TGF-beta promotes survival on mesencephalic dopaminergic neurons in cooperation with Shh and FGF-8." Neurobiol Dis 16(2): 300-10.

Roussa, E. and K. Krieglstein (2004a). "GDNF promotes neuronal differentiation and dopaminergic development of mouse mesencephalic neurospheres." Neurosci Lett 361(1-3): 52-5.

Roussa, E. and K. Krieglstein (2004b). "Induction and specification of midbrain dopaminergic cells: focus on SHH, FGF8, and TGF-beta." Cell Tissue Res 318(1): 23-33.

Rowland, B. D., S. G. Denissov, S. Douma, H. G. Stunnenberg, R. Bernards and D. S. Peeper (2002). "E2F transcriptional repressor complexes are critical downstream targets of p19(ARF)/p53-induced proliferative arrest." Cancer Cell 2(1): 55-65.

Sager, P. R. (1988). "Selectivity of methyl mercury effects on cytoskeleton and mitotic progression in cultured cells." Toxicol Appl Pharmacol 94(3): 473-86.

Sager, P. R., M. Aschner and P. M. Rodier (1984). "Persistent, differential alterations in developing cerebellar cortex of male and female mice after methylmercury exposure." Brain Res 314(1): 1-11.

Sah, V. P., L. D. Attardi, G. J. Mulligan, B. O. Williams, R. T. Bronson and T. Jacks (1995). "A subset of p53-deficient embryos exhibit exencephaly." Nat Genet 10(2): 175-80.

Saldeen, J., L. Tillmar, E. Karlsson and N. Welsh (2003). "Nicotinamide- and caspase-mediated inhibition of poly(ADP-ribose) polymerase are associated with p53-independent cell cycle (G2) arrest and apoptosis." Mol Cell Biochem 243(1-2): 113-22.

Santillano, D. R., L. S. Kumar, T. L. Prock, C. Camarillo, J. D. Tingling and R. C. Miranda (2005). "Ethanol induces cell-cycle activity and reduces stem cell diversity to alter both regenerative capacity and differentiation potential of cerebral cortical neuroepithelial precursors." BMC Neurosci 6: 59.

Sarkar, S. A. and R. P. Sharma (2002). "All-trans-retinoic acid-mediated modulation of p53 during neural differentiation in murine embryonic stem cells." Cell Biol Toxicol 18(4): 243-57.

Saucedo-Cardenas, O., J. D. Quintana-Hau, W. D. Le, M. P. Smidt, J. J. Cox, F. De Mayo, J. P. Burbach and O. M. Conneely (1998). "Nurr1 is essential for the induction of the dopaminergic phenotype and the survival of ventral mesencephalic late dopaminergic precursor neurons." Proc Natl Acad Sci U S A 95(7): 4013-8.

Schmid, P., A. Lorenz, H. Hameister and M. Montenarh (1991). "Expression of p53 during mouse embryogenesis." Development 113(3): 857-65.

Schubart, U. K., J. Yu, J. A. Amat, Z. Wang, M. K. Hoffmann and W. Edelmann (1996). "Normal development of mice lacking metablastin (P19), a phosphoprotein implicated in cell cycle regulation." J Biol Chem 271(24): 14062-6.

Seeley, M. R. and E. M. Faustman (1995). "Toxicity of four alkylating agents on in vitro rat embryo differentiation and development." Fundam Appl Toxicol 26(1): 136-42.

Shackelford, R. E., W. K. Kaufmann and R. S. Paules (1999). "Cell cycle control, checkpoint mechanisms, and genotoxic stress." Environ Health Perspect 107 Suppl 1: 5-24.

Shaulsky, G., N. Goldfinger, A. Peled and V. Rotter (1991). "Involvement of wild-type p53 in pre-B-cell differentiation in vitro." Proc Natl Acad Sci U S A 88(20): 8982-6.

Sherr, C. J. and J. M. Roberts (1995). "Inhibitors of mammalian G1 cyclin-dependent kinases." Genes Dev 9(10): 1149-63.

Sherr, C. J. and J. M. Roberts (1999). "CDK inhibitors: positive and negative regulators of G1-phase progression." Genes Dev 13(12): 1501-12.

Shirane, M., Y. Harumiya, N. Ishida, A. Hirai, C. Miyamoto, S. Hatakeyama, K. Nakayama and M. Kitagawa (1999). "Down-regulation of p27(Kip1) by two mechanisms, ubiquitin-mediated degradation and proteolytic processing." J Biol Chem 274(20): 13886-93.

Sicinski, P., J. L. Donaher, Y. Geng, S. B. Parker, H. Gardner, M. Y. Park, R. L. Robker, J. S. Richards, L. K. McGinnis, J. D. Biggers, J. J. Eppig, R. T. Bronson, S. J. Elledge and R. A. Weinberg (1996). "Cyclin D2 is an FSH-responsive gene involved in gonadal cell proliferation and oncogenesis." Nature 384(6608): 470-4.

Sicinski, P., J. L. Donaher, S. B. Parker, T. Li, A. Fazeli, H. Gardner, S. Z. Haslam, R. T. Bronson, S. J. Elledge and R. A. Weinberg (1995). "Cyclin D1 provides a link between development and oncogenesis in the retina and breast." Cell 82(4): 621-30.

Sidhu J. S., R. A. Ponce, M. A. Vredevoogd, X. Yu, E. Gribble, S. W. Hong, E. Schneider, and E. M. Faustman (2005). "Cell cycle inhibition by sodium arsenite in primary embryonic rat midbrain neuroepithelial cells." Toxicol Sci Epub ahead of print.

Sidhu, J. S., F. Liu, S. M. Boyle and C. J. Omiecinski (2001). "PI3K inhibitors reverse the suppressive actions of insulin on CYP2E1 expression by activating stress-response pathways in primary rat hepatocytes." Mol Pharmacol 59(5): 1138-46.

Sidhu, J. S. and C. J. Omiecinski (1998). "Protein synthesis inhibitors exhibit a nonspecific effect on phenobarbital-inducible cytochome P450 gene expression in primary rat hepatocytes." J Biol Chem 273(8): 4769-75.

Sionov, R. V. and Y. Haupt (1999). "The cellular response to p53: the decision between life and death." Oncogene 18(45): 6145-57.

Smidt, M. P., H. S. van Schaick, C. Lanctot, J. J. Tremblay, J. J. Cox, A. A. van der Kleij, G. Wolterink, J. Drouin and J. P. Burbach (1997). "A homeodomain gene Ptx3 has highly restricted brain expression in mesencephalic dopaminergic neurons." Proc Natl Acad Sci U S A 94(24): 13305-10.

Smith R., V. Bagga, R. A. Fricker-Gates (2003). "Embryonic neural progenitor cells: the effects of species, region, and culture conditions on long-term proliferation and neuronal differentiation." J Hematother Stem Cell Res 12(6):713-25.

Solberg, Y., W. F. Silverman and Y. Pollack (1993). "Prenatal ontogeny of tyrosine hydroxylase gene expression in the rat ventral mesencephalon." Brain Res Dev Brain Res 73(1): 91-7.

Stewart, Z. A. and J. A. Pietenpol (2001). "p53 Signaling and cell cycle checkpoints." Chem Res Toxicol 14(3): 243-63.

Storch, A., H. A. Lester, B. O. Boehm and J. Schwarz (2003). "Functional characterization of dopaminergic neurons derived from rodent mesencephalic progenitor cells." J Chem Neuroanat 26(2): 133-42.

Storch, A., M. Sabolek, J. Milosevic, S. C. Schwarz and J. Schwarz (2004). "Midbrain-derived neural stem cells: from basic science to therapeutic approaches." Cell Tissue Res 318(1): 15-22.

Sulik, K. K. and T. W. Sadler (1993). "Postulated mechanisms underlying the development of neural tube defects. Insights from in vitro and in vivo studies." Ann N Y Acad Sci 678: 8-21.

Sullivan A. M. and G. W. O'Keeffe (2005). "The role of growth/differentiation factor 5 (GDF5) in the induction and survival of midbrain dopaminergic neurons: relevance to Parkinson's disease treatment." J Anat 207(3): 219-26.

Takahashi T., R. S. Nowakowski, V. S. Caviness (1996). "The leaving of Q fraction of the murine cerebral proliferative epithelium: a general model of neocortical neurogenesis." J Neurosci 16(19):6183-96.

Takai H., K. Tominaga, N. Motoyama, Y. A. Minamishima, H. Nagahama, T. Tsukiyama, K. Ikeda, K. Nakayama, M. Nakanishi, K. Nakayama (2000). "Aberrant cell cycle checkpoint function and early embryonic death in Chk1(-/-) mice." Genes Dev 14(12):1439-47.

Tang, D., D. Wu, A. Hirao, J. M. Lahti, L. Liu, B. Mazza, V. J. Kidd, T. W. Mak and A. J. Ingram (2002). "ERK Activation Mediates Cell Cycle Arrest and Apoptosis after DNA Damage Independently of p53." J. Biol. Chem. 277(15): 12710-12717.

Taylor, W. R. and G. R. Stark (2001). "Regulation of the G2/M transition by p53." Oncogene 20(15): 1803-15.

Teixeira, L. T., H. Kiyokawa, X. D. Peng, K. T. Christov, L. A. Frohman and R. D. Kineman (2000). "p27Kip1-deficient mice exhibit accelerated growth hormone-releasing hormone (GHRH)-induced somatotrope proliferation and adenoma formation." Oncogene 19(15): 1875-84.

Temple S. (2001). "The development of neural stem cells." Nature 414(6859):112-7.

Thiel, G. (1993). "Synapsin I, synapsin II, and synaptophysin: marker proteins of synaptic vesicles." Brain Pathol 3(1): 87-95.

Tokumoto, Y. M., J. A. Apperly, F. B. Gao and M. C. Raff (2002). "Posttranscriptional regulation of p18 and p27 Cdk inhibitor proteins and the timing of oligodendrocyte differentiation." Dev Biol 245(1): 224-34.

Tokumoto, Y. M., D. G. Tang and M. C. Raff (2001). "Two molecularly distinct intracellular pathways to oligodendrocyte differentiation: role of a p53 family protein." Embo J 20(18): 5261-8.

Tominaga, M., S. Honda, A. Okada, A. Ikeda, S. Kinoshita, Y. Tomooka (2005). "A bipotent neural progenitor cell line cloned from a cerebellum of an adult p53-deficient mouse generates both neurons and oligodendrocytes." Eur J Neurosci 21(11): 2903-11.

Tong, W., H. Kiyokawa, T. J. Soos, M. S. Park, V. C. Soares, K. Manova, J. W. Pollard and A. Koff (1998). "The absence of p27Kip1, an inhibitor of G1 cyclin-dependent kinases, uncouples differentiation and growth arrest during the granulosa->luteal transition." Cell Growth Differ 9(9): 787-94.

Tsuji, K., K. Mizumoto, H. Sudo, K. Kouyama, E. Ogata and M. Matsuoka (2002). "p53-independent apoptosis is induced by the p19ARF tumor suppressor." Biochem Biophys Res Commun 295(3): 621-9.

Tsukada, T., Y. Tomooka, S. Takai, Y. Ueda, S. Nishikawa, T. Yagi, T. Tokunaga, N. Takeda, Y. Suda, S. Abe and et al. (1993). "Enhanced proliferative potential in culture of cells from p53-deficient mice." Oncogene 8(12): 3313-22.

Ueno, M., K. Katayama, H. Nakayama and K. Doi (2002). "Mechanisms of 5-azacytidine (5AzC)-induced toxicity in the rat foetal brain." Int J Exp Pathol 83(3): 139-50.

Vaghefi, H. and K. E. Neet (2004). "Deacetylation of p53 after nerve growth factor treatment in PC12 cells as a post-translational modification mechanism of neurotrophin-induced tumor suppressor activation." Oncogene 23(49): 8078-87.

van Lookeren Campagne, M. and R. Gill (1998). "Tumor-suppressor p53 is expressed in proliferating and newly formed neurons of the embryonic and postnatal rat brain: comparison with expression of the cell cycle regulators p21Waf1/Cip1, p27Kip1, p57Kip2, p16Ink4a, cyclin G1, and the proto-oncogene Bax." J Comp Neurol 397(2): 181-98.

Vermeulen, K., D. R. Van Bockstaele and Z. N. Berneman (2003). "The cell cycle: a review of regulation, deregulation and therapeutic targets in cancer." Cell Prolif 36(3): 131-49.

Vinson, R. K. and B. F. Hales (2003). "Genotoxic stress response gene expression in the mid-organogenesis rat conceptus." Toxicol Sci 74(1): 157-64.

Vitalis, T., O. Cases and J. G. Parnavelas (2005). "Development of the dopaminergic neurons in the rodent brainstem." Exp Neurol 191 Suppl 1: S104-12.

Vogel, D. G., P. S. Rabinovitch and N. K. Mottet (1986). "Methylmercury effects on cell cycle kinetics." Cell Tissue Kinet 19(2): 227-42.

Walsh, D. A. and V. B. Morris (1989). "Heat shock affects cell cycling in the neural plate of cultured rat embryos: a flow cytometric study." Teratology 40(6): 583-92.

Walum, E. and O. P. Flint (1990). "Midbrain micromass cultures: a model for studies of teratogenic and sub-teratogenic effects on CNS development." Acta Physiol Scand Suppl 592: 61-72.

Wang, C. X., J. H. Song, D. K. Song, V. W. Yong, A. Shuaib, and C. Hao (2005). "Cyclin-dependent kinase-5 prevents neuronal apoptosis through ERK-mediated upregulation of Bcl-2." Cell Death Differ, advance online publication, 4 November.

Weiss, B. and P. J. Landrigan (2000). "The developing brain and the environment: an introduction." Environ Health Perspect 108 Suppl 3: 373-4.

Whittaker, S. G. and E. M. Faustman (1991). "Effects of albendazole and albendazole sulfoxide on cultures of differentiating rodent embryonic cells." Toxicol Appl Pharmacol 109(1): 73-84.

Whittaker, S. G. and E. M. Faustman (1992). "Effects of benzimidazole analogs on cultures of differentiating rodent embryonic cells." Toxicol Appl Pharmacol 113(1): 144-51.

Whittaker, S. G., J. T. Wroble, S. M. Silbernagel and E. M. Faustman (1993). "Characterization of cytoskeletal and neuronal markers in micromass cultures of rat embryonic midbrain cells." Cell Biol Toxicol 9(4): 359-75.

Wijgerde, M., J. A. McMahon, M. Rule and A. P. McMahon (2002). "A direct requirement for Hedgehog signaling for normal specification of all ventral progenitor domains in the presumptive mammalian spinal cord." Genes Dev 16(22): 2849-64.

Williams, T. M., A. M. Ndifor, J. T. Near, R. R. Reams-Brown (2000). "Lead enhances NGF-induced neurite outgrowth in PC12 cells by potentiating ERK-MAPK activation." Neurotoxicology 21(6): 1081-9.

Wlodarczyk, B. C., J. C. Craig, G. D. Bennett, J. A. Calvin and R. H. Finnell (1996 a). "Valproic acid-induced changes in gene expression during neurulation in a mouse model." Teratology 54(6): 284-97.

Wlodarczyk, B. J., G. D. Bennett, J. A. Calvin and R. H. Finnell (1996b). "Arsenic-induced neural tube defects in mice: alterations in cell cycle gene expression." Reprod Toxicol 10(6): 447-54.

Woods, J. S., M. E. Ellis, F. J. Dieguez-Acuna, J. Corral (1999). "Activation of NF-kappaB in normal rat kidney epithelial (NRK52E) cells is mediated via a redox-insensitive, calcium-dependent pathway." Toxicol Appl Parmacol 154(3): 219-27.

Yamasaki L., T. Jacks, R. Bronson, E. Goillot, E. Harlow, N. J. Dyson (1996). "Tumor induction and tissue atrophy in mice lacking E2F-1." Cell 85(4):537-48.

Yamauchi, H., K. Katayama, M. Ueno, K. Uetsuka, H. Nakayama and K. Doi (2004). "Involvement of p53 in 1-beta-D-arabinofuranosylcytosine-induced rat fetal brain lesions." Neurotoxicol Teratol 26(4): 579-86.

Yan Y., D. Yang, E. D. Zarnowska, Z. Du, B. Werbel, C. Valliere, R. A. Pearce, J. A. Thomson, S. C. Zhang (2005). "Directed differentiation of dopaminergic neuronal subtypes from human embryonic stem cells." Stem Cells 23(6):781-90.

Yang, A., M. Kaghad, Y. Wang, E. Gillett, M. D. Fleming, V. Dotsch, N. C. Andrews, D. Caput, F. McKeon (1998). "p63, a p53 homolog at 3q27-29, encodes multiple products with transactivating, death-inducing, and dominant-negative activities." Mol Cell 2(3): 305-16.

Yang, A., N. Walker, R. Bronson, M. Kaghad, M. Oosterwegel, J. Bonnin, C. Vagner, H. Bonnet, P. Dikkes, A. Sharpe, F. McKeon, D. Caput (2000). "p73-deficient mice have neurological, pheromonal and inflammatory defects but lack spontaneous tumours." Nature 404(6773): 99-103.

Yang, W., J. Shen, M. Wu, M. Arsura, M. FitzGerald, Z. Suldan, D. W. Kim, C. S. Hofmann, S. Pianetti, R. Romieu-Mourez, L. P. Freedman and G. E. Sonenshein (2001). "Repression of transcription of the p27(Kip1) cyclin-dependent kinase inhibitor gene by c-Myc." Oncogene 20(14): 1688-702.

Yang, Y., C. C. Li and A. M. Weissman (2004). "Regulating the p53 system through ubiquitination." Oncogene 23(11): 2096-106.

Yu J. and L. Zhang (2005). "The transcriptional targets of p53 in apoptosis control." Biochem Biophys Res Commun 331(3):851-8.

Zhang L., A. Fletcher-Turner, M. A. Marchionnni, S. Apparsundaram, K. H. Lundgren, D. M. Yurek, K. B. Seroogy (2004). "Neurotrophic and neuroprotective effects of the neuregulin glial growth factor-2 on dopaminergic neurons in rat primary midbrain cultures." J Neurochem 91(6):1358-68.

Zheng M., C. L Leung, and R. K. Liem (1998). "Region-specific expression of cyclin-dependent kinase 5 (cdk5) and its activators, p35 and p39, in the developing and rat central nervous system. J Neurobiol 35: 141-59.

Zhu, X. H., H. Nguyen, H. D. Halicka, F. Traganos and A. Koff (2004). "Noncatalytic requirement for cyclin A-cdk2 in p27 turnover." Mol Cell Biol 24(13): 6058-66.

Zindy, F., J. J. Cunningham, C. J. Sherr, S. Jogal, R. J. Smeyne and M. F. Roussel (1999). "Postnatal neuronal proliferation in mice lacking Ink4d and Kip1 inhibitors of cyclin-dependent kinases." Proc Natl Acad Sci U S A 96(23): 13462-7.

Zindy, F., J. van Deursen, G. Grosveld, C. J. Sherr and M. F. Roussel (2000). "INK4d-deficient mice are fertile despite testicular atrophy." Mol Cell Biol 20(1): 372-8.

Zuccato, C., L. Conti, E. Reitano, M. Tartari, E. Cattaneo (2005). "The function of the neuronal proteins shc and huntingtin in stem cells and neurons: pharmacologic exploitation for human brain diseases." Ann N Y Acad Sci 1049: 39-50.

Zwolak, J. W., J. J. Tyson and L. T. Watson (2005). "Parameter estimation for a mathematical model of the cell cycle in frog eggs." J Comput Biol 12(1): 48-63.

APPENDIX

Quantification of Western blots presented in Chapters 4 and 5

Densitometry for Figure 5.4A: Comparisons of differentiation markers expressed in p53+/+ and p53-/- cultured midbrain NPCs.

NESTIN

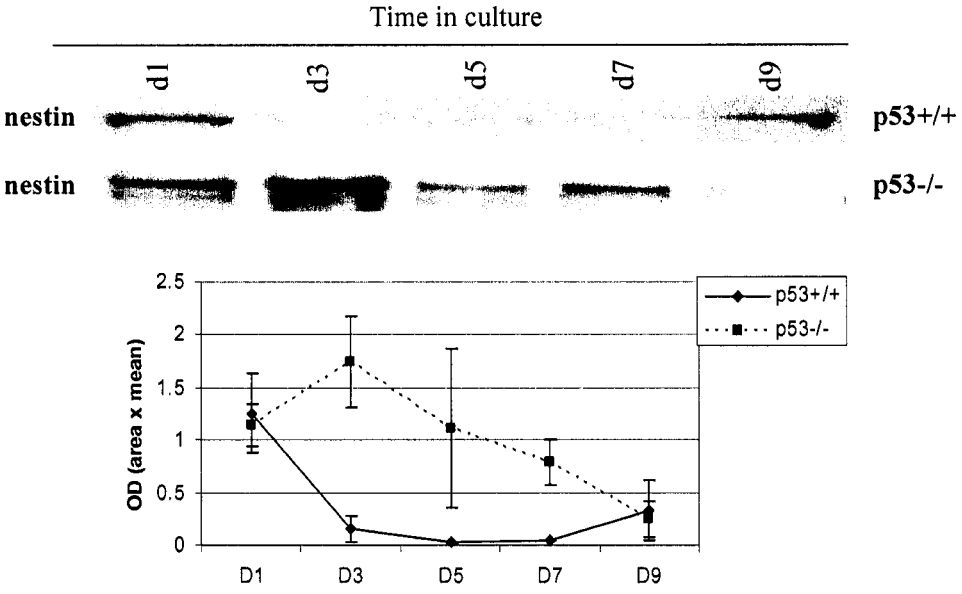

GAP-43

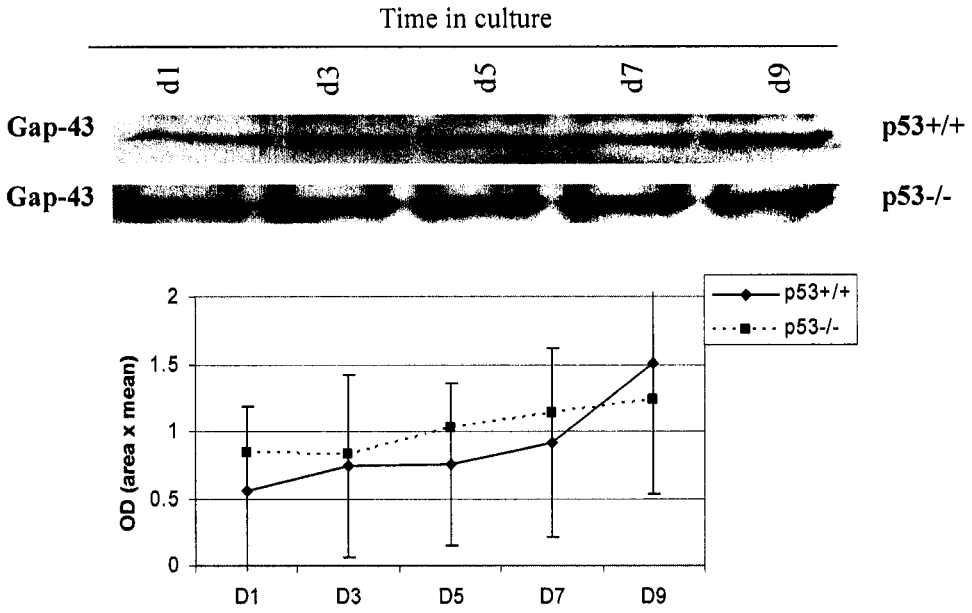
Time in culture
d1
d3
d5
d7
d9
Gap-43
p53+/+
Gap-43
p53-/-
OD (area x mean)
2
1.5
1
0.5
0
D1
D3
D5
D7
D9
p53+/+
p53-/-

NF-L

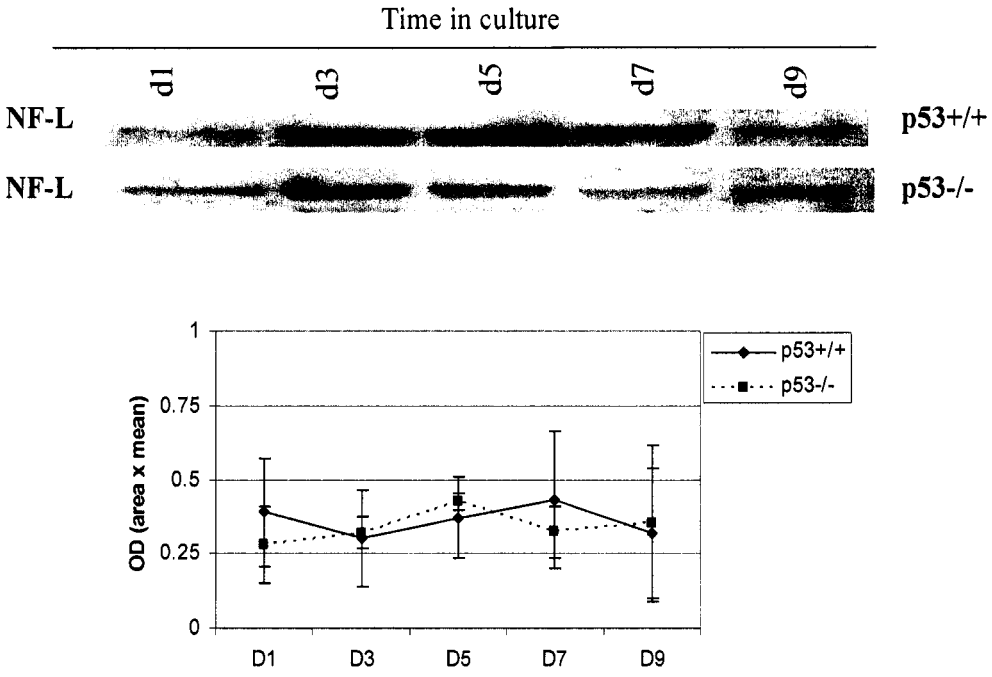
Time in culture
d1
d3
d5
d7
d9
NF-L
p53+/+
NF-L
p53-/-
OD (area x mean)
1
0.75
0.5
0.25
0
D1
D3
D5
D7
D9
p53+/+
p53-/-

TH

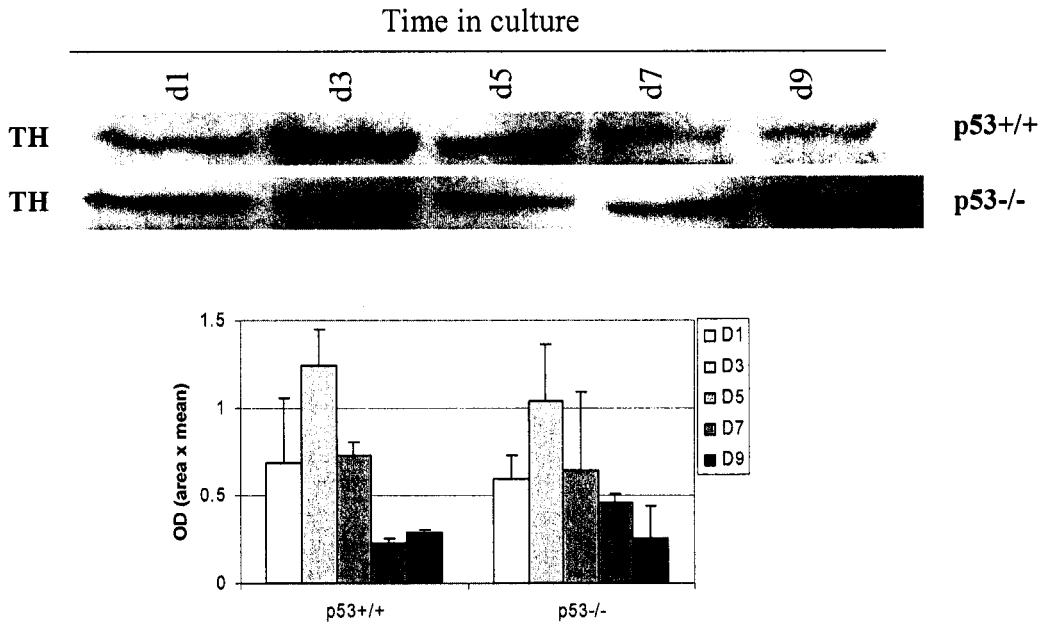
Time in culture
d1
d3
d5
d7
d9
TH
TH
p53+/+
p53-/-
1.5
1
0.5
0
OD (area x mean)
D1
D3
D5
D7
D9
p53+/+
p53-/-

VITA

Elizabeth J. Gribble attended the University of Puget Sound in Tacoma, Washington and graduated Humboldt State University cum laude in Arcata, California in 1999 with a Bachelor of Science in Molecular and Cellular Biology. She chose the University of Washington to study Environmental Health with a focus in Developmental Toxicology and Risk Assessment after encountering the inspiring work of her future advisor, Dr. Elaine Faustman. Elizabeth's research interests include cell cycle control, mechanisms of neurodevelopmental toxicity, and the development and use of appropriate models for developmental toxicological investigations and risk assessment. Beyond academia, Elizabeth has remained sane while pursuing her Ph.D. by running, climbing, doing yoga, living in and traveling to beautiful places, and playing with her dog, Zora, and husband, Matt.